THE $C^{13}(He^3, a)C^{12}$ REACTION AND THE STRUCTURE OF O^{16}

by

Henry R. Weller

Department of Physics
Duke University

Date: 21 Sept. 1967

Approved:

N. R. Roberson, Supervisor

E. G. Bilpuch

L. E. Evans

David A. Smith

A dissertation submitted in partial fulfillment of the requirements for the degree of Doctor of Philosophy in the Department of Physics in the Graduate School of Arts and Sciences of Duke University

1968

ABSTRACT

(Physics)

THE $C^{13}(He^3, \alpha)C^{12}$ REACTION AND THE STRUCTURE OF O^{16}

by

Henry R. Weller

Department of Physics
Duke University

Date: _____

Approved:

_____
N. R. Roberson, Supervisor

_____

_____

_____

An abstract of a dissertation submitted in partial fulfillment of the requirements for the degree of Doctor of Philosophy in the Department of Physics in the Graduate School of Arts and Sciences of Duke University

1968

THE $C^{13}(He^3, \alpha) C^{12}$ REACTION AND THE STRUCTURE OF O^{16}

by

Henry R. Weller

We have measured the angular distributions of the outgoing alpha particles from the $C^{13}(He^3, \alpha)C^{12}$ reaction in 100 keV steps from 5.1 to 8.4 MeV for the ground and first two excited state alpha groups. Elastic angular distributions resulting from the scattering of He^3 by C^{13} and C^{12} were measured at He^3 energies of 6.0, 7.0, and 8.0 MeV. Excitation curves of the alpha particles, protons and He^3 ions resulting from the bombardment of C^{13} with He^3 were measured at various angles.

We began the analysis by examining the applicability of the Distorted Wave Born Approximation using code JULIE. This also entailed using the Optical Model (Code HUNTER) to obtain the input parameters for JULIE for the incoming channel. In this case we also investigated the effects of adding a resonance term to the optical amplitude as formulated and coded by Tamura. Next we observed some features of our data which suggest a compound nucleus mechanism. Namely, symmetry about 90°

in the angular distributions and resonant like structure in the yield curves. Using the formalism of Blatt and Biedenharn and other considerations, we were able to make a probable spin assignment of $J^{\pi} = 3^{-}$ to a state in O^{16} at 27.6 MeV. This result also indicates a compound nucleus interpretation of j dependence for our data. We also considered the implications of the statistical compound nucleus theory in two ways. First we attempted to see how the ratios of total cross sections were predicted from approximate transmission coefficients. Next we examined the data to see how consistent it was with Ericson's theory of fluctuations. Then utilizing the doorway state concept of intermediate structure it seems possible to reconcile the features of our data which are single level in essence with the apparent statistical behavior. However, we are still left with the question of the doorway state mechanism and no clear computational technique. A general computational technique is needed and found in the Eigenchannel formalism. Although the complete problem is not yet solved, an approximation within the Eigenchannel calculation allows us to relate theory and experiment.

ACKNOWLEDGMENTS

I wish to acknowledge the help and suggestions of my research advisor Dr. N. R. Roberson in performing this experiment, particularly for encouraging the development of the doubly ionized He^3 beam and the mass identification technique, and for his expert guidance in using the on-line computer facilities. I am also indebted to Dr. D. R. Tilley for his help and advice in procuring the data.

Dr. Max Huber's enthusiastic discussions of the data were most valuable. I feel priviledged to have been shown a "reasonable treatment of nuclear reactions" by Dr. Michael Danos. I want to thank Dr. R. M. Drisko for his hospitality and advice while I was at Oak Ridge using the programs HUNTER and JULIE. I also appreciated Dr. Taro Tamura's instruction in using his code JUPITOR I. Discussions with my colleague Dr. M. Divadeenum were very helpful. I am very grateful to Dr. Wahsweiler for his communications from Frankfurt with regard to the eigenchannel calculations. Finally, I want to thank the people who helped in processing the somewhat voluminous data of this experiment and Mrs. J. Bailey for her excellent work on the illustrations.

H.R. W.

TABLE OF CONTENTS

LIST OF FIGURES

LIST OF TABLES

THE $C^{13}(He^3, a)C^{12}$ REACTION AND THE STRUCTURE OF O^{16}

Chapter I

INTRODUCTION

Nuclear reactions may be conveniently classified in terms of the time scale in which they occur. At one end of the time scale are the "compound nucleus" reactions which occur in times on the order of 10^{-14} seconds; at the other end are the "direct reactions" which occur in times on the order of 10^{-23} seconds. A direct reaction is also characterized as involving only a few degrees of freedom, whereas a compound nucleus involves many degrees of freedom.

In the case of direct reactions, let us consider three separate approximations: stripping (pickup), knock out, and heavy particle stripping. For example the $C^{13}(He^3, a)C^{12}$ reaction can be viewed as a neutron pickup reaction in which case the interaction between the He^3 ion and the neutron is considered to be dominant. Or one can take the knock-out picture and suppose that the interaction between the He^3 and the a particle in the target is dominant. Finally, in the heavy particle stripping assumption the Be^9-He^3 interaction is supposed to be effective. In all cases the

direct interaction is treated as a perturbation. For these reactions, since the incident wave packet is not appreciably delayed in passing through the nucleus, the phases of the partial waves in the incident channel are correlated with the partial waves in the exit channel. Thus, for direct reactions, there will be strong interference effects which may result in strong forward or backward peaking of the angular distributions of the emitted particles. In addition, due to the short lifetime, the direct reaction assumption implies a slowly varying cross section as a function of energy (widths of several MeV).

According to the compound nucleus model of Neils Bohr, (1) the existence of a rapidly varying structure in the continuum is attributed to long lived compound states. In these states an available excitation energy exceeding threshold is shared among many nucleons, none of which has enough energy to escape. These states typically have very narrow widths ($\sim$5 keV). In Bohr's original hypothesis, it was assumed that after equilibrium is reached, the system loses all 'memory' of its mode of formation. Thus, there is no correlation between the modes of formation and decay other than that required by the most elementary conservation laws such as those of energy and angular momentum. As a consequence, the decay of the compound nucleus is independent of its mode of formation.

The complexity of the compound nucleus can vary from one nuclear state (J^{π}) in one extreme, to so many that a statistical hypothesis becomes feasible. The observation of rapidly varying cross sections in the statistical region where the level width Γ is expected to be much

larger than the level spacing D, led to the development of Ericson's statistical theory of fluctuations. This theory takes into account a slowly varying non fluctuating component (the direct reaction part). It uses statistical techniques to describe the data, and so does not give a detailed account of observed cross sections.

Recently more general mechanisms have been introduced in order to account for so called intermediate resonance structure. Structures have been observed which have lifetimes too short to be conventional compound nucleus structures, and too long to be single particle resonances associated with the optical model, but which seem to have definite quantum numbers. (2) These intermediate resonance structures are supposed to be accounted for if we view the reaction as a sequential process. In Feshbach's terminology the first stage of this process is called the doorway state. The mechanism for the production of the doorway state is supposed to have many equivalent (complimentary) descriptions. In the case of a few open channels, if the target is describable in terms of the shell model and the residual interaction describing the possible excitations of the target by the incident particle is a sum of two body forces, then the doorway state consists of a two particle one hole state. This state can decay directly or can couple to higher generations (3p2h, 4p3h, etc.) to give rise to fine structure. (3) If the target is better described in terms of the collective model, then the doorway state consists of the target nucleus excited to a vibrational level and the incident particle dropping into a single particle level. Another description employs a double

R matrix theory dividing the nucleus into an inner complex part, an intermediate region, and an outside region so that only part of the compound nucleus is involved in the resonance. (4) Still other models have been suggested. For example LeCoteur, (5) Moldauer, (6) and Griffin (7) have independently described a statistical intermediate resonance model with some success in accounting for several experimental observations.

In the energy region of high excitations in which there are many open channels Feshbach has suggested a new mechanism for the production of doorway states. These doorway states are said to be those linear combinations of open channel wavefunctions which are particularly stable, i.e., have a relatively small width. (8) Of course this region is also supposed to contain Ericson fluctuations, so that there is a major problem in separating the intermediate resonances from the statistical fluctuations.

From the expression for the average scattering amplitude in the case when several reaction channels are open, Feshbach has shown that we may analyze doorway state resonances by using techniques identical with those employed in the study of compound resonances. (9) Another result is that the doorway state resonance can make its appearance in all exit channels, a result which provides a criterion which assists in the detection of these resonances; namely, it is sufficient that correlated intermediate structure exist simultaneously in the exit channels. It has been pointed out,(9) however, that the doorway state need not be

detectable in all exit channels, for the branching ratio for a particular decay of the doorway state may be very small. Very roughly speaking, the doorway state may act as a doorway for only some of the possible reaction channels, and this in fact is expected to be the case when many channels are open.

We can list some clues which may be useful in detecting intermediate resonances:

1. The existence of intermediate widths in the energy dependence.
2. The simultaneous existence of the structure in several open exit channels (i.e., a strong correlation in the energy dependence of the cross sections for different exit channels indicates the presence of intermediate resonances).
3. Angular distributions which vary smoothly as the energy is changed within the energy range covered by the intermediate structure.

It should be emphasized that the doorway state resonances will have definite quantum numbers.

The bombardment of C^{13} with He^3 ions provides a means of exciting O^{16} above the giant dipole region with relatively low energy (2. to 8. MeV) beams (see Figure 1). A recent $He^3(C^{13},\gamma_0)O^{16}$ experiment of Puttaswamy and Kohler (10) indicates that the compound nucleus O^{16} is significantly involved in this process. Previous studies of the $C^{13}(He^3,\alpha)C^{12}$ (11, 12, 13) reaction have concentrated on viewing the reaction as proceeding via a direct pickup process, an assumption which

Figure 1. Reaction Diagram for the $C^{13}(He^3, a)C^{12}$ Reaction.

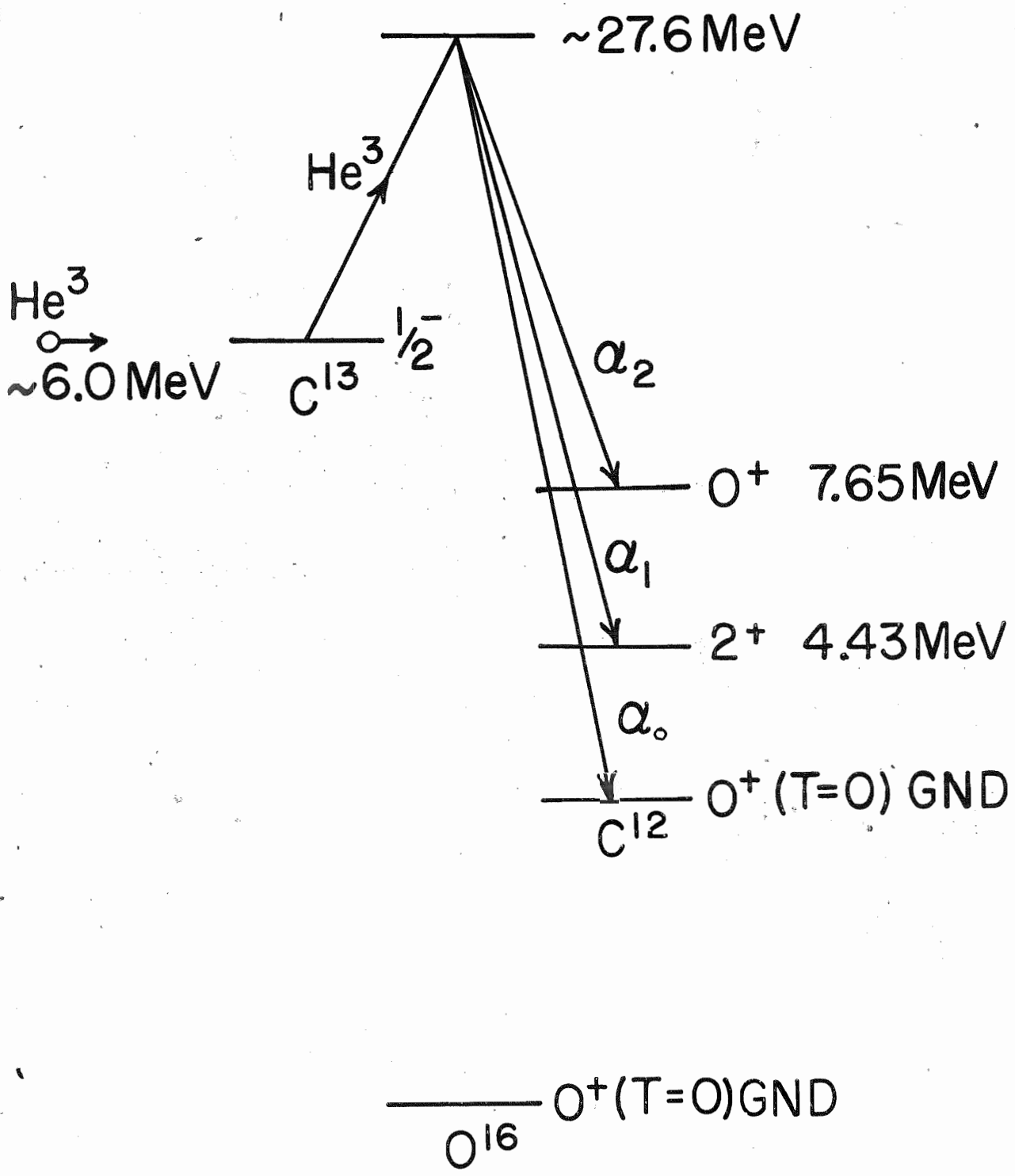

Reaction Energy Level Diagram

implies that the single particle states of C^{13} are the essential nuclear structure features which determine the reaction data. These studies were made at bombarding energies below 5. MeV and above 12. MeV, and did not attempt to account for any energy dependence in the cross sections. Studies have been made using the $N^{15}(p,\alpha)C^{12}$ reaction (14, 15) to test the statistical theories of Ericson et al. In this reaction the compound nucleus O^{16} was studied between the energies of 18. - 25. MeV. So it appeared that the $C^{13}(He^3,\alpha)C^{12}$ reaction would be subject to a similar analysis since He^3 energies from 2 to 8 MeV correspond to O^{16} excitation energies from 24 to 29 MeV. So a detailed study of the $C^{13}(He^3,\alpha)C^{12}$ reaction was attempted with the following objectives:

1. To study the direct reaction theory as represented in the Distorted Wave Born Approximation (DWBA) for He^3 energies from 5. to 8. MeV.
2. To study the applicability of Ericson's Statistical Theories and compare the results to those obtained from the $N^{15}(p,\alpha)C^{12}$ study.
3. To search for intermediate resonances.

The nucleus O^{16} is a particular interesting one in view of the extensive experimental and theoretical work which has been done on it in the past. For this reason a reaction theory which relies on nuclear structure knowledge is at an advantage here. Such a theory, the eigenchannel reaction theory of Danos and Greiner, (16) will be described later and the results of a calculation using this theory will be related to our experiment.

Chapter II

EXPERIMENTAL APPARATUS AND PROCEDURE

A. The He^3 Beam

The development of a doubly ionized He^3 beam seemed attractive, as this would allow us to obtain an 8.0 MeV projectile from the 4.0 MeV Duke Van de Graaff Accelerator. For this purpose a bench replica of the terminal ion source was constructed. After initial experimentation, we decided to install a small magnet between the bottle and the einzel lens (the einzel lens was used to refocus the beam after deflection).(17) The purpose of this magnet was to enable control of the ratio of singly to doubly ionized He^3 ions. This was valuable for it allowed acceleration of a double ionized beam without a large single ionized beam, the later being undesirable since it could cause troublesome upcharge loading of the accelerator. The initial design of the magnet was based on semi-empirical formulae. (18) We then measured the field through the magnet in small intervals using a Hall probe and fed this information into a program which calculated the trajectory of the beam. After one alteration we were

satisfied with the design. A cross-section of the final source is shown in Figure 2.

B. Target Preparation

The carbon target used in this experiment was 50 - 60% enriched C^{13}. The isotope was obtained in the form of methyl iodide from the Isomet Corporation of Palisades Park, New Jersey. The technique of cracking on a thin nickel foil and dissolving the foil in acid, as described in Appendix I, was used to obtain a self supporting target of about 100 $\mu g/cm^2$ thickness.

C. Angular Distribution and Excitation Curve Measurements

1. $C^{13}(He^3, \alpha)C^{12}$

The first measurement made was of the angular distributions of the alpha particles leading to the ground and first two excited states of C^{12} resulting from the reaction $C^{13}(He^3, \alpha)C^{12}$. These angular distributions were measured at 5.0, 6.0, 7.0, and 8.0 MeV bombarding energies. A 300 micron Silicon Solid State detector was used for these measurements. Data was accumulated by means of a 400 channel analyzer.

The solid state detector, collimated with a 1/16 inch diameter collimator, was set into the charged particle scattering chamber designed

Figure 2. Cross Section of He^3 Ion Source.

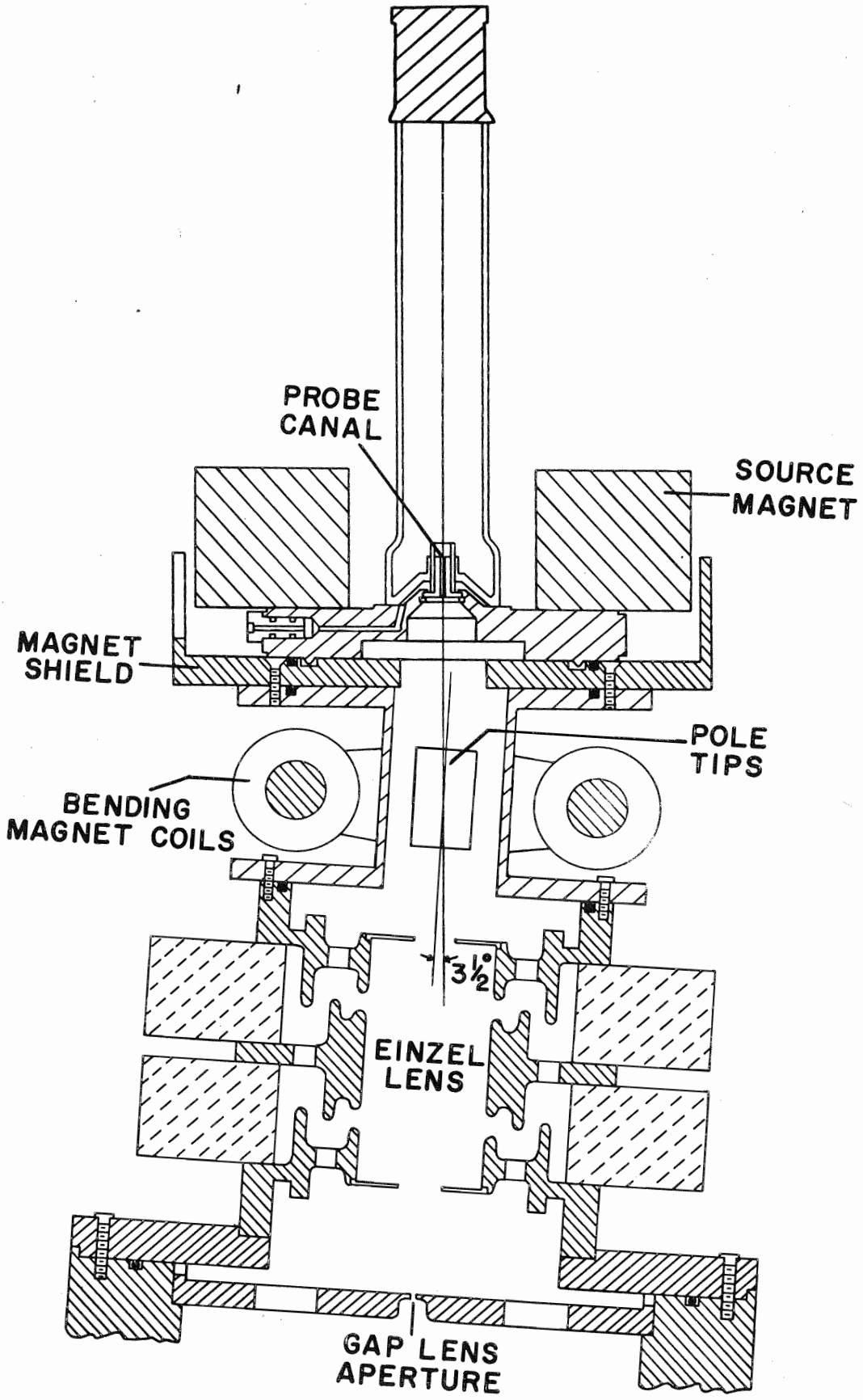
PROBE
CANAL
SOURCE
MAGNET
MAGNET
SHIELD
POLE
TIPS
BENDING
MAGNET COILS
3½°
EINZEL
LENS
GAP LENS
APERTURE

by Gerke.(19) The beam was collimated so that the beam spot was less than 1/8 inch diameter on the center of the target. The beam after passing through the target entered a Faraday cup, whereupon it was collected and integrated. Typical beam currents of 100 - 150 x 10^{-9} amperes were used. In this and subsequent measurements, the total charge accumulated was used for normalizing the runs of different angles and energies. Whenever practical, a monitor detector was also used to check this normalization.

A typical spectrum obtained is shown in Figure 3. Each run lasted about 30 minutes. The clean spectrum is due to the high energies of the alpha particles which we are detecting, and meant that no background subtraction was necessary. Typical sums obtained from the peaks were about 100 - 200 counts. The results of these measurements are shown in Figures 9, 10, and 11 of Chapter IV. The determination of the absolute cross section will be discussed below in section D.

The excitation curves of the outgoing α particles were taken at 30° and 90° using two detectors and procedures as described above. The energy steps of 20 keV on the machine corresponded to 40 keV beam energy steps. The target was about 20 keV thick to 5. MeV alpha particles, and due to 5 keV machine energy variations, the uncertainty in energy of the doubly charged beam was about 10 keV, so that the overall resolution was about 30 keV. Each energy from 2.0 to 8.0 MeV took about 30 minutes to obtain satisfactory statistics. The results of these measurements are shown in Figure 13 of Chapter IV.

Figure 3. Charged Particle Spectrum of the Alpha Groups from the $C^{13}(He^3, \alpha) C^{12}$ Reaction.

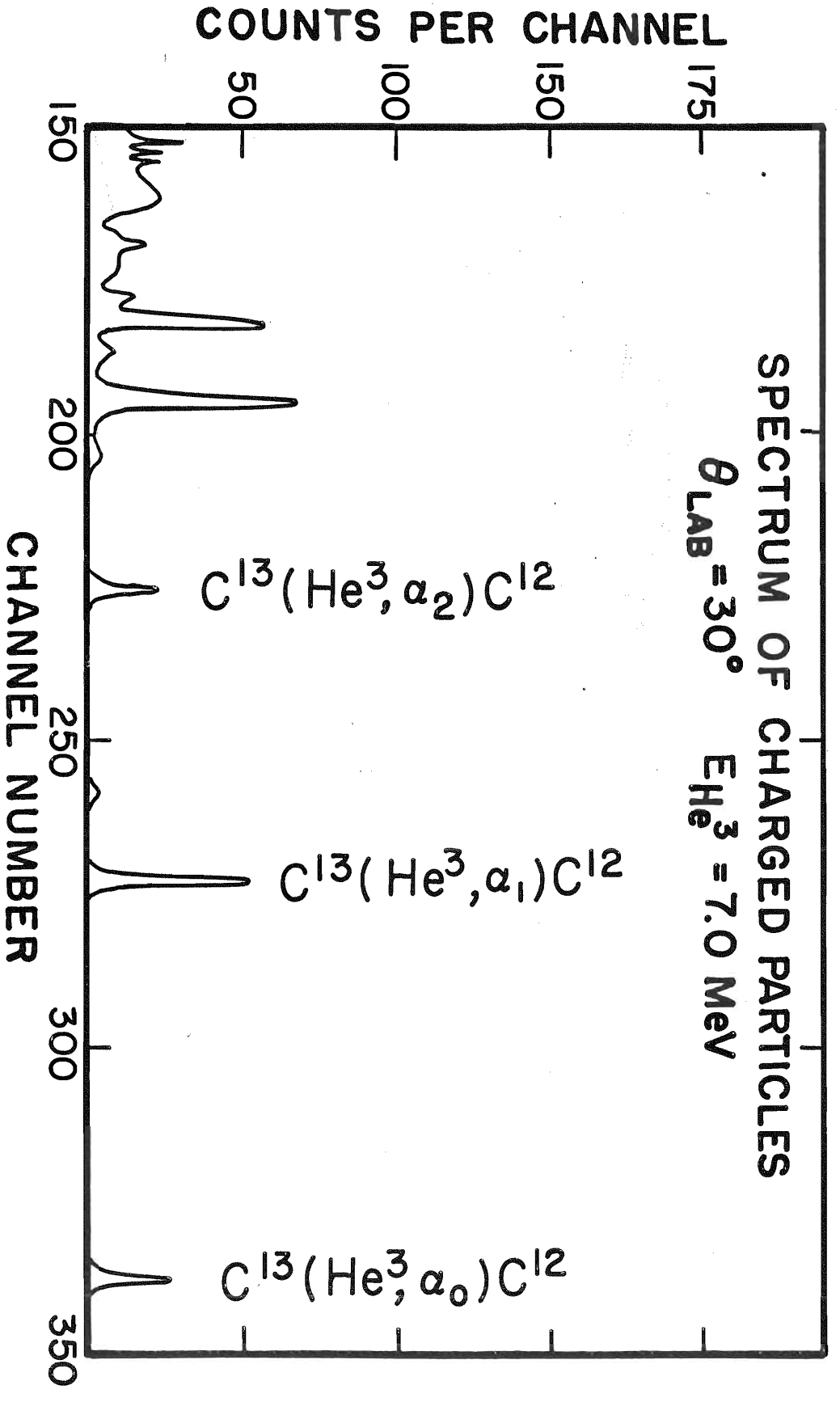
COUNTS PER CHANNEL
50
100
150
175
150
200
250
300
350
CHANNEL NUMBER
SPECTRUM OF CHARGED PARTICLES
$\theta_{LAB} = 30°$
$E_{He^3} = 7.0$ MeV
$C^{13}(He^3, \alpha_2)C^{12}$
$C^{13}(He^3, \alpha_1)C^{12}$
$C^{13}(He^3, \alpha_0)C^{12}$

Finally four detectors were installed in the chamber such that four settings gave points in 10° steps from 20° through 160° inclusive (90° being taken twice). The biases on the post-amplifiers were set so that pulses resulting from particles less energetic than a_2 were not analyzed. The four detectors were routed into the TMC multichannel analyzer, acting as four 100 channel analyzers. The solid angles were normalized from the geometric dimensions. These normalizations were checked by interchanging the detectors with one another. This technique enabled us to obtain one angular distribution every two hours and was used to obtain angular distributions in 100 keV steps from 5.1 to 8.4 MeV. An absolute energy correction made at the end of the run indicated that the energy intervals were actually 117 keV.

2. $C^{13}(He^3, p)N^{15}$

Measurement of the excitation curves of the high energy ($\sim 18.$ MeV) protons resulting from the $C^{13}(He^3, p)$ reaction required use of 2 mm thick Li drifted silicon detectors. Two were used, one at 30°, another at 150°. Data were stored in an on line computer programmed as two 1024 channel analyzers. A typical 30° spectrum is shown in Figure 4. The data resulting from these measurements are shown in Figures 17 and 18 of Chapter IV.

Figure 4. Charged Particle Spectrum from the Li Drifted Detector.

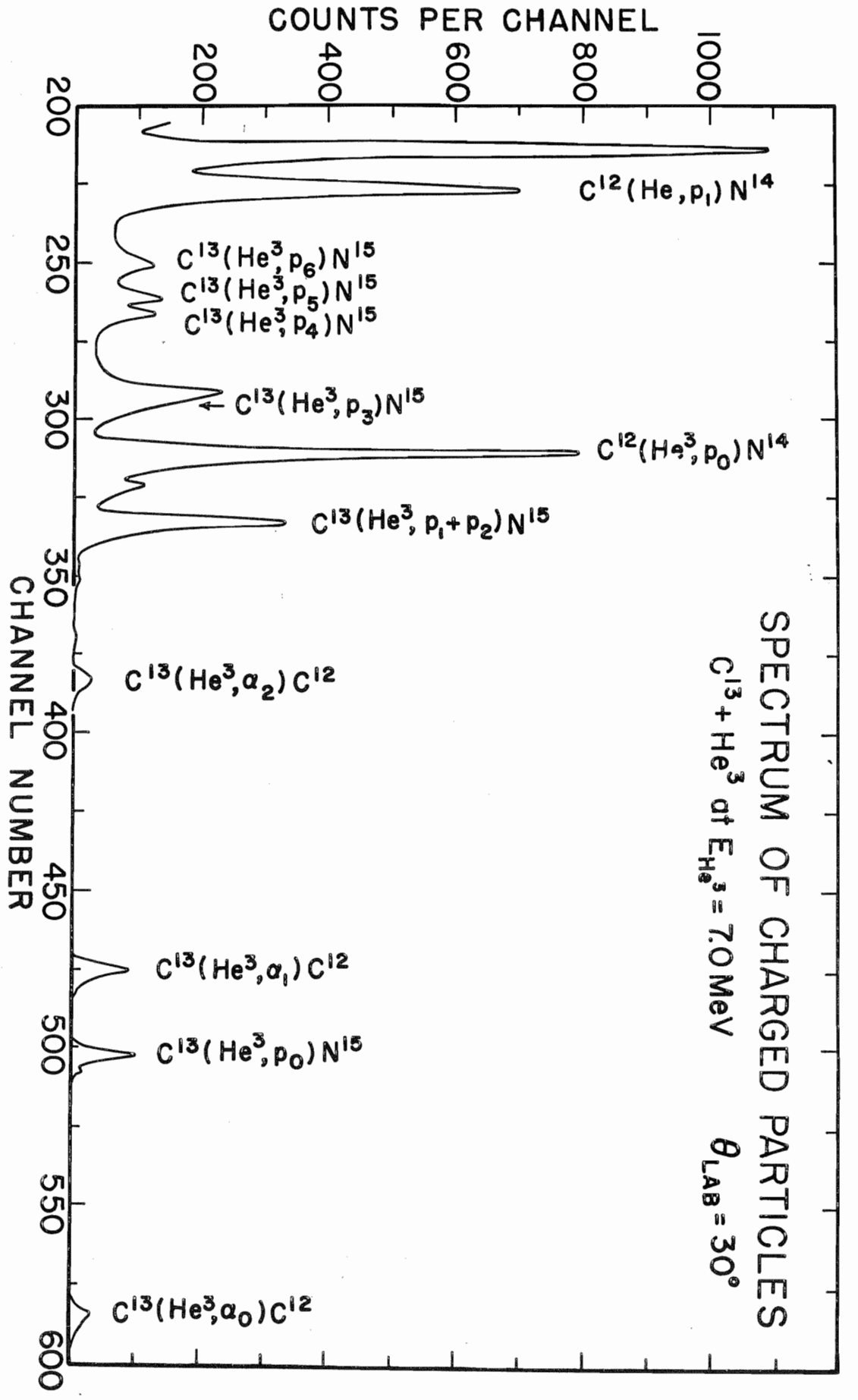
COUNTS PER CHANNEL
200
400
600
800
1000
CHANNEL NUMBER
200
250
300
350
400
450
500
550
600
$C^{12}(He, p_1)N^{14}$
$C^{13}(He^3, p_6)N^{15}$
$C^{13}(He^3, p_5)N^{15}$
$C^{13}(He^3, p_4)N^{15}$
$C^{13}(He^3, p_3)N^{15}$
$C^{12}(He^3, p_0)N^{14}$
$C^{13}(He^3, p_1+p_2)N^{15}$
$C^{13}(He^3, \alpha_2)C^{12}$
$C^{13}(He^3, \alpha_1)C^{12}$
$C^{13}(He^3, p_0)N^{15}$
$C^{13}(He^3, \alpha_0)C^{12}$
SPECTRUM OF CHARGED PARTICLES
$C^{13} + He^3$ at $E_{He^3} = 7.0$ MeV
$\theta_{LAB} = 30°$

3. $C^{13}(He^3, He^3)C^{13}$

The elastic angular distributions were taken with a mass telescope system composed of a proportional counter and solid state detector. The design is based on that of R. R. Carlson. (20) This apparatus provided an easy means of identifying the elastically scattered He^3 particles from the nearby alpha particles resulting from the $C^{12}(He^3, \alpha)C^{11}$ reaction. The proportional counter assembly is shown in Figure 5. Some essential features of this counter include using a spring rod to provide tension on the high voltage wire. The .004 inch tungsten wire was copper plated on both ends so that it could be soldered to the spring rod on one end, and so that a small bead could be soldered to the other end to hold the wire in the glass globule. It was also found that the counter would not work until the wire was flashed in a vacuum. The gas used in the counter was obtained from the Matheson Company of East Rutherford, New Jersey, and was 95% Argon, 05% CO^2. A pressure of several centimeters of Mercury was used, the actual pressure being determined empirically so as to give the best resolution. The window of the counter was a 1 micron nickel foil. In order to avoid a pressure gradient on this foil, when evacuating the target chamber, sufficient plumbing was utilized so as to enable evacuation of the proportional counter while the chamber was being pumped down. Then the proportional counter was filled with the gas mixture. During operation the proportional counter was refilled daily to assure purity. An operating voltage of 600 - 800 volts was found to be satisfactory.

Figure 5. Cross Section of Proportional Counter in Extended Position.

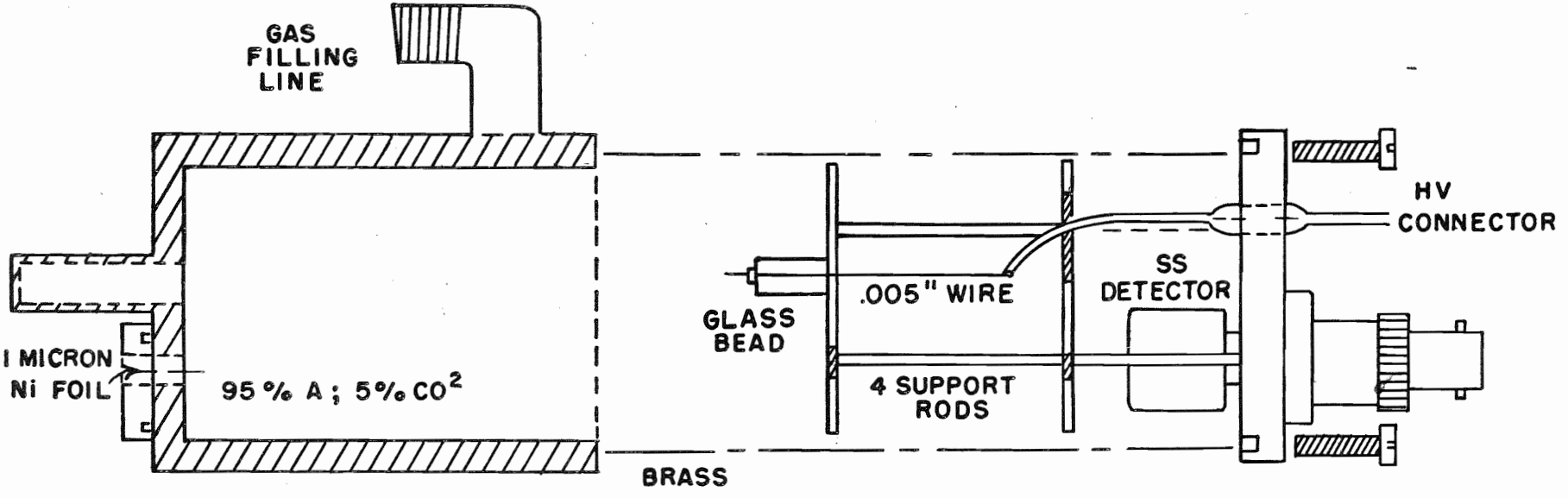
GAS
FILLING
LINE
1 MICRON
Ni FOIL
95 % A ; 5% CO2
GLASS
BEAD
.005" WIRE
4 SUPPORT
RODS
SS
DETECTOR
HV
CONNECTOR
BRASS

The electronic circuit associated with the proportional counter assembly is shown in Figure 6. The two linear signals were fed into two analog-to-digital converters (ADC's), and the computer was programmed as a two-parameter analyzer with the energy on the vertical axis and the energy loss on the horizontal axis. A typical spectrum observed from this system is shown in Figure 7. The four major peaks seen in the contour view are from two different mass numbers. The two peaks to the left are the He^3 elastic particles from C^{12} and C^{13} while the remaining two peaks are alpha particles. The counts in the lower left hand side are from unresolved protons, deuterons and tritons.

At a later date the data was read back into the computer and the groups were summed with the aid of a light pen. The computer was programmed to output the cross-section in absolute units in the center of mass system; target thickness and solid angle being known. The experimental angular distributions are shown in Figure 21 of Chapter IV.

D. Absolute Cross Section Determination

In order to obtain the absolute cross section, an angular distribution was taken at 2.0 MeV He^3 energy for the $C^{13}(He^3, \alpha)C^{12}$ reaction. Then using the data of H. D. Holmgren, (21) who measured the absolute cross section at 2.0 MeV by means of the $C^{13}(p, \gamma)N^{14}$ reaction, we were able to normalize our data to absolute units. A later measurement of the absolute cross section by means of Rutherford scattering

Figure 6. Block Diagram of Proportional Counter Assembly Electronics.

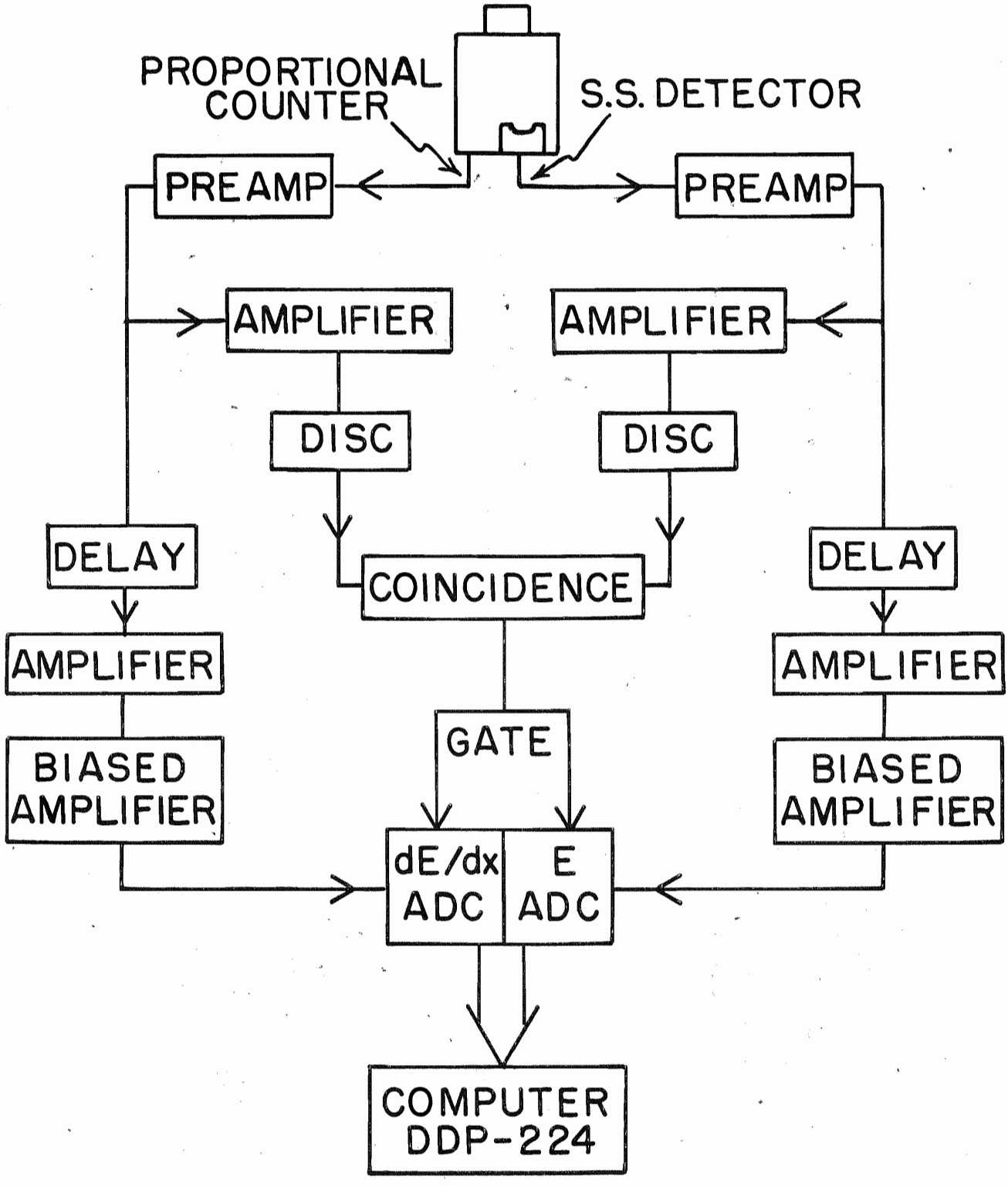
PROPORTIONAL COUNTER
S.S. DETECTOR
PREAMP
PREAMP
AMPLIFIER
AMPLIFIER
DISC
DISC
DELAY
COINCIDENCE
DELAY
AMPLIFIER
AMPLIFIER
GATE
BIASED AMPLIFIER
BIASED AMPLIFIER
dE/dx ADC
E ADC
COMPUTER DDP-224

Figure 7. Contour (top) and Isometric (bottom) View of 2-Dimensional Spectrum.

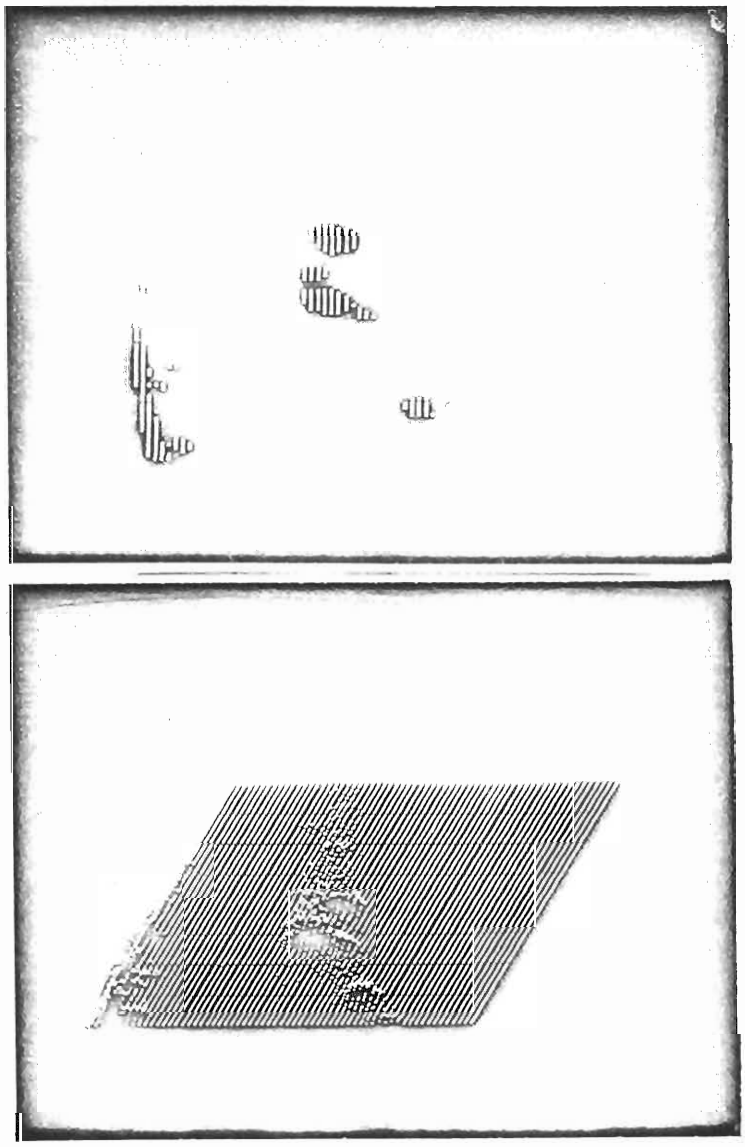

$He^3 + C^{13}$ SPECTRUM
7.0 MeV 120°

agreed with these results to within statistics.

In this later measurement the target thickness was determined by using a 2.0 MeV He^3 beam and taking an elastic scattering angular distribution in the forward angles. This 2.0 MeV beam was of necessity singly charged. This was because the 2.0 MeV doubly charged beam required running the Van de Graaff at 1.0 MeV where it does not run well. Using a singly charged beam meant measuring the stripping efficiency of the target. This was measured by placing the target in and out of the beam path several times and measuring the charge accumulated for a preset time under steady beam conditions. An average value of 92 percent $\pm$ 5 percent was obtained. With this information the angular distribution data provided a measurement of the target thickness by assuming pure Rutherford scattering. The shape of the distribution substantiated this assumption quite well. This measurement however was of the total target thickness which was a composite of C^{12} and C^{13}.

In order to get the C^{13} thickness the target thickness of a natural C^{12} target was measured. In measuring the elastic scattering of He^3 from C^{13} at 6.0, 7.0, and 8.0 MeV it had also been necessary to measure the scattering from C^{12} at the same energies. This was done because for angles less than 90° the elastically scattered He^3 particles from C^{12} and C^{13} were unresolved, so that by matching the back angle data for the C^{12} scattering from both targets and obtaining a normalization constant, the pure C^{12} data in the forward angles could be sub-

tracted from the composite $C^{12} + C^{13}$ forward angle data. So with these data the C^{12} target thickness told us the absolute cross section of the C^{12} elastic data. Then we knew the thickness of C^{12} in the composite target. Knowing the total thickness of the $C^{12} + C^{13}$ target enabled us to evaluate the thickness of the C^{13} in the composite target.

There was some problem with the C^{12} buildup on the target. This was monitored in two ways. First a monitor detector was used. By comparing the spectra from the C^{12} and the $C^{12} + C^{13}$ target, peaks peculiar to the C^{12} target were selected and summed. This gave a check on the C^{12} content during the course of measuring an angular distribution. Also, representative angular distributions were taken at each energy at the end of the experiment to check the total C^{12} buildup. The agreement between the two measurements was good.

E. Accelerator Energy Calibration

The absolute energy of the accelerated beam was measured in two ways. First, using an Am^{241} source, we took a spectrum with the multichannel analyzer using a calibration such that there were about 5 keV per channel. We then put the detector at a forward angle (eg. 30°) and adjusted the beam energy until the elastic peak fell into the same channel as did the Am^{241} alphas. Then, taking account of the energy loss through the target, a simple kinematical calculation determined the energy of the machine from the known energy of the Am^{241} alpha particles. It

was estimated that this technique determined the energy to within 20 keV.

Immediately following our run, a Li(p, n) threshold measurement was made to check our absolute energy calibration. This result agreed with our measurement within the expected error. In subsequent runs we were able to use the 6.0 MeV resonance observed in the C^{13} $(He^3, \alpha) C^{12}$ reaction as a check of the absolute calibration.

Chapter III
THEORY

In this chapter we will examine some of the basic ideas and present the basic formulae of the different theoretical approaches which will be used in the analysis of the data. An attempt will be made to point out the approximations involved in each approach.

A. The Compound Nucleus

1. Widely Spaced Levels

At very low excitation energies in the compound nucleus, for example just above the threshold for neutron emission and for medium weight nuclei, the widths of the nuclear levels are usually very narrow (as narrow as a few electron volts), and their average spacing is usually large enough so that they are completely separated. If the compound nucleus is formed by the excitation of one of these levels, then the assumption that the formation and decay of the compound nucleus are completely independent is obviously valid. The Breit-Wigner formalism for describing the cross sections for the excitation of these levels has been

extremely successful in describing many kinds of experimental data in this energy region. In this formalism, the cross section for the reaction leading from state a to state b is written

$$\sigma(a,b) = \sigma_c(a)\,\Gamma_b/\Gamma \tag{1}$$

where $\sigma_c(a)$ is the cross section for the formation of a compound nucleus by the particle a and Γ_b/Γ is the probability that the particle b is emitted by the compound state. Thus, the formula for describing the reaction can be separated into two independent parts.

The angular distribution of reaction products going from channel a to channel a' when only one compound nuclear state (J^π) is involved and in the absence of non resonant processes is (22)

$$\frac{d\sigma(a'|a)}{d\Omega} = \frac{\lambda^2/4}{(2I+1)(2i+1)\left[(E-E_{J\pi})^2+(1/2\Gamma_{J\pi})^2\right]} \cdot \sum (-1)^{s'-s}\bar{Z}(\ell_1 J \ell_2 J; sL)$$

$$\cdot \bar{Z}(\ell_1' J \ell_2' J; s' L) \cdot P_L(\cos\theta) \cdot \left[g(a'\ell_1' s' \,|\, J^\pi) g(a'\ell_2' s' \,|\, J^\pi) g(a\ell_1 s / J^\pi)\right.$$

$$\left. \cdot g(a\ell_2 s \,|\, J^\pi)\right] \cdot \cos\left[\delta(a\ell_1' s' \,|\, J^\pi) - \delta(a'\ell_2' s' \,|\, J\pi) + \delta(a\ell_1 s \,|\, J\pi) - \delta(a\ell_2 s \,|\, J\pi)\right] \tag{2}$$

where $\vec{s}$ is the channel spin defined as $\vec{s} = \vec{I} + \vec{i}$, I being the spin of the target and i the spin of the projectile. The spin of the state (J) must satisfy the equation $\vec{J} = \vec{\ell} + \vec{s}$, $\vec{\ell}$ being the orbital angular momentum. The sum in this equation represents a sum over all quantum numbers, the allowed values being determined by the triangle relations associated with the $\bar{Z}$ coefficients. The $\bar{Z}$ coefficients are defined by Blatt, Biedenharn, and Rose (23) and have been tabulated. (24) The factors g are related to

the partial widths $\Gamma(a\ell s|J\pi)$ by $\Gamma(a\ell s|J\pi) = g^2(a\ell s|J\pi)$, and the δ's are their associated phases. Since ℓ_1 and ℓ_2 represent possible routes between the same initial and final states (as do ℓ_1' and ℓ_2') it follows that they must have the same parity so that

$$\ell_1 + \ell_2 \text{ and } \ell_1' + \ell_2'$$

are even. From the property of the $\bar{Z}$ coefficients that $\ell_1 + \ell_2 + L$ must be even, it follows that L is even. Therefore only even Legendre Polynomials are involved and so the distribution is symmetric about 90°.

2. Statistical Theory (Hauser-Feshbach Formula)

As the excitation energy increases however, the level spacing rapidly decreases. At the same time, the probability for emission of the incident particle increases, and many new decay channels open up. These energy dependent partial widths must be added to the total width, and the result is that the total width rapidly increases as the excitation energy increases. For a sufficiently high excitation energy, the compound levels have begun to overlap. When this occurs, there is no guarantee that the independence hypothesis holds.

In order to re-establish the independence hypothesis, the assumption is usually made that in the region where many levels overlap and where the average total width is much larger than the average level spacing for a given angular momentum J and parity π ($\langle\Gamma^{J\pi}\rangle >> D_{J\pi}$), that the widths and phases of the partial amplitudes involved in the calculations are

randomly distributed and uncorrelated. Thus, when the contributions from many levels are summed, the cross terms will cancel, eliminating interference between different partial waves. The further assumption of random distribution of partial widths makes it possible again to separate the cross section into two parts, one corresponding to the formation of the compound nucleus, and the other to its decay. In this case the differential cross section may be written as (22)

$$\frac{d\sigma}{d\Omega}(a|a') = \frac{\lambda^2}{8}\sum\frac{(2J+1)}{(2I+1)}(-1)^{s-s'}\bar{Z}(\ell J \ell J; sL)\,\bar{Z}(\ell' J \ell' J'; s' L) \cdot P_L(\cos\theta) \cdot \frac{T^J_{a'\ell's'}\,T^J_{a\ell s}}{\sum T^J_{a''\ell''s''}} \tag{3}$$

which is the Hauser-Feshbach formula. Here $T^J_{a\ell s}$ is the transmission coefficient which represents the probability that the incident particle in channel a will be absorbed to form a compound state of spin J. The term $\sum T^J_{a''\ell''s''}$ is a sum of transmission coefficients for all competing channels a'' into which the particle can be emitted while conserving energy, parity, and angular momentum. From the properties of the $\bar{Z}$ coefficients we note that L is even so that the angular distribution is symmetric about 90°. The transmission coefficient can be written for the case where $\Gamma >> D$ as (25)

$$T^J_{a\ell s} = 2\pi\, S(\ell, J, E)\, P(\ell, E) \tag{4}$$

where the black nucleus penetrability $P(\ell, E)$ contains the size effect, and the strength function $S(\ell, J, E)$ contains the effect of the details of the

optical model. Under the black nucleus assumption $T^{J}_{a\ell s}$ is proportional to $P(\ell, E)$. $P(\ell, E)$ is given by

$$P(\ell, E) = \frac{kR}{F_\ell^2(kR) + G_\ell^2(kR)} \tag{5}$$

where F_ℓ (kR) and G_ℓ (kR) are the regular and irregular Coulomb wave-functions, where k is the wave number of the incident particle and R is the channel radius, defined as $R = r_o(A_T^{1/3} + A_P^{1/3})$ with $r_o = 1.3$ fermi, A_T = mass number of the target and A_P = mass number of the projectile. The integrated cross section for a given reaction under the assumption of many overlapping levels can be written as (22)

$$\sigma_R(a'|a) = \pi \lambda^2 \sum \frac{2J+1}{(2I+1)(2i+1)} \frac{T^{(J)}_{a'\ell's'} \; T^{(J)}_{a\ell s}}{\sum T_{a''\ell''S''}^{(J)}} \tag{6}$$

3. Fluctuations

It has been established theoretically and experimentally that, in nuclear reactions for which the excitation of the intermediate nucleus is high enough that the mean level width Γ is much greater than the mean level spacing D, fluctuations will occur in the reaction cross section. The theory of statistical fluctuations has been developed principally by Ericson, Brink, and Stephen. (25, 26, 27) The physical reason for the occurence of random fluctuations in the compound nucleus cross section is as follows: the statistical theory of nuclear reactions, as discussed in the previous section, rests on the assumption of independence of formation and decay.

This implies that the incident wave packet must have ceased interacting when the decay occurs. The interaction time is $T = \Delta x/v$ (Δx is the size of the incident packet, v its group velocity). Independence implies $\tau >> T$ (τ the lifetime of the compound nucleus). The uncertainty principle implies $\Delta_p = \hbar/\Delta x$ or $\Delta E = \Delta_p \cdot v$ for the incident packet. The compound lifetime also corresponds to an energy uncertainty Γ so we can write the independence requirement as

$$\tau = \hbar/\Gamma >> \frac{\Delta x}{v} = \hbar/\Delta_p \cdot v = \hbar/\Delta E \tag{7}$$

or

$$\Gamma << \Delta E \tag{8}$$

So there will be interference effects when this condition is not fulfilled. That is, the independence hypothesis may not hold for large Γ so that the incoming and outgoing partial waves can interfere, giving rise to fluctuations.

Ericson's theory (26) provides general formulas for the fluctuations and their interference with direct reactions in terms of correlation functions for the integrated and differential cross sections as well as for the B_L coefficients (see equation 24) in the Legendre expansion of the cross section. According to this theory the scattering amplitude, $S_{aa'}(E)$, from channel a to channel a' can be physically divided into two parts, one which varies slowly with energy, which is associated with direct interactions or, in the case of elastic scattering, with potential scattering, and one which is associated with a long lived compound system characterized by intermediate states i. Writing the scattering amplitude as in Feshbach's

unified theory of nuclear reactions (26) we get

$$S_{a\,a'}(E) = S^{(p)}_{a\,a'} + i \sum_i a_i / E - E_i \qquad (9)$$

where the states i have energy E_i and amplitudes a_i. Now one writes $a_i = \langle a \rangle + \delta_{a_i}$ which separates the average value from the fluctuating part of the amplitude. Then it can be shown that in the region of $\Gamma >> D$ one can write

$$S_{a\,a'}(E) = \langle S_{a\,a'} \rangle + S^{fl}_{a\,a'}(E) \qquad (10)$$

where $S^{fl}_{a\,a'}(E)$ is the fluctuating part of the scattering amplitude. Hence we see that the fluctuating compound contributions to the scattering matrix are associated with the fluctuations in the amplitudes. Now using the relation

$$\sigma_{a\,a'}(E) = \pi \lambda_a^2 \left| S_{a\,a'}(E) \right|^2 \qquad (11)$$

the average cross section can be written as

$$\langle \sigma_{a\,a'}(E) \rangle = \pi \lambda_a^2 \langle |S_{a\,a'}(E)|^2 \rangle = \pi \lambda_a^2 |\langle S_{a\,a'} \rangle|^2 + \pi \lambda_a^2 \langle |S^{fl}_{a\,a'}(E)|^2 \rangle$$

$$= \sigma_D + \langle \sigma^{fl} \rangle \qquad (12)$$

that is, a direct term and a fluctuating compound term.

Ericson has shown that the cross section $d\sigma / d\Omega$ at energy E will be correlated with the cross section at energy $(E + \delta)$ only if δ is less than or equal to Γ. A relative correlation function is defined as below

$$C(\delta) = F(E, \delta) / \langle \sigma(E) \rangle^2 \qquad (13)$$

where the notation $\langle\ \rangle$ indicates an energy average. $F(E, \delta)$ is the correlation coefficient defined as

$$F(E,\delta) = \langle (\sigma(E+\delta) - \langle\sigma(E)\rangle)(\sigma(E) - \langle\sigma(E)\rangle)\rangle \simeq \langle\sigma(E+\delta)\,\sigma(E)\rangle - \langle\sigma\rangle^2 \quad (14)$$

$C(\delta)$ may be written as

$$C(\delta) = \left[\langle\sigma(E)\,\sigma(E+\delta)\rangle / \langle\sigma(E)\rangle^2\right] - 1 \quad (15)$$

For a finite range of data it has been shown (29) that a better $C(\delta)$ is computed from

$$C_p(\delta) = \frac{\langle\sigma(E)\,\sigma(E+\delta)\rangle}{\langle\sigma(E)\rangle\langle\sigma(E+\delta)\rangle} - 1 \quad (16)$$

Writing the scattering amplitude as a sum of resonance terms of constant decay width $\Gamma >> D$ leads to the expression

$$C(\delta) = \Gamma^2/(\Gamma^2 + \delta^2) \quad (17)$$

However, direct interactions also lead to a reduction of fluctuations. If we call y_D the relative contribution of the direct amplitude to the cross section defined by

$$y_D = \sigma_D/\langle\sigma\rangle \quad (18)$$

then, assuming that the relative amount of direct interaction in each channel is equal, the resulting expression for $C(\delta)$ is (30)

$$C(\delta) = (1 - y_D^2)\,\Gamma^2/(\Gamma^2 + \delta^2) \quad (19)$$

In most nuclear reactions several amplitudes contribute simultaneously owing to the additional freedom associated with the spins of the particles and the nuclei. In this case the magnitude of the fluctuation effects is often reduced since the observed cross section is the sum of several partial cross sections. If we denote the spins of the projectile, emitted particle, initial nucleus, and final nucleus by i, i', I, and I', respectively, and the

projections along the incident direction by $\beta = m, m', M, M'$, then the differential cross section to a specific final state can be expressed as a sum of "basic" partial cross sections σ_β

$$\sigma = \sum_\beta \sigma_\beta \tag{20}$$

The partial cross sections are in general not independent. In particular, it follows from parity conservation that $\sigma_\beta = \sigma_{-\beta}$. It is therefore easily seen that the maximum number of independent partial cross sections consistent with this restriction is related to the total spin weight $g = (2i + 1)(2i' + 1)(2I + 1)(2I' + 1)$ by

$$N^{max} = (1/2)\, g \quad (g \text{ even}) \qquad N^{max} = (1/2)(g + 1) \quad (g \text{ odd}).$$

N is called the statistical damping factor. Introducing this effect into our expression for $C(\delta)$ results in (30)

$$C(\delta) = N^{-1}(1-y_D^2)\Gamma^2/(\Gamma^2 + \delta^2) \tag{21}$$

The angular cross correlation function defined by

$$C(\theta,\theta') = \frac{\langle \sigma(\theta,E)\, \sigma(\theta', E+\delta)\rangle}{\langle \sigma(\theta,E)\rangle \langle \sigma(\theta',E)\rangle} - 1 \tag{22}$$

and the group correlation function

$$C(a,a') = \frac{\langle \sigma_a(E)\ \ \sigma_{a'}(E+\delta)\rangle}{\langle \sigma_a(E)\rangle \langle \sigma_{a'}(E)\rangle} - 1 \tag{23}$$

are also useful in searching for group and angular cross correlations by examining the relative sizes of these coefficients for various groups and angles.

Another statistical test which can often provide information

about the amount of direct interaction contributing to the cross section has been discussed by Ericson. (26) An angular distribution can always be written as an expansion in terms of Legendre Polynomials

$$d\sigma/d\Omega = \sum_{L} B_L P_L(\cos\theta) \tag{24}$$

A correlation coefficient defined by

$$F(E,\delta) = \langle \sigma(E+\delta)\,\sigma(E)\rangle - \langle\sigma\rangle^2 \tag{25}$$

can also be written as an expansion in Legendre polynomials

$$F(E,\delta) = \sum_{L_1 L_2} F(L_1, L_2)\, P_{L_1}(\cos\theta)\, P_{L_2}(\cos\theta) \tag{26}$$

where δ and E are contained in the $F(L_1, L_2)$ coefficients. In the case for $\delta = 0$ it has been shown that (26)

$$F(L_1, L_2) = \langle B_{L_1} B_{L_2}\rangle - \langle B_{L_1}\rangle\langle B_{L_2}\rangle \ . \tag{27}$$

Ericson has shown that those values of $F(L_1, L_2)$ are zero for which $L_1 + L_2$ is odd for reactions in which there is no contribution from direct processes. Thus a comparison of the $F(L_1, L_2)$'s for $L_1 + L_2$ odd to those for which this is even can provide some indication concerning the mixture of the two mechanisms. This result is actually stating that the odd and even terms are uncorrelated. It follows that, while at any particular energy the angular distribution of statistical reactions is made up of two independent parts, one symmetric about 90 degrees, the other asymmetric, the asymmetric part will vanish when the angular distributions are averaged over a range of energies large compared to Γ. (26)

Finally, Stephen (28) has predicted a theoretical probability

distribution for the cross section with a statistical reaction and a direct reaction occurring together. This can be written as

$$\frac{dP}{d\eta} = \frac{N e^{-Ny_D/(1-y_D)}}{(1-y_D)} \left(\frac{\eta}{y_D}\right)^{(N-1)/2} \cdot e^{-N\eta/(1-y_D)} \cdot I_{N-1}\left[\frac{2N(\eta y_D)^{1/2}}{1-y_D}\right] \tag{28}$$

where $$\eta = \sigma(E) / \langle\sigma(E)\rangle$$

and I_n (arg) is the n^{th} order modified Bessel function of integral order and real argument. All other symbols have their previously defined meaning.

B. Direct Reactions

1. The Distorted Wave Born Approximation

We now leave the concept of the compound nucleus and go to the opposite extreme: direct reaction theory and the Distorted Wave Born Approximation (DWBA). The DWBA is an approximation used for describing a reaction in which a so called direct reaction mechanism is present. Such a treatment is possible due to the few degrees of freedom associated with the direct reaction assumption as discussed in section I. This calculation takes into account the distortion of the incoming and outgoing waves by the Coulomb and nuclear potentials. In addition to these interactions the direct reaction theory introduces as a perturbation an additional interaction which produces non elastic processes.

The basic expression for the transition amplitude in the dis-

torted wave theory for the reaction A(a, b) B is (31)

$$T = \int d\vec{r}_{aA} \int d\vec{r}_{bB}\, \phi^{(-)*}_{bB}(\vec{k}_b, \vec{r}_{bB}) \langle b, B | V | a, A \rangle\, \phi^{(+)}_{aA}(\vec{k}_a, \vec{r}_{aA}) \qquad (29)$$

for a particle a incident with relative momentum $\vec{k}_a$ and b emitted with relative momentum $\vec{k}_b$. The quantities $\phi^{(-)}$ and $\phi^{(+)}$ are the incoming and outgoing distorted waves, respectively. They are obtained by solving the elastic scattering problems in the entrance and exit channels using the optical model. The matrix element is for the interaction between the internal states of the colliding pairs and represents the effective interaction for scattering from one elastic scattering state to another. It contains the nuclear structure information.

In the case of the pick-up reaction, (He^3, a), 'a' is the alpha particle and 'b' is the He^3. The interaction is taken as V_{bx}, where x is the transferred neutron. Under the zero range approximation, the matrix element reduces to the product of the relative reduced width (spectroscopic factor), and the quantity

$$\psi_x(\vec{r}_{xA})\ D(\vec{r}_{bx}) \qquad (30)$$

where $\psi_x(\vec{r}_{xA})$ is the bound state wave function for the captured particle x in B, where B = A + x.

$$D(\vec{r}_{bx}) = V_{bx}(\vec{r}_{bx})\, \psi_a(\vec{r}_{bx}) \qquad (31)$$

which, in the zero range approximation is just $D_o\, \delta(\vec{r}_{bx})$, where D_o can be evaluated from the binding energy of the neutron in the alpha particle. Now $\psi_x(r_{xA})$ can be expanded as a core plus a neutron in some shell model orbit. In the language to be used below, this corresponds to a

choice of form factor. The differential cross section can be written (31) in the form

$$\frac{d\sigma}{d\Omega} = \frac{2s_a+1}{2s_A+1} \sum_{\ell sj} \frac{C D_o^2}{(2s+1)} \quad \sigma_{\ell sj}(\theta) \tag{32}$$

The computer code Julie (31) calculates the quantity $\sigma_{\ell sj}(\theta)$ given by

$$\sigma_{\ell sj}(\theta) = \frac{m_B^5 m_b m_a}{m_A^3 (m_a+m_A)(m_b+m_B)} \quad \frac{9.268}{k_b^3 k_a} \sum_m \left|\beta_{sj}^{\ell m}\right|^2 \tag{33}$$

where the $\beta_{sj}^{\ell m}$ factors are quantities which can be expressed in terms of the partial distorted waves $\chi_L(kr)$ and the form factors. The factor C is determined so that the first factor in the sum of equation (32) is the spectroscopic factor. In this form the characteristics of the particular reaction under study are expressed entirely in what are called radial form factors $F_{\ell sj}(r)$ which appear in the factors $\beta_{sj}^{\ell m}$ as an integral

$$\int dr_i \chi_{Lb}^{(b)}\left(\frac{m_A}{m_b} k_b r\right) F_{\ell sj}(r) \chi_{La}^{(a)}(k_a r) \tag{34}$$

For a pickup reaction if it is assumed that the neutron is in a definite orbital $N\ell$, then $F_{\ell sj}(r)$ is the radial wavefunction of the picked up nucleon.

The spectroscopic factor S is a measure of the probability that in the initial nuclear state all but one of the nucleons will arrange themselves in a configuration corresponding to the final state. It appears as the coefficients in the shell model expansion of the wave functions of the initial state in terms of the final state plus a nucleon. That is

$$V^{J_B}_{m_B}(\vec{\xi}_A, \vec{r}_n) = \sum_{\ell,j} \sqrt{S_{\ell,J}} \left[V^{J}_{m_J}(\vec{\xi}_A)\, \phi^{\ell}_{n}(\vec{r}_n) \right]_{m_B}^{J_B} \qquad (35)$$

where $\vec{\xi}_A$ are the intrinsic coordinates of the nucleus A and $\vec{r}_n$ is the neutron co-ordinate. In this notation B is the target for a pickup reaction. In equation (35), for simplicity we have neglected the spin of the captured neutron. These coefficients can be calculated from shell model theory for a chosen coupling scheme.

Bassel, Drisko, and Satchler (31) give the differential cross section for the (He^3, a) reaction as

$$\sigma(\ell, j) = 1.63\, S(\ell, j)\, \sigma_{jul}(\ell, j) \qquad (36)$$

Due to assumptions implicit to the formalism, the neglect of the internal wave functions of the He^3, the neglect of finite range, and the neglect of non-local effects, the absolute cross section is not correctly predicted. So one writes

$$\sigma_{ex}(\ell, j, E) = K(E)\, \sigma(\ell, j, E) \qquad (37)$$

with the factor K(E) assumed independent of ℓ and j, but not of bombarding energy. This factor was determined in our experiment by insisting that the ground state spectroscopic factor be equal to one, an assumption which results from viewing C^{13} in the jj coupling scheme as C^{12} plus a $p_{1/2}$ neutron.

2. The Optical Model

The full treatment of even so simple a process as elastic scattering is prohibitively complicated. Each nucleon in the incident

particle interacts with each nucleon in the target, and each of these interactions is a formidable complex of central, spin orbit, exchange, and tensor components. A complete treatment of the interaction between two nucleons is exceedingly difficult. The interaction between more than two nucleons cannot be attempted without a series of simplifying assumptions.

The initial development of the optical model was due to Fernbach, Server, and Taylor.(32) They analyzed the results of Cook, Macmillan, Petersen, and Sewell (33) and found that nuclei show considerable transparency to 90 MeV neutrons, in disagreement with the compound nucleus model. This led them to propose that the elastic scattering of nucleons by nuclei be compared with the scattering of a wave by a refracting and absorbing sphere. Classically, this may be represented by a complex refractive index. They were able to obtain a self consistent description of the total absorption cross-sections for the scattering of 90 MeV neutrons for a range of nuclei by estimating the refractive index from known nucleon-nucleon cross-sections.

The natural extension of these semi-classical studies of high energy scattering is to apply quantum-mechanical techniques and solve the Schroedinger equation appropriate to scattering by a complex potential. The first application to lower energies, with a full quantum mechanical solution of scattering by a complex potential, was made by LeLevier and Saxon in 1952. (34).

Since a generally satisfactory account of nucleon scattering can be obtained with the optical model, (35) it is natural to try to extend

it to the scattering of composite particles like deuterons, helium 3 nuclei, and alpha particles.

The nuclear and Coulomb interactions of the incoming and outgoing waves with the nucleus are described in the Distorted Wave Born Approximation by the Optical Model. The approach of the optical model is to replace all of the interactions of the incident nucleon with the nucleus by an average potential in the Schroedinger equation and to then solve the scattering problem. The potential is assumed to have a real part, which gives rise to elastic scattering, and an imaginary part, which represents absorption. The complex potential of the optical model is that potential which generates an elastic scattering amplitude equal to the energy average over the narrow compound nucleus resonances of the exact scattering amplitude. The successful interpretation of experimental results in terms of this model were first shown by Feshbach, Porter, and Weisskopf. (36)

In order to calculate the elastic scattering cross section we must find the amplitude of the outgoing waves for the elastic channel. So we must solve the Schroedinger equation with the potential being the optical potential.

$$\nabla^2\psi + \frac{2\mu}{\hbar^2}(E - U)\psi = 0 \tag{38}$$

The optical potential is taken to have the form

$$U = V(r) + V_{so}(r)\,\vec{\ell}\cdot\vec{\sigma} + i\left[W(r) + W_s(r)\right] + V_c(r) \tag{39}$$

where

$$
\begin{aligned}
V(r) &= -V\,(1+e^{x})^{-1} & x &= (r - r_o A^{1/3})/a \\
V_{so}(r) &= V_{so}\, f_{so}(x) & f_{so}(x) &= \left(\frac{\hbar}{mc}\right)^2 \frac{1}{r}\frac{d}{dr}\,(1+e^{x})^{-1} \\
W(r) &= -W(1+e^{y})^{-1} & y &= (r - r_g A^{1/3})/b \\
W_s(r) &= \mathcal{T}_4 \frac{d}{dy}\,(1+e^{y})^{-1} & & \qquad (40) \\
V_c(r) &= Z_a Z_A e^2/r\,, & & r \geq r_c A^{1/3} \\
&= \frac{Z_a Z_A e^2}{2 r_c A^{1/3}}\left(3 - \frac{r^2}{r_c^2 A^{2/3}}\right), & & r \leq r_c A^{1/3}
\end{aligned}
$$

3. The Optical Model Plus Resonance Formulation

The optical model potential is an average potential which has removed rapidly varying cross sections from the problem. The structure associated with the optical potential has a width of several MeV, and these so called single particle resonances are several MeV apart. For a range of data corresponding to a few MeV, therefore, the optical parameters are expected to vary smoothly with energy. A recent analysis (37) of the elastic scattering of protons by C^{12} showed that the optical parameters had to be varied drastically from energy to energy, a feature which contradicts the basic concept of the optical model. In an attempt to account for this energy dependence, Tamura has formulated and coded a scattering amplitude which is a sum of optical model and Breit-Wigner terms. The hope is that intermediate resonance like structure in elastic scattering

can be accounted for and possibly assigned quantum numbers. One might think of this amplitude as representing a background due to many overlapping resonances (optical part), plus an amplitude to account for an intermediate structure (eg. a doorway state) in the midst of the other states.

The scattering amplitude $S(\theta)$ may be written as (37)

$$S(\theta) = A(\theta) + B(\theta)\,(\vec{\sigma} \cdot \vec{n}) \quad \text{for } i = 1/2;\ I = 0. \tag{41}$$

where $\vec{\sigma}$ is the spin of the projectile and $\vec{n}$ is the unit vector perpendicular to the plane of scattering. And

$$A(\theta) = A_{op}(\theta) + \frac{1}{k}\sum_{\lambda} \exp(2i\sigma_\ell)\,\frac{R_\lambda + i\,I_\lambda}{(E-E_\lambda) + \frac{1}{2}i\Gamma_\lambda} \times \left[(\ell+1)\,\delta_{j,\ell+\frac{1}{2}} + \ell\,\delta_{j,\ell-\frac{1}{2}}\right] P_\ell^0(\cos\theta)$$

and

$$B(\theta) = B_{op}(\theta) + \frac{1}{k}\sum_{\lambda} \exp(2i\sigma_\ell)\,\frac{R_\lambda + i\,I_\lambda}{(E-E_\lambda) + \frac{1}{2}i\Gamma_\lambda} \times \left[\delta_{j,\ell+\frac{1}{2}} - \delta_{j,\ell-\frac{1}{2}}\right] P_\ell^1(\cos\theta) \tag{42}$$

where $A_{op}(\theta)$ and $B_{op}(\theta)$ are the usual optical scattering amplitudes. σ_ℓ is the Coulomb phase shift. The numerators of the resonance term $(R_\lambda + i\,I_\lambda)$ are assumed to be complex. The elastic scattering cross section $d\sigma(\theta)$ is obtained from equation (41) as

$$d\sigma(\theta) = 1/2\ \ Tr\ S^*(\theta)\,S(\theta) \tag{43}$$

C. The Eigenchannel Reaction Theory

In many situations the approximations discussed above are apparently quite good and relatively little nuclear structure information is required to describe reaction data. However, in general this is not

true. A technique for solving the continuum problem which does not necessitate any reaction mechanism assumption has been formulated by Danos and Greiner. (16) This is a technique by means of which the eigenstates of the S matrix, that is the eigenchannels (defined by the eigenvalue equation $SV^{(\alpha)} = E_{\alpha} V^{(\alpha)}$), can be computed directly. Considering only one particle open channels we begin by writing the assymptotic wave function as

$$\psi = \sum_c \left[A_c \mathcal{O}_c + B_c \mathcal{O}_c \right] \tilde{\psi}_c \tag{44}$$

where $\mathcal{O}_c$ and $\mathcal{O}_c$ are the radial parts of the incoming and outgoing particle in channel c, and everything else is in $\tilde{\psi}_c$, namely, the wavefunction of the A-1 system together with the angular parts of the projectile particle. Then all information about scattering is contained in B/A. So we define the S matrix via the relation

$$B_c = -\sum_{c'} S_{c\,c'} A_{c'} \tag{45}$$

Now we define the logarithmic derivative (b) of the radial wave function $f_c(x)$ as a function of the phase shift δ at the radius $r = a$

$$b = \frac{\partial \ln (f_c (kr))}{\partial \ln r} \Bigg| \quad r = a \tag{46}$$

For neutral particles $f_c(x)$ is given by

$$f_c(x) = \frac{x}{k} \left[\cos \delta j_{\ell}(x) - \sin \delta \, \eta_{\ell}(x) \right] \text{ where } x = kr \tag{47}$$

For charged particles the spherical Bessel functions are replaced by Coulomb functions. The value of a is determined by the requirement of channel orthogonality. (38)

We want to compute the scattering at energy E, momentum k.

So we guess a phase shift $\delta^{(1)}$ and compute $b^{(1)}$ using equations (46) and (47). Then solve

$$\left\{ \frac{d^2}{dr^2} - \frac{\ell(\ell+1)}{r^2} + \frac{2m}{\hbar^2} (E_\lambda - V) \right\} \phi_\lambda = 0 \tag{48}$$

with the boundary condition

$$\left. \frac{\partial \ln \phi_\lambda}{\partial \ln r} \right|_{r=a} = b^{(1)} \tag{49}$$

and repeat this procedure until we find some $E_\lambda = E$.

The self consistent values of $b = b^{(n)}$ obtained corresponds to what are called the natural boundary conditions and give the required value of the scattering phase shift δ. Denoting the amplitude of the standing waves of an eigenstate of the S matrix in the experimental channel c by $V_c^{(\beta)}$, the S matrix is given by

$$S_{cc'} = \sum_{\beta} V_c^{(\beta)} e^{2i\delta^{(\beta)}} V_{c'}^{(\beta)*} \tag{50}$$

a knowledge of $V^{(\beta)}$ and $\delta^{(\beta)}$ as functions of energy thus allows the complete description of all one particle reactions. The steps for such a calculation may be summarized as follows

1. At energy E the wave numbers k_c are obtained for all open channels from binding energies and the spectrum of the bound states of the daughter nucleus.
2. An eigenphaseshift δ is assumed.
3. The logarithmic derivative of the radial wavefunction in the assymptotic region in all open channels are computed at $r = a$.

4. Sets of single particle wavefunctions for the different channels are obtained for a real Saxon Woods potential using these logarithmic derivatives as boundary conditions.
5. Orthonormal sets of particle hole states are now constructed with these single particle wavefunctions and the Hamiltonian is diagonalized in the space of these particle hole states. The eigenvalues obtained are plotted as a function of δ for fixed E. The eigenphases are found as crossing points of an eigenvalue curve with the line E. The eigenphases are then plotted as a function of energy.

Of course the technique presented here has been restricted to single particle channels. However, the essential method can be generalized to many particle cases. (38) (39)

A case where the reaction is dominated by a single compound state should be describable by a single level Breit-Wigner formula. In the eigenchannel language this corresponds to the domination of the reaction by a single eigenchannel, which has at the resonance energy an eigenphase $\pi/2$. Then all other channels can be relegated to the background. In general all eigenchannels contribute comparably to the reaction amplitude, thus it is necessary to find all eigenchannels and all eigenphases.

Chapter IV

DATA ANALYSIS

A. The Distorted Wave Born Approximation

We begin by discussing the analysis of the angular distribution data at 5.0, 6.0, 7.0, and 8.0 MeV in terms of the DWBA assuming a pick-up mechanism. These angular distributions were taken in 5^{o} steps. The calculations were performed at the Oak Ridge National Laboratory using the DWBA code JULIE developed by Bassel, Drisko and Satchler. (31) The input for this calculation includes the optical potentials which describe the incoming and outgoing channel elastic scattering problems. A discussion of our analysis which resulted in the incoming ($C^{13}(He^{3}, He^{3})C^{13}$) channel parameters will be postponed until later. However, the outgoing parameters ($C^{12}(\alpha, \alpha)C^{12}$) were obtained from the work of Carter, Mitchell and Davis, (40) since the energies of the alpha particles could not be obtained with our accelerator. These parameters are somewhat ambiguous because of resonant structures in the alpha scattering from C^{12}. The parameters finally used were those obtained from off-resonance data. This same set has also been used by Kellogg (13) at 12., 15., and

18. MeV and found to be the best available. Other sets of parameters were tried for our data, but no improvement was seen to result. The outgoing parameter set is given below:

V	W	r_o	a	r_g	b	r_c	V_{so}	24
110.	0.0	1.87	0.5	1.87	0.3	1.22	0.0	16.0

where the energies are in MeV and the geometrical parameters are in fermis.

In addition to the entrance and exit channel optical parameters, the following quantities were used in the Julie calculations:

ℓ = orbital angular momentum of the picked-up neutron

j = total angular momentum of the picked-up neutron

N = radial quantum number of the picked-up neutron

B_N = binding energy of the picked-up neutron in the potential well prior to pick-up

S_a = spin of the incoming projectile

r_o, r_c, a = well parameters for the bound state neutron; nuclear radius, Coulomb radius, and diffusivity for the Saxon-Woods well

S = spin of the picked-up neutron

Q = the reaction Q value

r_c = lower cutoff of radial integration

The quantum numbers of the picked-up neutron for the transitions to the ground and first two excited states are quite well known from known spins and parities of the states involved and the shell model level scheme. Thus they should be p 1/2, p 3/2, and p 1/2, respectively.

Besides the work of Kellogg these values have also been tested in a $C^{13}(p,d)C^{12}$ reaction study. (41)

In using JULIE one must also specify the number of partial waves and the radial integration steps. It was found that 17 partial waves were sufficient for the entrance channel and 18 for the exit channel. The radial integration steps were specified according to the advice of Drisko and are known to be adequate. (42)

Finally, it was found that no fits were obtainable without the use of a lower cutoff. So the cutoff radius, r_c, became another free parameter. It was found that the results were very sensitive to the choice of lower cutoff, as shown in Figure 8. Values of this parameter were taken from 2.0 to 5.5 f in steps of .25 f. Upper cutoffs of 20 f were used for all calculations. The results of the 360 calculated angular distributions were compared to the measurements. The best fits along with the experimentally determined angular distributions are shown in Figures 9, 10, and 11. The error bars indicate the statistical error. The criterion used for the best fit was to emphasize the forward angle data. This appeared to be the most objective means of normalizing the data to the experiment.

Considerable effort was expended in attempting to keep the value of the lower cutoff parameter fixed for the various groups and energies when selecting the best fits. It has been suggested that the use of the lower cutoff tends to accentuate the relative contribution of the higher partial waves by suppressing the contributions in the nuclear interior which supposedly come primarily from the lower partial waves.

Figure 8. Cutoff Dependence of JULIE Calculation of $C^{13}(He^3, a)C^{12}$ Angular Distributions. The value of r_c, the cutoff parameter, is listed with each curve in fermi.

$C^{13}(He^3, \alpha_1) C^{12}$ at 7.0 MeV

UPPER CUTOFF 10. Fermi

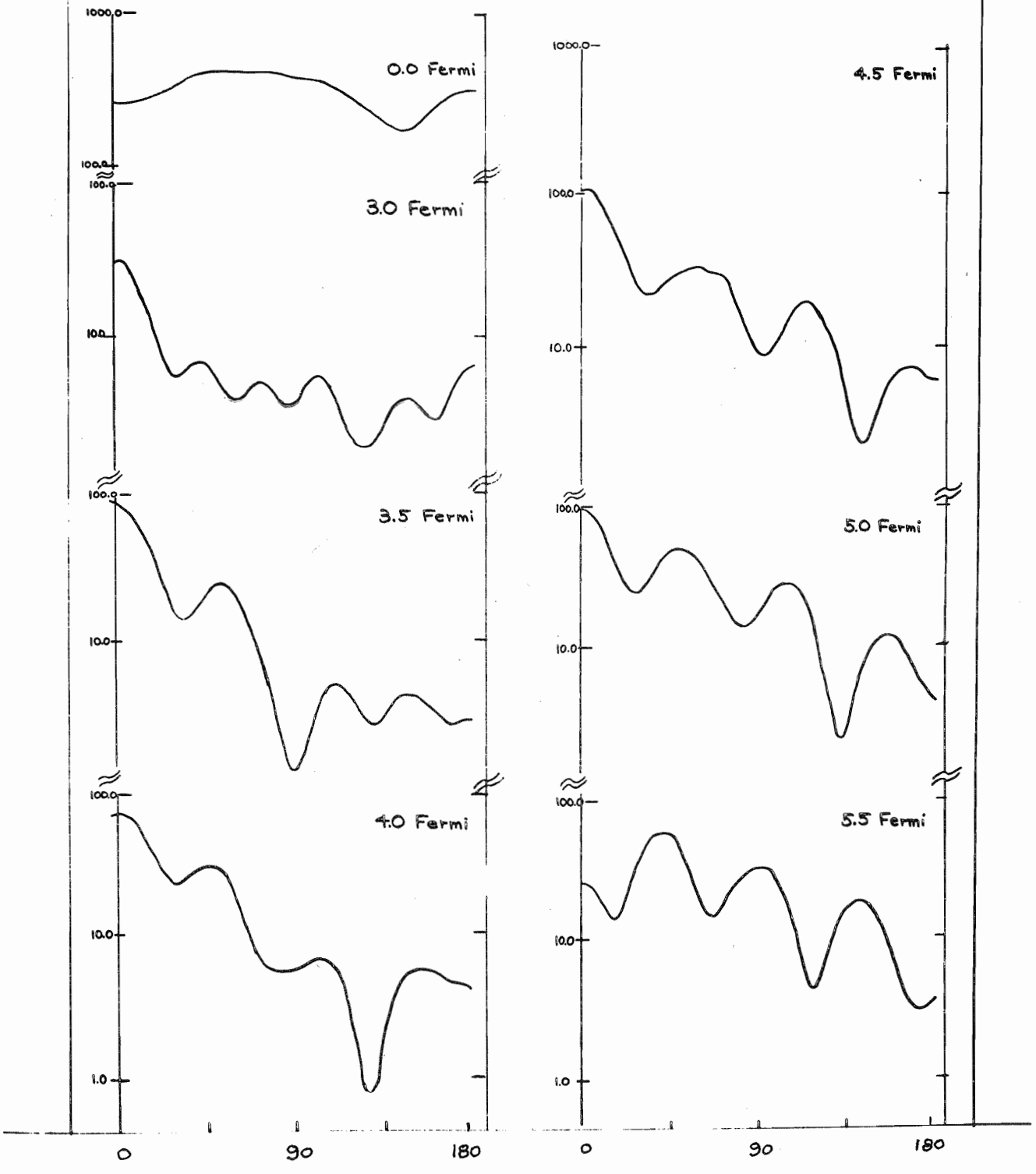

Figure 9. JULIE Fits to The Ground State α Particles

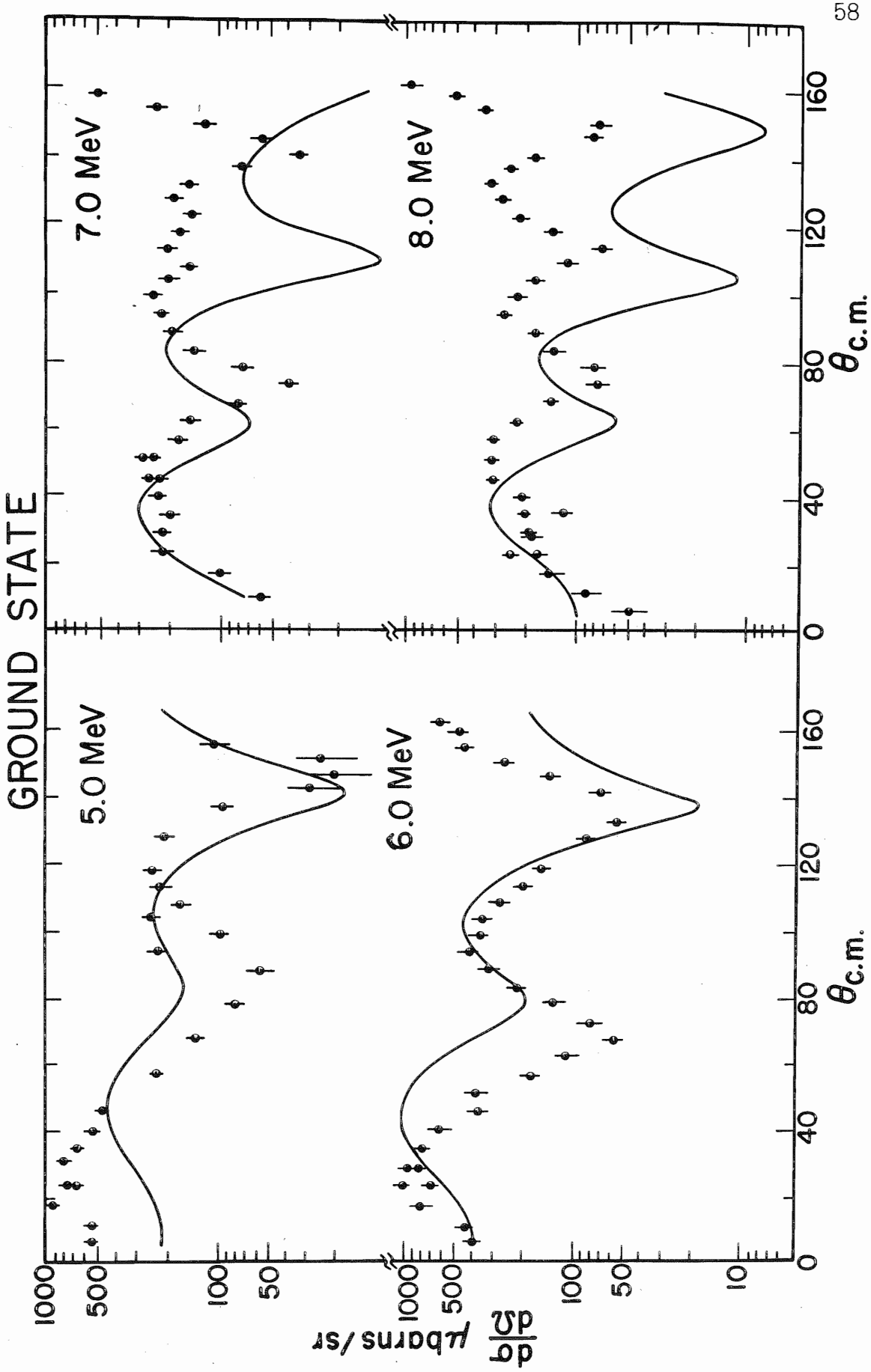
GROUND STATE
5.0 MeV
6.0 MeV
7.0 MeV
8.0 MeV
dσ/dΩ μbarns/sr
θc.m.
θc.m.
1000
500
100
50
10
0
40
80
120
160

Figure 10. JULIE Fits to The First Excited State Alpha Particles

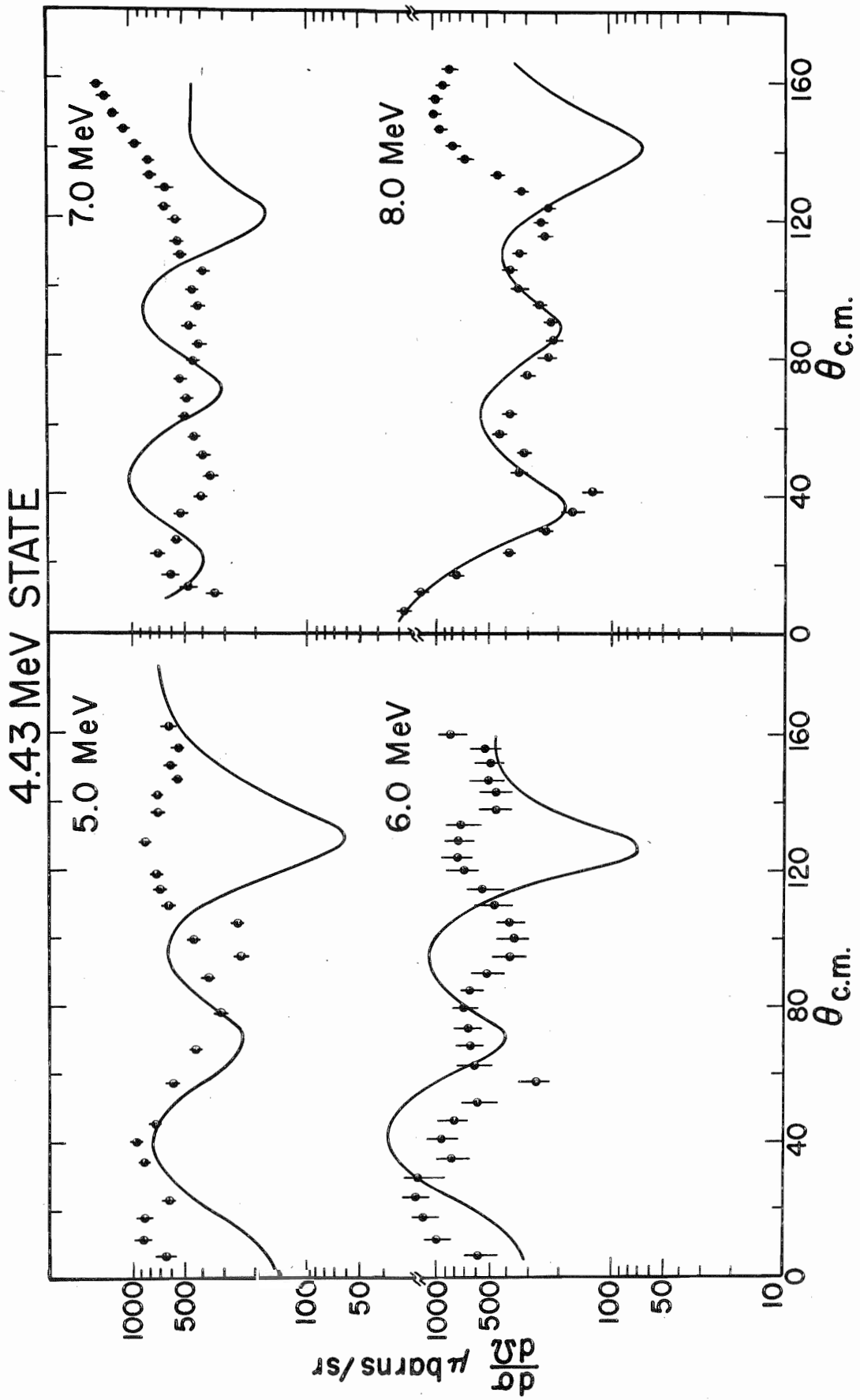
4.43 MeV STATE
5.0 MeV
6.0 MeV
7.0 MeV
8.0 MeV
dσ/dΩ μbarns/sr
θc.m.
θc.m.
1000
500
100
50
10
0
40
80
120
160

Figure 11. JULIE Fits to the Second Excited State Alpha Particles

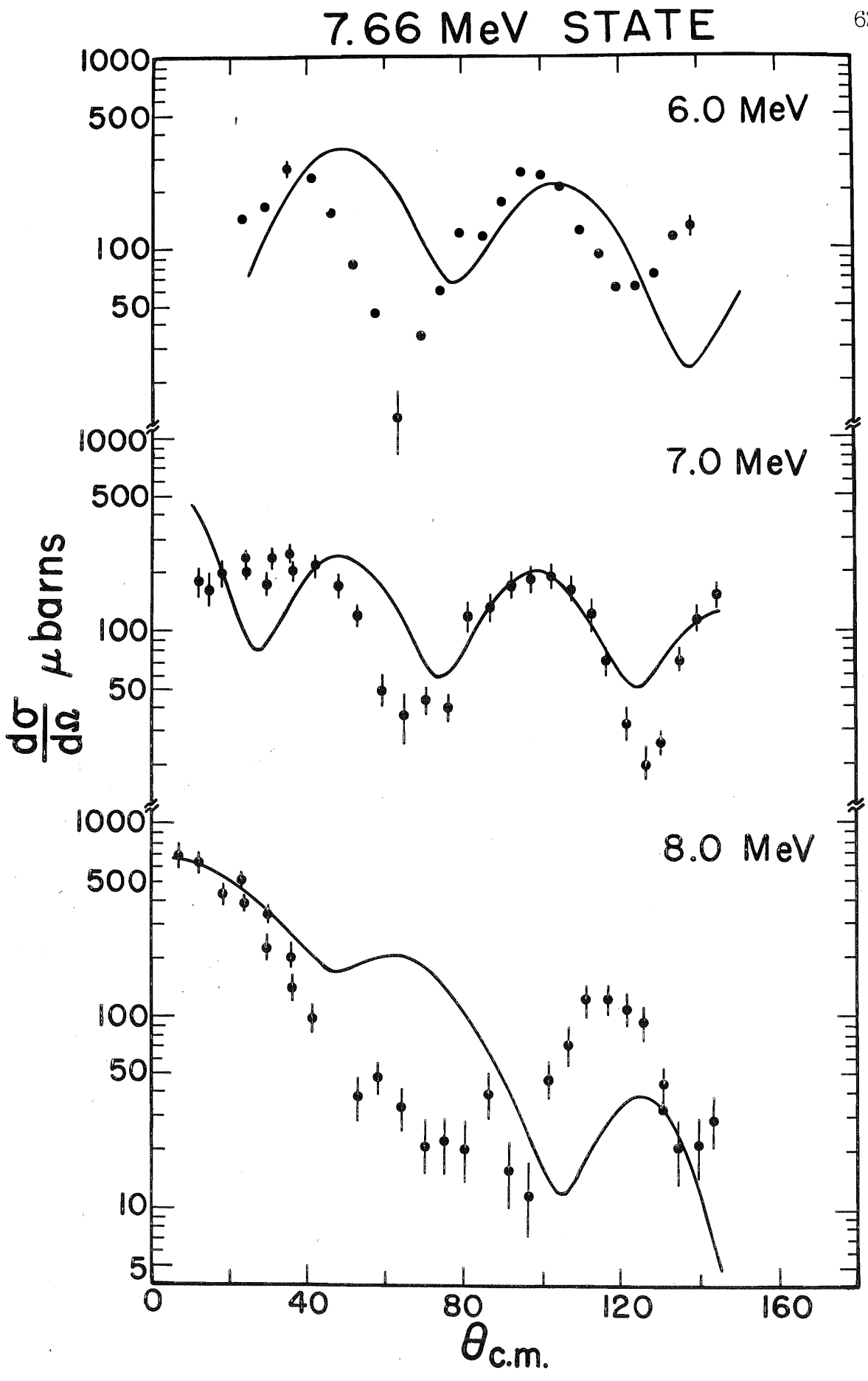
7.66 MeV STATE
6.0 MeV
7.0 MeV
8.0 MeV
dσ/dΩ μbarns
θc.m.
1000
500
100
50
10
5
0
40
80
120
160

However, when we examined the coefficients $\bar{\beta}_L$ which are the coefficients in the expansion

$$\beta^0 = \sum_L \bar{\beta}_L^0 P_L(\cos\theta); \beta^1 = \sum_L \bar{\beta}_L^1 P_L^1(\cos\theta); \sigma(\theta) = N\left[|\beta^0|^2 + 2|\beta^1|^2\right] \quad (51)$$

as a function of r_c, this was not found to be true. In many cases the lower partial waves became more important at higher values of r_c.

Buck and Rook (43) have suggested that the use of r_c simulates the effect of coupling to other channels than those taken account of in the usual DWBA calculation. However, it is important to realize that the use of r_c admits to the failure of the DWBA as formulated in code JULIE. (42) Allowing this parameter to be free permits one to obtain better fits to the experiment, but the meaning of the results is questionable. In fact, our studies show that a particular choice of r_c can set all even Legendre polynomials large, which means 90° symmetry. So that perhaps one is effecting a compound nucleus resonance in this way.

With these difficulties in mind we can take the best fits obtained and extract relative spectroscopic factors as defined in equation (36). In table 1 we have presented the factor K(E) necessary to make S = 1 for the ground state along with the resulting spectroscopic factors for the other two states. This choice follows from the assumption that the C^{13} ground state results from a p 1/2 neutron bound to a C^{12} core. A calculation of the relative spectroscopic factor for the first excited state has been reported by French and MacFarlane. (39) Their results are shown

Table 1. Relative Spectroscopic Factors, Radial Cutoffs and Normalization Factors from JULIE Fits

Cutoffs in Fermis					
Level J^{π}	E_{excit}	5.0 MeV	6.0 MeV	7.0 MeV	8.0 MeV
0^+	0	5.0	5.0	5.5	5.5
2^+	4.43	5.5	5.5	5.25	4.5
0^+	7.66	-	5.5	5.25	3.5

DWBA Spectroscopic Factors						
J^{π}	E_{excit}	S_5	S_6	S_7	S_8	$\langle S \rangle$
0^+	0	1	1	1	1	1
2^+	4.43	4.0	3.3	6.6	2.4	4.07
0^+	7.66	-	.83	3.3	2.4	2.18
	K(E) =	2.5	6.0	1.5	2.5	

$$(\sigma_{ex} = 1.63\ K(E) \times S\ \sigma_{JUL})$$

in Figure 12. We see that the results of our 8.0 MeV data correspond to a spin-orbit parameter of about .25, indicating intermediate coupling. The large value obtained for the spectroscopic factor for a_2 seems hard to explain. A pure jj picture of C^{13} implies that this value should be zero. So either there are configurations such as $p3/2^{-2}d5/2^{2}p1/2$ in the ground state of C^{13} or the mechanism is wrong. The relative spectroscopic factors obtained at 13. - 18. MeV by Kellogg are about 0.08, although these values are somewhat questionable due to the cut-off ambiguity. However, the values we find seem completely outside any explanation based on configuration mixing and so we can only conclude that the mechanism assumption as represented in JULIE is incorrect. It should be noted that at 6 MeV, a very large value of K(E) is necessary to make $S_o = 1$.

The failure of the DWBA as represented in code JULIE does not in itself rule out direct reactions for it may be that other modes are important. This would correspond to a different choice of form factor. However, for heavy particle stripping the zero range approximation used would be quite unreasonable. (31) Programs which perform distorted wave treatments for knock-out (45) and heavy particle stripping (46) modes are in preparation, but are not yet available. Plane wave formalisms are not considered to be useful, although much work has been done on adding plane wave modes. (11) However, the large number of free parameters make such calculations relatively unmeaningful, not to mention the large discrepancies usually found in the calculated values of spectroscopic factors.

Figure 12. Relative Spectroscopic Factors of French and MacFarlane as a Function of the Spin Orbit Parameter η . η is proportional to the strength of the $\ell \cdot s$ term in the shell model Hamiltonian.

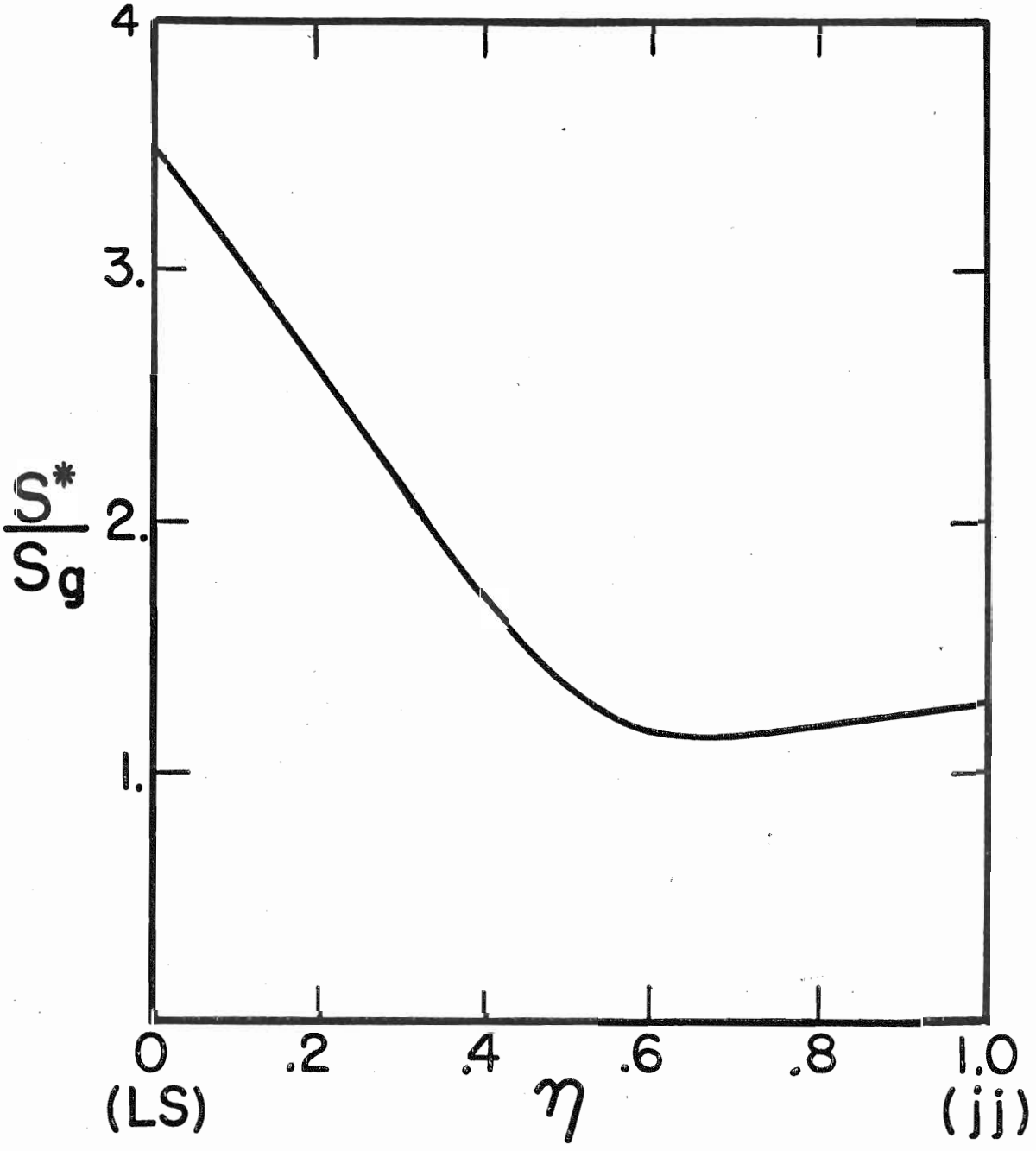
4
3.
2.
1.
$\frac{S^*}{S_g}$
0
(LS)
.2
.4
.6
.8
1.0
(jj)
η

B. Compound Nucleus Analysis

At this point we began to study the possibility of compound nucleus formation. The structure observed in the excitation curves shown in Figure 13 clearly indicates some non-direct processes. The solid lines shown in the figure are simple smooth lines drawn through the data. The observation of some uncorrelated structures and the high excitation energy ($\sim$ 27. MeV) of the compound nucleus O^{16} encouraged a statistical analysis. Previous work which analyzed $N^{15}(p,\alpha)C^{12}$ data at energies corresponding to an excitation of O^{16} at energies from 18.7 to 23.8 MeV has been performed by G. M. Temmer (14) and, more recently, by I. Nonaka et al. (15) at the somewhat higher energies of 21.5 to 26.0 MeV. Using the fluctuation theories as discussed in Section A, Part 3, Temmer found a value of Γ of 250 keV while Nonaka found a value of Γ of 400 keV. So we would expect a value of Γ slightly larger than 400 keV from our data since our energies are from 24.5 to 29.0 MeV in O^{16}. Arguments concerning the validity of the assumption $\Gamma >> D$ in this region were discussed in these papers and will not be repeated here. Due to our relatively poor statistical sample it was realized that the reliability of statistical quantities extracted from our data would be poor, however the general behavior of the data could be examined this way. Besides this we felt such an analysis could provide us with additional insight into the validity of the assumption $\Gamma >> D$ for our reaction.

This analysis began with a calculation of the correlation

Figure 13. Excitation Curves of a_o and a_1 at 30° and 90°.

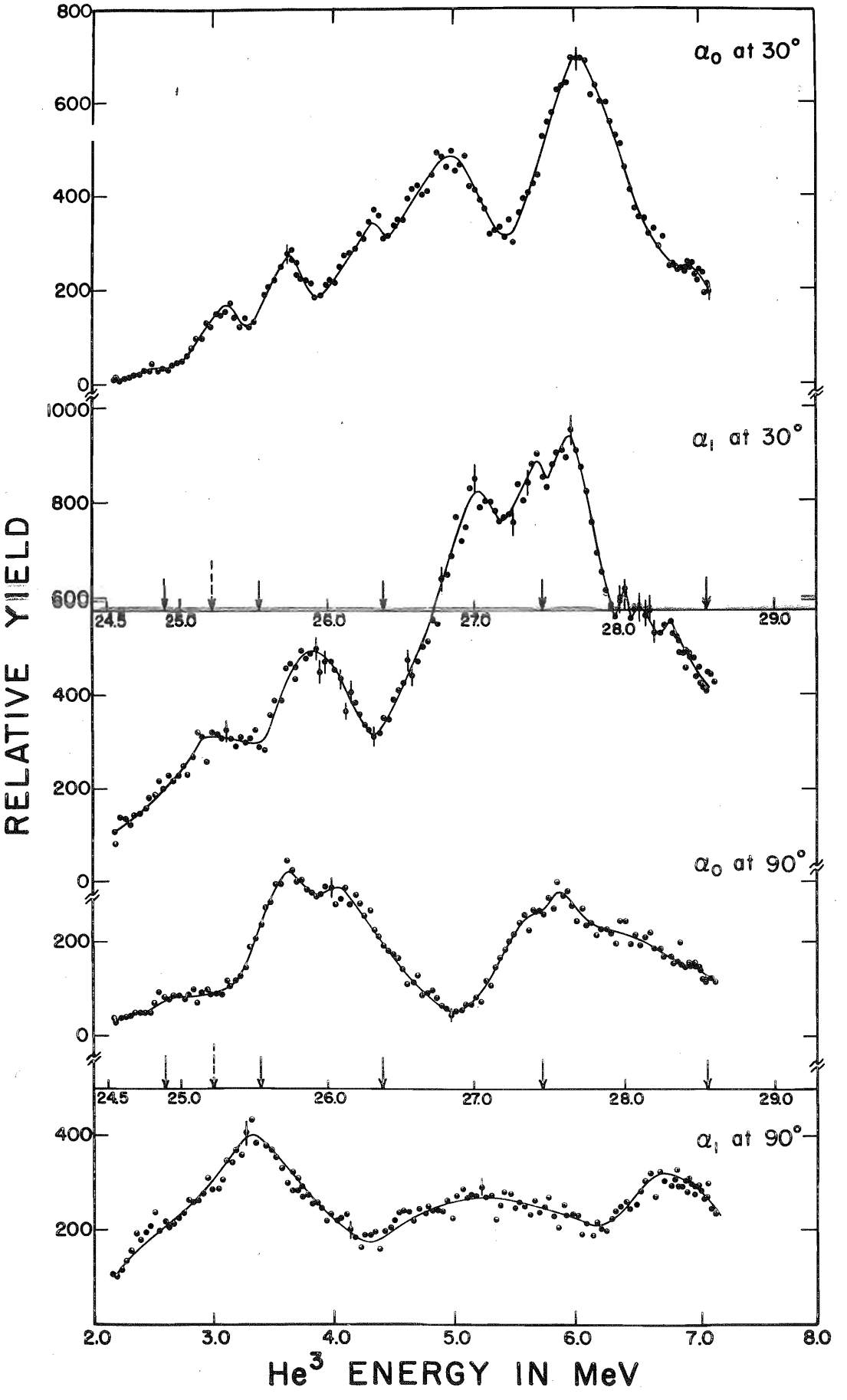
α_0 at 30°
α_1 at 30°
α_0 at 90°
α_1 at 90°
RELATIVE YIELD
He^3 ENERGY IN MeV
800
600
400
200
0
1000
800
600
400
200
0
200
0
400
200
24.5
25.0
26.0
27.0
28.0
29.0
2.0
3.0
4.0
5.0
6.0
7.0
8.0

coefficients: auto, group, and angular cross-correlations were computed and plotted as a function of delta according to equations (16), (22), and (23). The resulting auto correlation coefficients are shown in Figure 14a. The value of Γ (the self coherence energy) is obtained from these curves as shown. An average value of Γ of about 500 keV was obtained. The large variations in Γ may be due to our poor statistical sample.

With a coherence energy of about 500 keV a range of data of 10 gamma or 5.0 MeV could theoretically look as shown in Figure 14b. This curve was calculated by Dallmore and Hall (31) from the equation for the scattering amplitude (f(E))

$$f(E) = (2ik)^{-1} \sum_i \frac{(\gamma x \gamma)i}{(E-E_i + i\,\Gamma/2)} \qquad (52)$$

For the matrix elements $(\gamma x \gamma)i$ stochastic numbers were chosen which were real and had a normal distribution of mean zero and standard deviation unity. Equal level spacing was assumed. We observed the similarity in the structure obtained here and our data for a_o taken at 30°.

The group and angular cross correlation calculations told us what was apparent to the eye. Namely that there is a strong correlation between the 30° yield curves from a_o and a_1 around 6.0 MeV He^3 energy.

The next step in the statistical analysis was to calculate the probability distributions as prescribed by Brink and Stephen (see equation (28)). For this the so-called statistical damping factors N need to be estimated. The upper limit for N is 2 for a_o and 10 for a_1. Using these values and the relation

Figure 14. (a) Auto Correlation Coefficients

(b) Theoretical Excitation Curve of Dallmore and Hall.

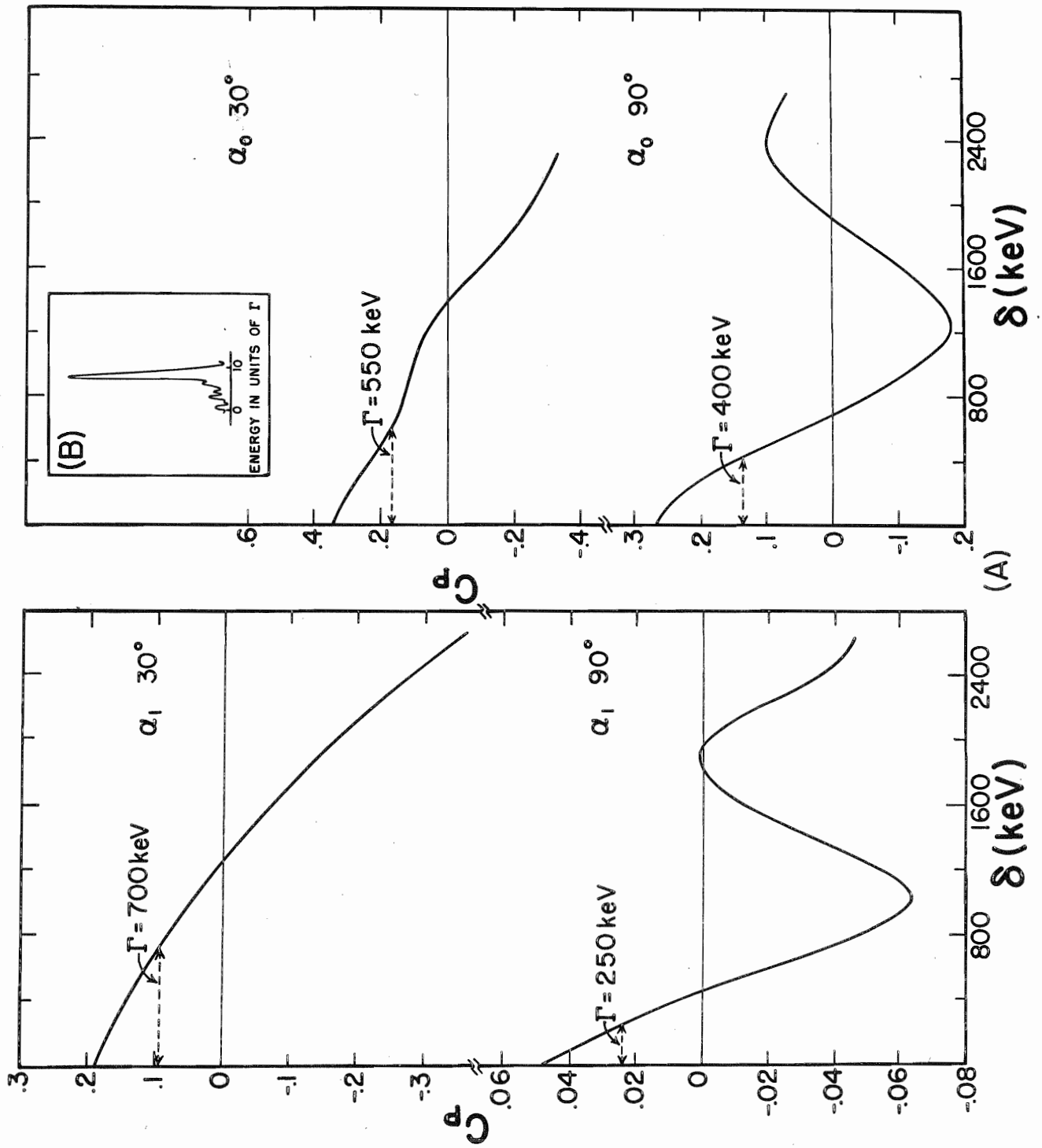
(A)
(B)
α_0 30°
α_0 90°
α_1 30°
α_1 90°
Γ = 550 keV
Γ = 400 keV
Γ = 700 keV
Γ = 250 keV
ENERGY IN UNITS OF Γ
δ (keV)
C_p

$$C(0) = 1 - y_D^2 / N \qquad (53)$$

with C(0) as determined from the previous auto correlation calculations, one can evaluate y_D for a given N. Of course, there is a degeneracy between N and y_D for the other values of N allowed, however, an upper limit on N of 2 does not leave much ambiguity in N. The fits are not sensitive enough to the various combinations to choose between them. Using values of N equal to the upper limit we obtained the fits shown in Figure 15. In the case of a_1 at 30^o the largest possible value of N is 5. Larger values give a negative number for y_D^2. The theoretical curve is essentially unchanged for N = 2, for which we have also indicated the value of y_D. The modified Bessel functions involved in this calculation were calculated using the integral representation and Gaussian integration. (47) The large values of y_D indicate that direct processes are responsible for a major part of the cross section.

Further statistical tests were possible at a later date when more data, namely measurements of angular distributions as a function of energy, were taken. These results, which again give good qualitative agreement, are postponed for discussion until those data can be presented.

According to Ericson: "two independent tests of the compound nuclear assumption are (a) that the ratios of partial cross sections to two residual states c_1' and c_2' depend only on the respective transmission coefficients $T_{c_1'}$ and $T_{c_2'}$ and (b) that the fluctuations are properly described." Having investigated (b) we now attempt to evaluate (a). Using

Figure 15. Probability Distributions of Excitation Curves. Histogram represents experimental data.

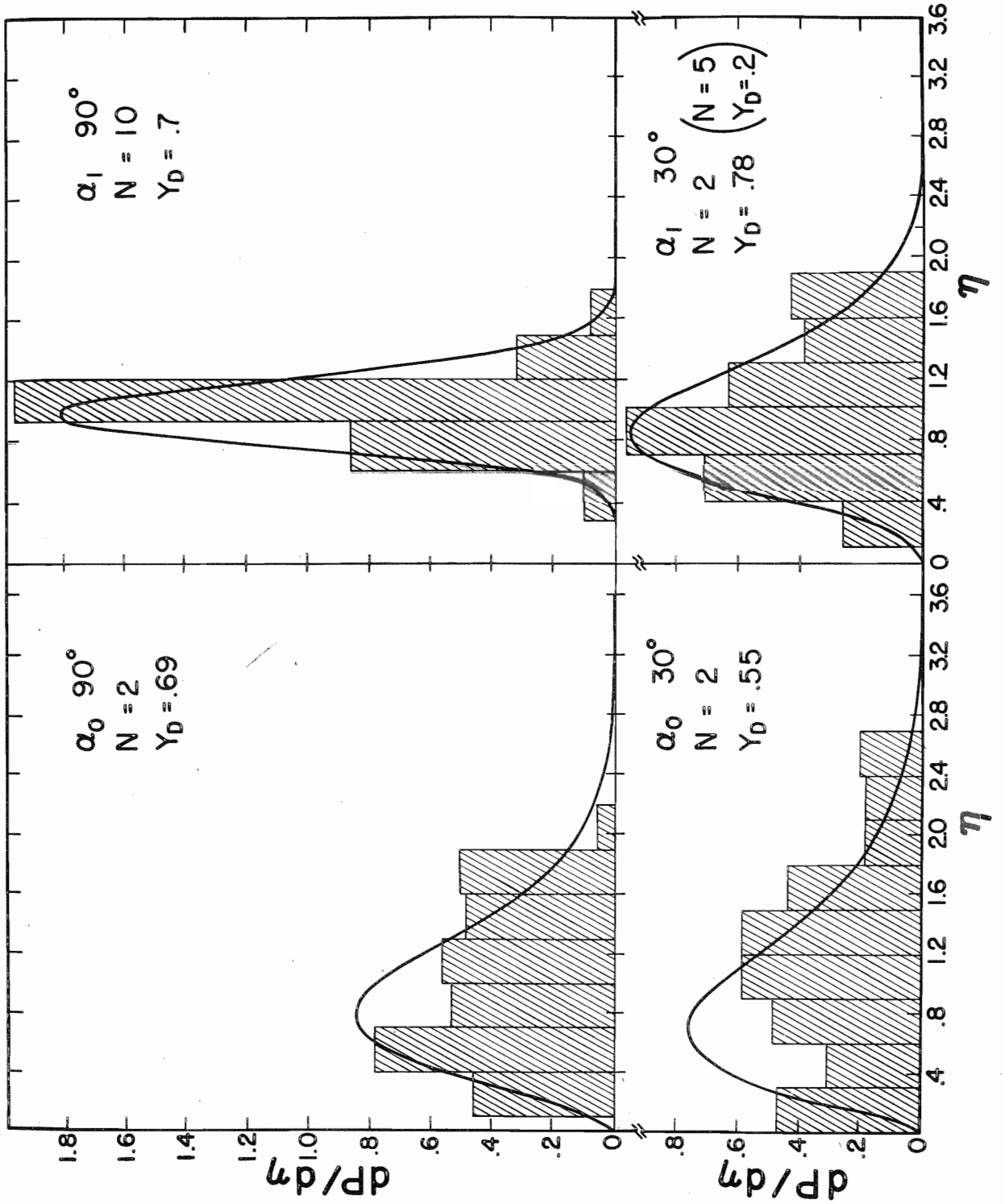
α_1 90°
N = 10
Y_D = .7
α_1 30°
N = 2 (N = 5)
Y_D = .78 (Y_D = .2)
α_0 90°
N = 2
Y_D = .69
α_0 30°
N = 2
Y_D = .55
dP/dη
η

the approximation that the transmission coefficients are proportional to the penetrability factors (48) defined as $P_\ell = \rho / F_\ell^2 + G_\ell^2$ where F_ℓ and G_ℓ are the Coulomb functions and $\rho = kR$ (R being the channel radius), we calculated the branching ratios for various values of J^π of the compound nucleus using the program of M. Gursky. (49) These are given below:

J^π	a_1 / a_o	a_2 / a_o
0^+	.86	.74
1^-	1.6	.73
2^+	2.4	.70
3^-	2.35	.67
4^+	2.26	.61
Average	1.9	0.69

The experimental values obtained by integrating the angular distributions are shown in table 2. Also included are the values obtained from Kellogg's data at 12., 15., and 18. MeV. Thus we see that we can understand the branching on the basis of Coulomb and angular momentum barrier effects alone. That is, a_o is greater than a_2 as a result of the Coulomb barrier, whereas a_1 is greater than a_o as a result of angular momentum conservation. Here we observe that the average value is not very different from a particular spin parity value so that if one spin dominated the cross section at a particular energy, the effect on the integrated cross section ratios could be small.

So we have found that apparently there is appreciable direct reaction present and that the statistical compound theory which takes this into account can give a general description of our data.

Table 2. Ratios of Measured Integrated Cross Sections. The values for 12, 15, and 18 MeV are taken from reference 13.

	6.0	7.0	8.0	12.0	15.0	18.0
a_2/a_o	.43	.70	.48	.61	.36	.33
a_1/a_o	2.0	2.8	1.5	2.8	2.5	2.2

Having provided this evidence for the validity of the statistical compound assumption we now make the following observations:

1. There is a strong correlation between the 30^{o} yield curves for a_o and a_1 at 6.0 MeV. Resonant structure of about 600 keV width appears at 6.0 MeV in the alpha zero curve.
2. The angular distributions for a_o and a_2 are of similar shape at 6.0 MeV.
3. The angular distributions at 6.0 MeV are closely symmetric about 90^{o}.

With these observations we now decided to attempt to fit the angular distributions at 6.0 MeV by assuming a single level. To do this we used the formalism of Blatt and Biedenharn (see equation (2·)). We began by assuming various values of J and attempted to get the observed shapes. It was found that a 3^- level could best account for the data. One has

$$\vec{s} + \vec{\ell} = \vec{J} = \vec{s'} + \vec{\ell'} \tag{54}$$

where the channel spin s is defined as

$$\vec{s} = \vec{i} + \vec{I} \tag{55}$$

where $\vec{i}$ is the spin of the projectile and $\vec{I}$ is the spin of the target. So for the case of $J = 3^-$ one has

$$s = 1 \qquad s' = 0$$
$$\ell = 2, 4 \qquad \ell' = 3 \qquad \text{for } a_o \text{ and } a_2$$

and

$$s = 1 \qquad s' = 2$$
$$\ell = 2, 4 \qquad \ell' = 1, 3, 5 \qquad \text{for } a_1$$

Because of the simplifications resulting from having only one partial wave in the outgoing channel, we first fit the data for the 0^+ transitions to fix

the amounts of $\ell=2$ and $\ell=4$ in the incoming channel. Assuming equal magnitudes and phases for these gave the shape for a_o shown in Figure 16. The calculated shape was normalized to fit the data. The fit to a_2 is now obtained if we set Γ (a_o 30/3$^-$)= 2 Γ (a_2 30/3$^-$) to give the proper normalization. The case for a_1 is more complicated. Making the simplest assumption of equal widths and phases for the $\ell = 1$, 3 and 5 contributions gave the shape shown in Figure 16. The number of parameters in a_1 make further searching meaningless. Besides it is clear that the deviation from symmetry implies a more complicated nature for this state. However, we see that these data behave quite alot like those for a reaction proceeding through a single level 3$^-$ state.

It was now decided that in order to determine if the 6.0 MeV structure is a resonance in the compound nucleus, data at more angles and for more channels were required to better establish the observed correlation. Thus we decided to take the (He^3, p) excitation curves at 30^o and 150^o using two lithium drifted silicon detectors. In addition, we obtained the He^3 elastic excitation curve using the proportional counter system. Finally, the $N^{14}(d,a)C^{12}$ data of Chaudri (50) was examined at energies corresponding to the same 27.6 MeV excitation in O^{16}. The results of these measurements are shown in Figures 17, 18, and 19. We have also included the (He^3, a_o) group at 30^o for comparison. Again, the solid lines are simple, smooth lines drawn through the data. The collected evidence for the resonant structure at 27.6 MeV is quite strong. Only the a_2 group at 30^o fails to show any structure at 6.0 MeV bombarding energy. However, as will be shown later, the total cross section for a_2 does show resonant structure at 6.0 MeV.

Figure 16. Single Level Fits to 6.0 MeV Angular Distributions.

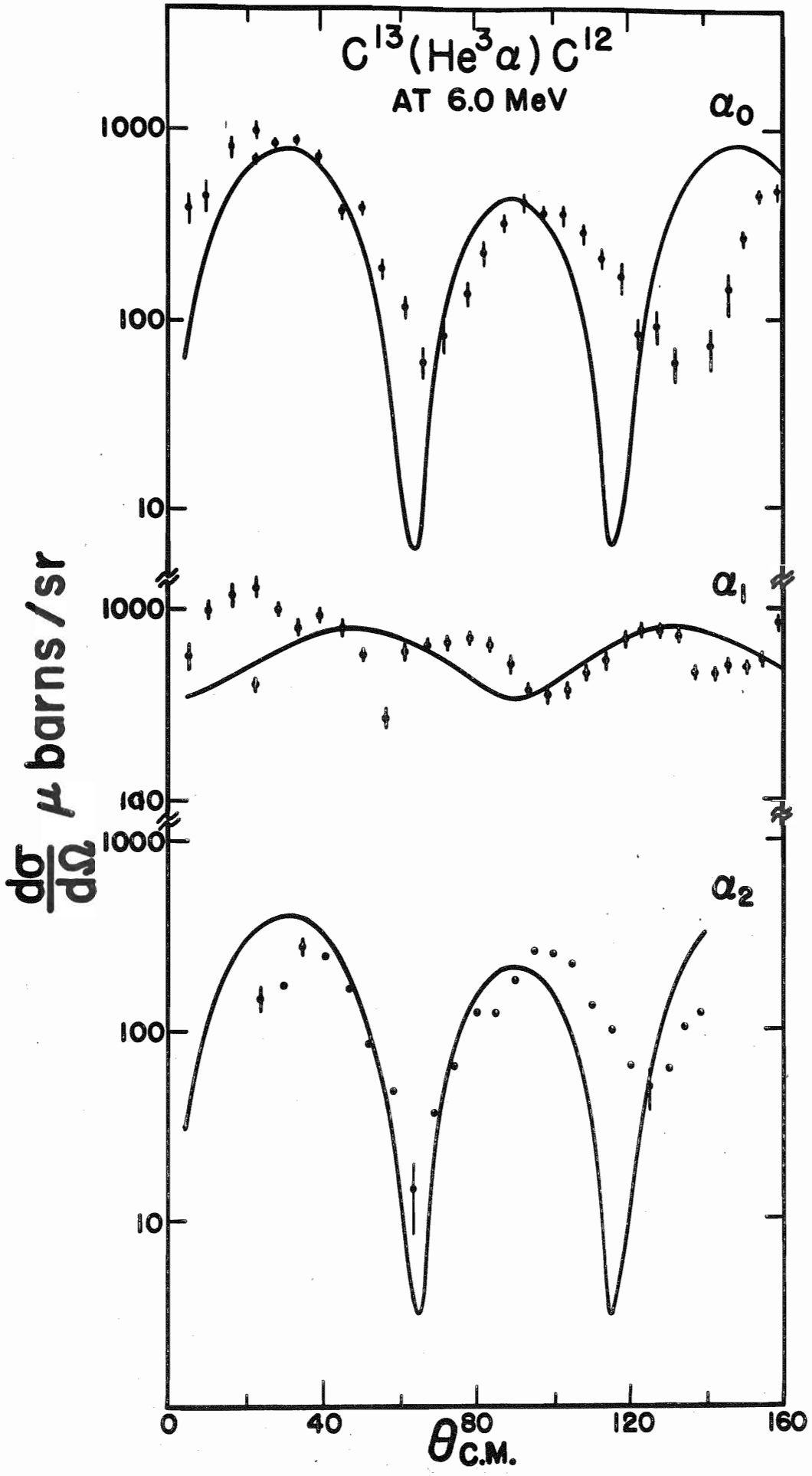
C13(He3α)C12
AT 6.0 MeV
α0
α1
α2
1000
100
10
1000
100
1000
100
10
dσ/dΩ μ barns/sr
0
40
80
120
160
θC.M.

Figure 17. Excitation Curves Showing 27.6 MeV State in O^{16}.

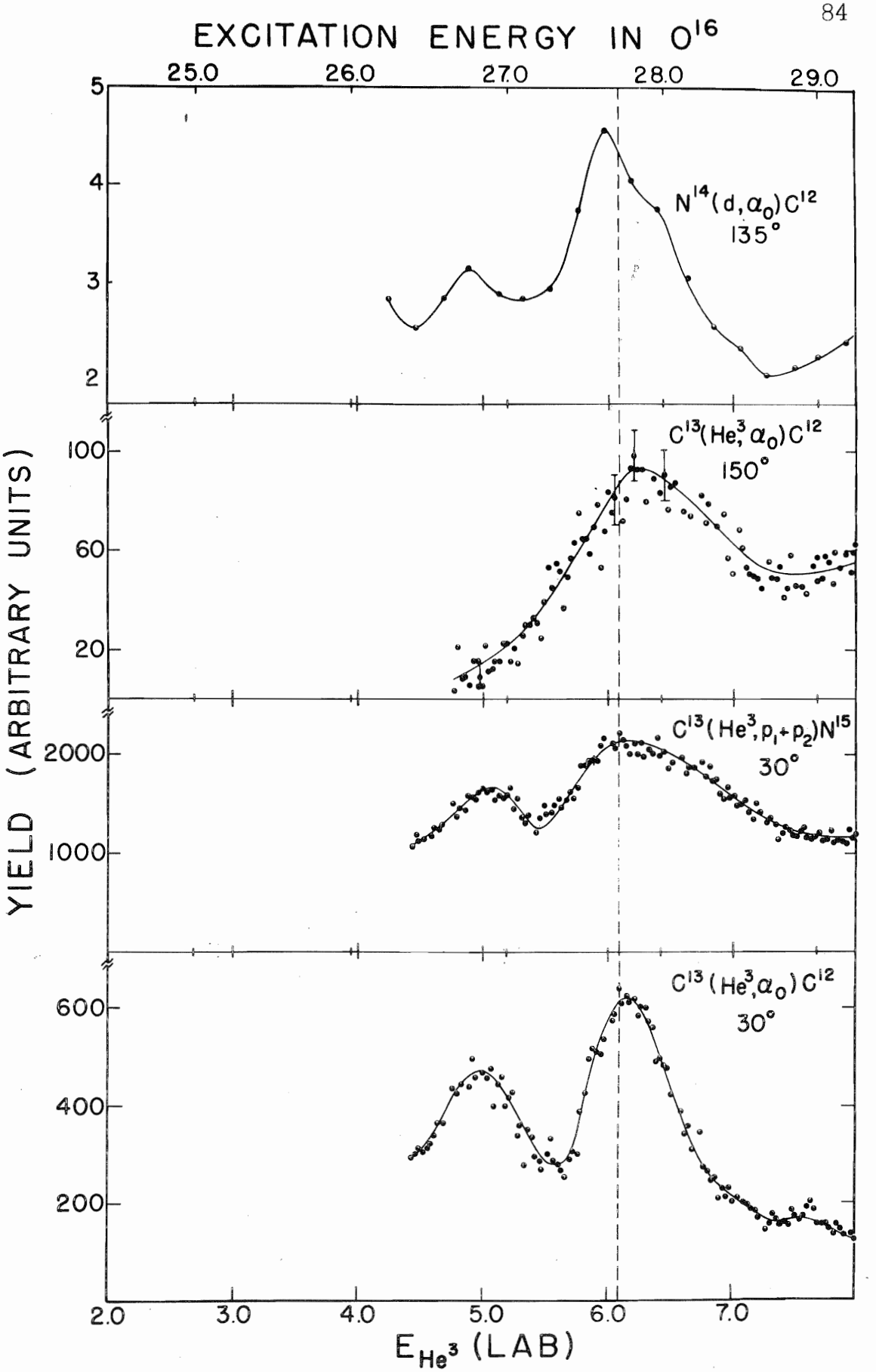
EXCITATION ENERGY IN O16
25.0
26.0
27.0
28.0
29.0
N14(d,α0)C12
135°
C13(He3,α0)C12
150°
C13(He3,p1+p2)N15
30°
C13(He3,α0)C12
30°
YIELD (ARBITRARY UNITS)
EHe3 (LAB)
2.0
3.0
4.0
5.0
6.0
7.0

Figure 18. Excitation Curves Showing 27.6 MeV State in O^{16}.

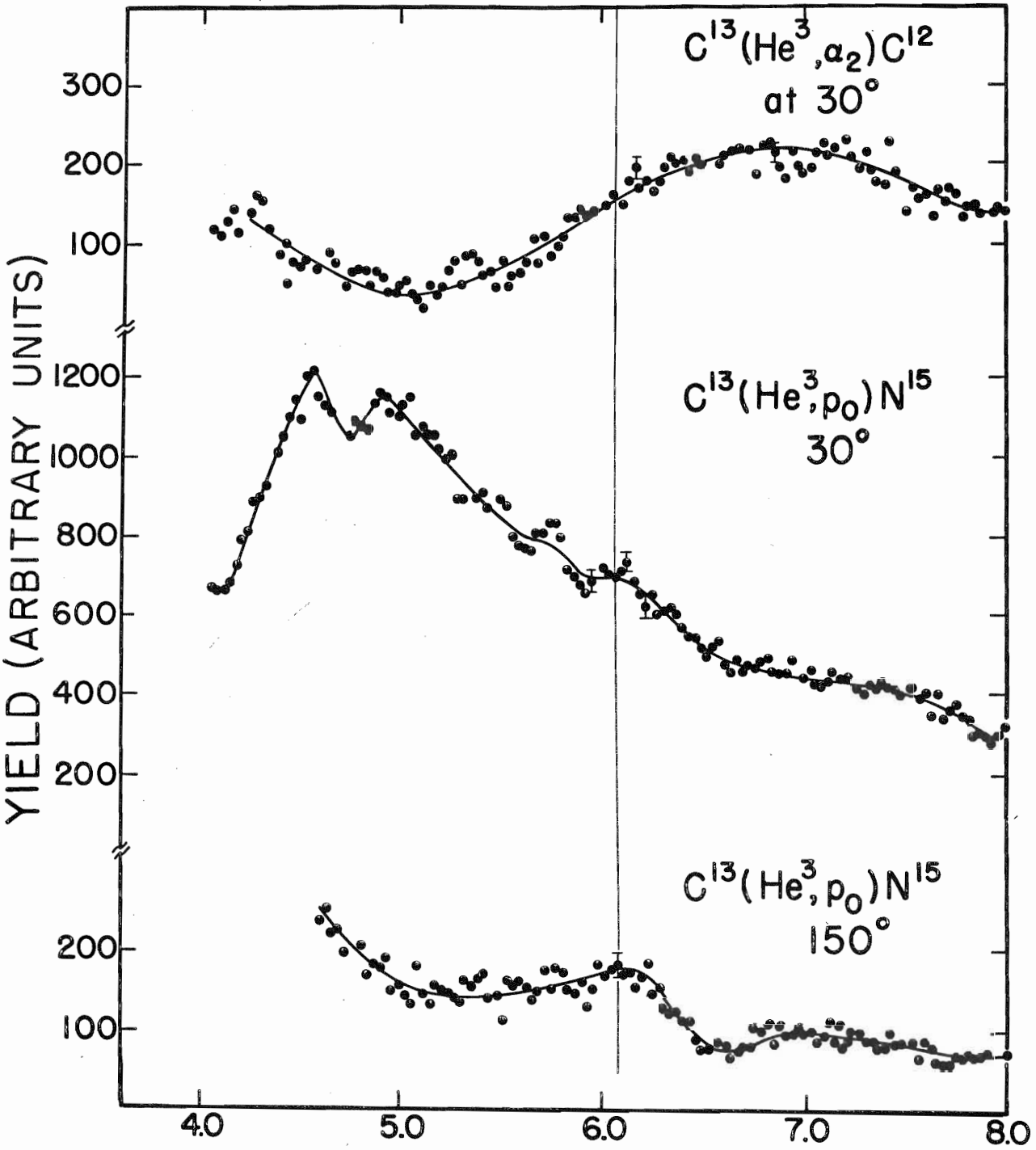
$C^{13}(He^3,\alpha_2)C^{12}$
at 30°
$C^{13}(He^3,p_0)N^{15}$
30°
$C^{13}(He^3,p_0)N^{15}$
150°
YIELD (ARBITRARY UNITS)
300
200
100
1200
1000
800
600
400
200
200
100
4.0
5.0
6.0
7.0
8.0

Figure 19. Excitation Curve for Elastic Scattering of He^3 by C^{13}.

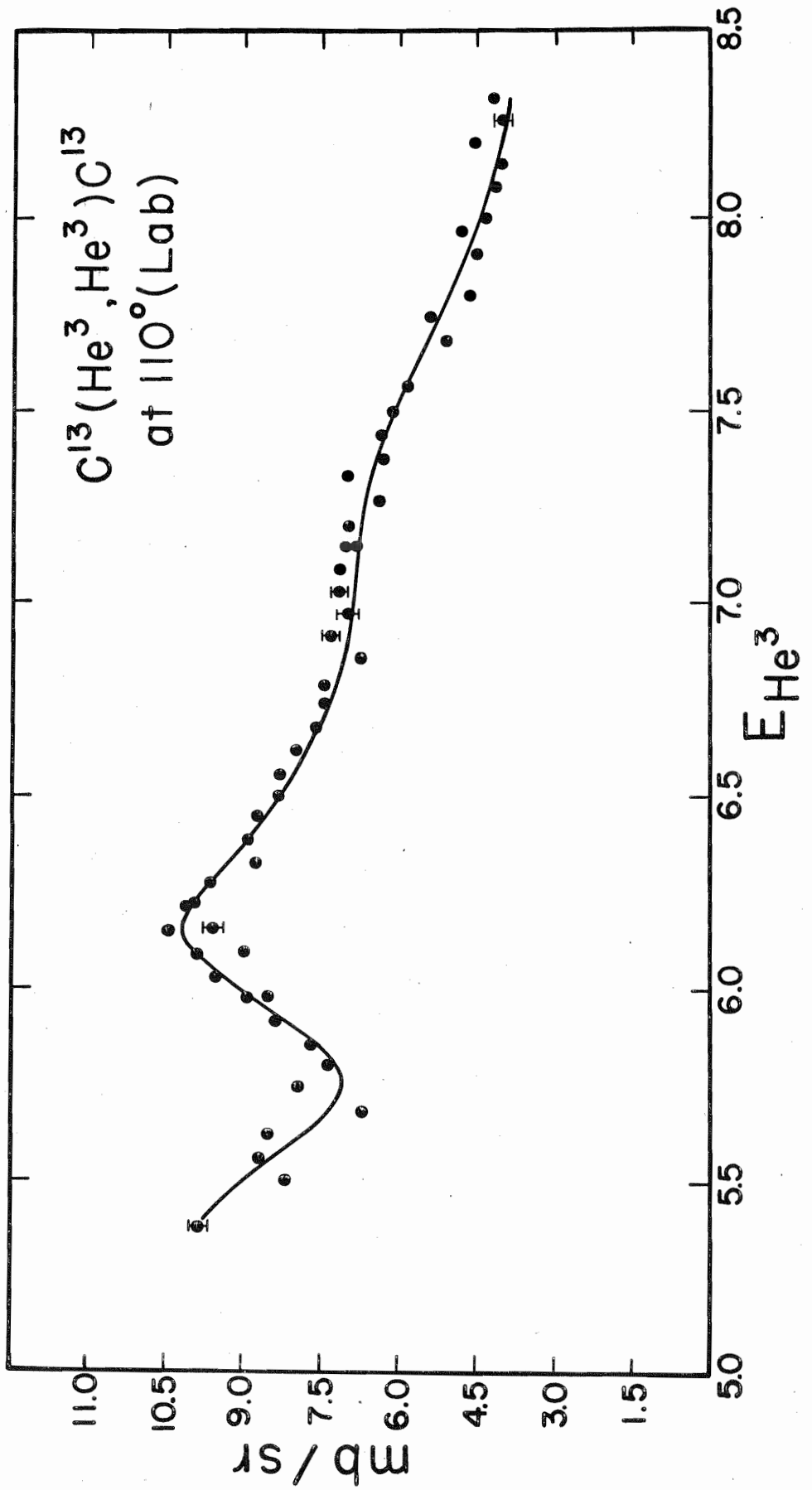
$C^{13}(He^3,He^3)C^{13}$
at 110°(Lab)
mb/sr
11.0
10.5
9.0
7.5
6.0
4.5
3.0
1.5
5.0
5.5
6.0
6.5
7.0
7.5
8.0
8.5
E_{He^3}

An interesting result of this analysis is with regard to so-called j dependence. (51) It was found that the ratios of the angular distributions of a_1/a_2 and a_1/a_o showed similar pronounced structure, whereas a_o/a_2 was relatively flat as shown in Figure 20. In this same reaction at 12. to 18. MeV it was observed that the a_1 data was relatively flat compared to a_o and a_2. Kellogg (13) suggested that this is a j dependence of the picked up neutron, j being 3/2 for a_1 and 1/2 for a_o and a_2. Here we see that from a compound nucleus viewpoint this effect at our energies can be attributed to angular momentum conservation. Namely for the 2^+ state more partial waves are allowed, which can have the effect of less rapid oscillations. A similar result would be expected to hold for a single level or for a collection of overlapping levels. In the statistical case this effect can be put in terms of the statistical damping factor N as has been discussed earlier. The same ratios of cross sections as predicted by the DWBA calculations are also shown in Figure 20. There is no agreement with the experimental ratios.

C. Optical Model Analysis

As was seen earlier in Figure 19, the elastic scattering excitation curve shows the effect of the proposed 3^- resonance. To investigate the energy dependence of the elastic scattering it was decided to perform an optical model plus resonance analysis. Before this was attempted, we carried out a simple optical model analysis of the 6.0, 7.0, and 8.0 MeV

Figure 20. Ratios of Angular Distributions of α Particles and Predicted Ratios from DWBA and Compound Nucleus Fits.

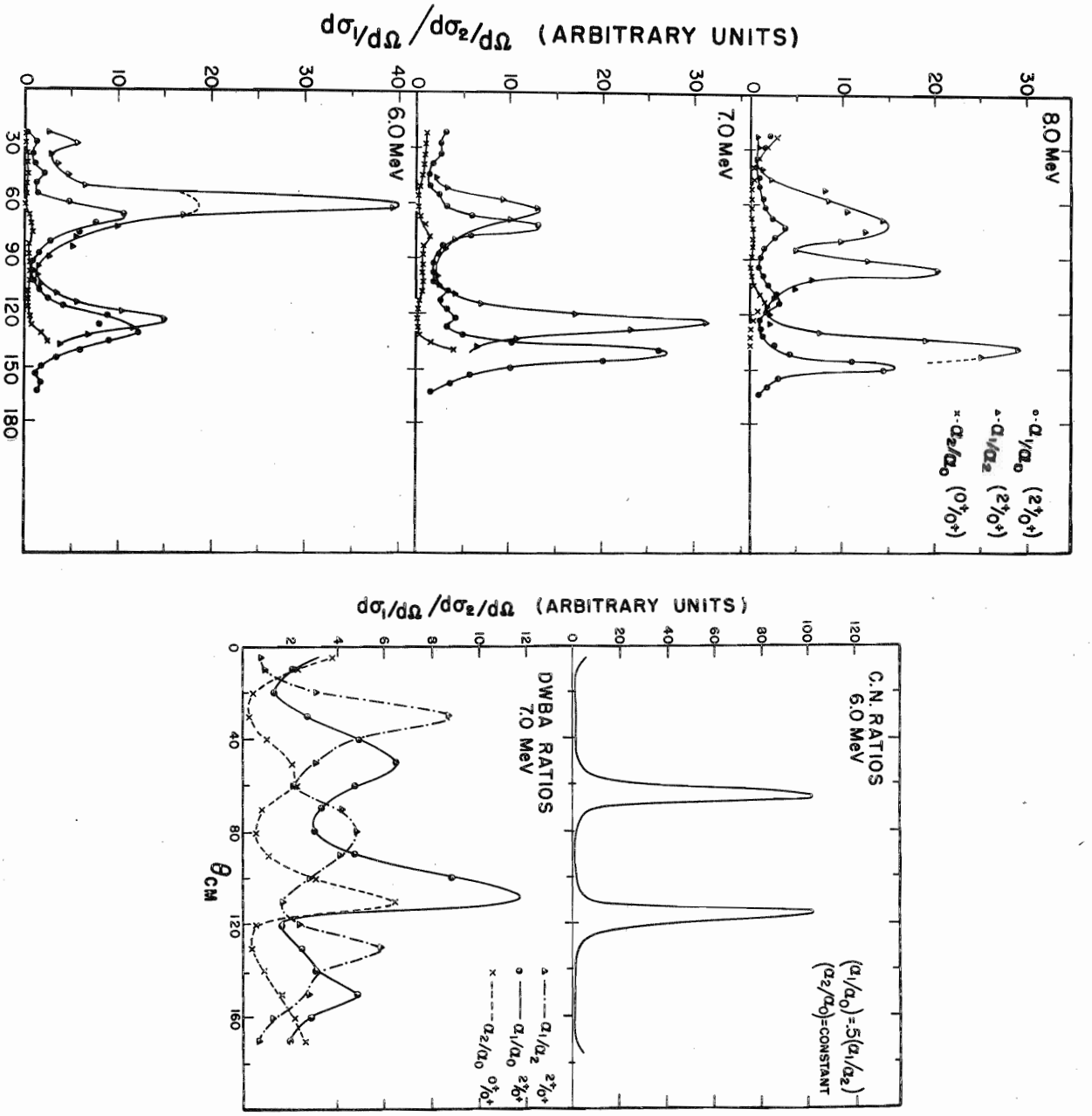
8.0 MeV
7.0 MeV
6.0 MeV
$d\sigma_1/d\Omega / d\sigma_2/d\Omega$ (ARBITRARY UNITS)
C.M. ANGLE
$\circ$-α_1/α_0 ($2^+/0^+$)
Δ-α_1/α_2 ($2^+/0^+$)
$\times$-α_2/α_0 ($0^+/0^+$)
C.N. RATIOS
6.0 MeV
$(\alpha_1/\alpha_0)=.5(\alpha_1/\alpha_2)$
(α_2/α_0)=CONSTANT
DWBA RATIOS
7.0 MeV
Δ —·— α_1/α_2 $2^+/0^+$
$\circ$ —— α_1/α_0 $2^+/0^+$
$\times$ - - - α_2/α_0 $0^+/0^+$
θ_{CM}

elastic scattering angular distributions. This served two purposes: first it provided the entrance channel parameters for our DWBA calculation, and second it gave us a guide in selecting the parameters to be used in the resonance analysis.

For the optical model analysis the computer code HUNTER develped by Drisko (42) was used at the Oak Ridge National Laboratory. A potential (see equation (39)) which provided independent geometry for the real and imaginary potentials was used. The HUNTER program accepts the experimental data for the elastic scattering as well as initial guesses at the parameters for some form of the optical potential. It then conducts a variation of these parameters, seeking to minimize χ^2 where

$$\chi^2 = \sum_i \frac{|\sigma_{ex(i)} - \sigma_{th(i)}|^2}{|\Delta \sigma_{ex(i)}|^2} \qquad (56)$$

The manner of the search is conducted in a specific way by the user. That is, one may vary any number of parameters in any desired order.

For our initial fit we decided to work with the C^{12} data at 8.0 MeV. This was because we had more confidence in the absolute cross section for the C^{12} data (since the technique for measuring target thickness here is quite straight forward). We took the optical parameters of Kellogg (13) for C^{13} at 12., 15., and 18. MeV and energy extrapolated V and W down to 8.0 MeV. Next a small correction was made to V to account for the symmetry term due to the one less neutron in C^{12} compared to C^{13}. This value of 2.0 MeV was suggested by Drisko. (42) A search was now

made with the initial set of parameters given by

$V = 162, \quad W = 4.43, \quad R_o = .93, \quad r_c = 1.4, \quad a = .81, \quad r_g = 2.25, \quad b = .65$

Only V, W, and r_g were allowed to vary. So we are using a three parameter search. An excellent fit to the C^{12} data at 8.0 MeV was obtained. Using these parameters as initial values, we found that a good fit could be obtained for the C^{13} data if it was normalized by a factor of 2. This factor could be accounted for because of the complicated technique employed in measuring the C^{13} target thickness. Searches were now conducted for the 6.0 and 7.0 MeV data for C^{12} and C^{13}. The results, which are rather satisfactory, are shown in Figure 21. The parameters for our data and for the 12., 15., and 18. MeV data are shown in table 3.

Some comments with regard to the parameters: first, the large value of r_g is thought to be a consequence of the fact that the He^3 particle starts interacting with the nucleus at a rather large radius, and second the energy dependence of V, i.e., decreasing with increasing E, can be explained as a result of averaging over nucleon-nucleon potentials. This average contains overlap integrals between the wave functions of the incident particles and the target nucleus, and decreases with increasing energy. Also the repulsive core becomes more important at higher energies, which acts so as to decrease the average interaction. (35)

The increase of W with energy is thought to be a result of the Pauli Principle. (35) Since states of low energy are filled first, there are more available states at higher energies, and thus W is greater. Finally, we found that the use of a spin orbit term did not improve the fits

Figure 21. Elastic Scattering Data for C^{12} and C^{13} and Optical Model Fits.

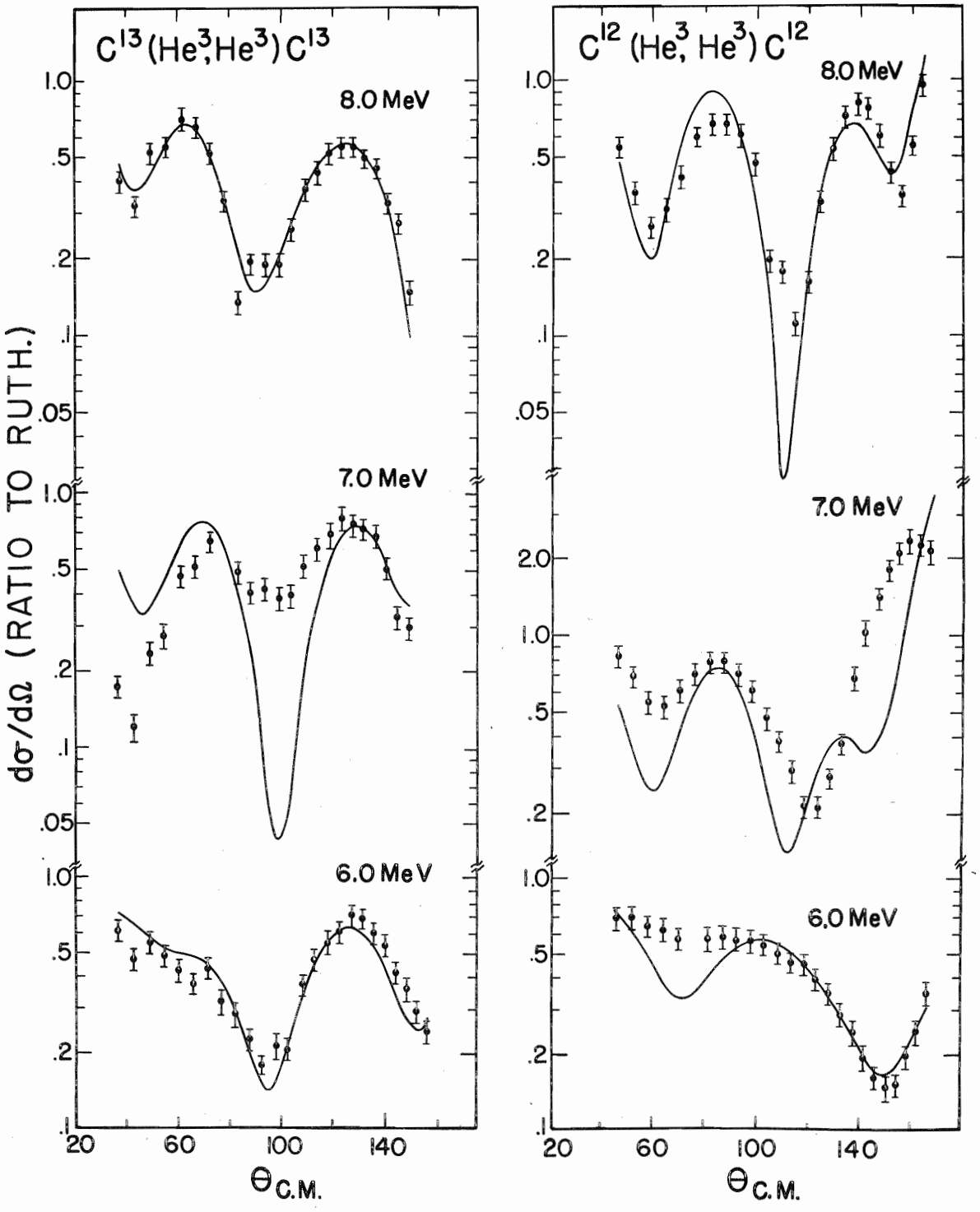
C13(He3,He3)C13
8.0 MeV
7.0 MeV
6.0 MeV
dσ/dΩ (RATIO TO RUTH.)
1.0
.5
.2
.1
.05
20
60
100
140
θC.M.
C12 (He3, He3) C12
8.0 MeV
7.0 MeV
6.0 MeV
2.0
1.0
.5
.2
.1
.05
20
60
100
140
θC.M.

Table 3. Optical Model Parameters. Here the parameters r' and a' are referred to in the text as r_g and b.

Optical Parameters $C^{13}(He^3, He^3)C^{13}$								
V	W	r_o	a	r'	a'	r_c	V_{so}	He^3 Lab Energy
156.	6.8	.93	.81	2.25	.65	1.4	6.	18.
158	6.75			2.25			6.	15.
161.	5.37			2.25			6.	12.
161.4	4.73			2.56				8.
156.5	2.45			2.75				7.
173.9	4.55			2.26				6.
$C^{12}(He^3, He^3)C^{12}$								
165.	4.43	.93	.81	2.05	.65	1.4		8.
165.2	4.43			1.90				7.
139.5	5.5			2.25				6.

obtained for our data, and so it was omitted.

Having obtained optical potentials which fit the C^{12} and C^{13} data in a reasonable way, we felt that we had a good optical potential. We now investigated the effects of adding a 3^- resonance to the optical potential to explain the energy dependence of the angular distributions. Although the optical model gave a good fit for the angular distribution, it does not account for the excitation curve taken at 110^o as shown in Figure 19.

To try to include this data in the analysis we used the program developed by Tamura for an optical model plus resonance analysis (as discussed in section B.3). We used the 8.0 MeV optical parameters from C^{13} and added a 3^- resonance (based on the results of our previous analysis of the alpha data). The 8.0 MeV parameters were chosen because they gave the most consistent results both with regard to the higher energy data of Kellogg, and our 8.0 MeV C^{12} data. Since we have a target of spin 1/2 and a projectile spin of 1/2, we can have $\ell = 2$ or $\ell = 4$ (i.e., d or g waves) involved. To account for this it was necessary to put in two resonance terms, a d wave and a g wave. This meant 6 parameters, two of which were approximately known. It was found that this amplitude could fit the data, but the fit was not an improvement over the pure optical model fit at 6.0 MeV. However, we then had a resonance structure in the excitation curve as well as a fit to the angular distribution, so that this amplitude does account for more data than a pure optical amplitude could. No statement can be made concerning the proof of the 3^- assignment from

this analysis, however, as the number of parameters is too large and too free to be able to single out a spin assignment. Our conclusion, then, is that although the proposed state appears in the elastic channel, its effect is not severe enough to study it with this approach using the available data. Perhaps measuring the elastic angular distributions in small ($\sim$ 100 keV) intervals as a function of energy will help to solve this problem.

With this experience in using the Tamura code, we now decided to attempt to account for the energy dependence in the excitation curve for C^{12} as shown in Figure 22 for a scattering angle of 140^{o}. There is an apparent broad resonance at 7.0 MeV. Here the optical model was not able to account for the back angle peaking in the angular distribution data at 7.0 MeV. Besides, C^{12} has spin zero, so that the number of parameters is two less than in the case of C^{13}.

Here again we took the 8.0 MeV optical potential, this time for C^{12}. We then tried searching for various values of ℓ. It was found that a p wave could give the best fit to the 7.0 MeV angular distribution. The results are shown in Figure 23. Therefore, there is apparently a $3/2^{-}$ or $1/2^{-}$ state in O^{15} near 17.5 MeV.

In the initial fit of the angular distribution we had put $\Gamma = 1.2$ MeV. When we calculated the elastic scattering as a function of energy we found that the shape at 140^{o} was too wide. In order to improve this we re-calculated the resonance parameters so as to keep the angular distribution on top of the resonance the same, but for different values of Γ. We then ran Tamura's program for various Γ's to get the best agreement

Figure 22. Excitation Curve of $C^{12}(He^3, He^3)C^{12}$ Elastic Scattering at 140°.

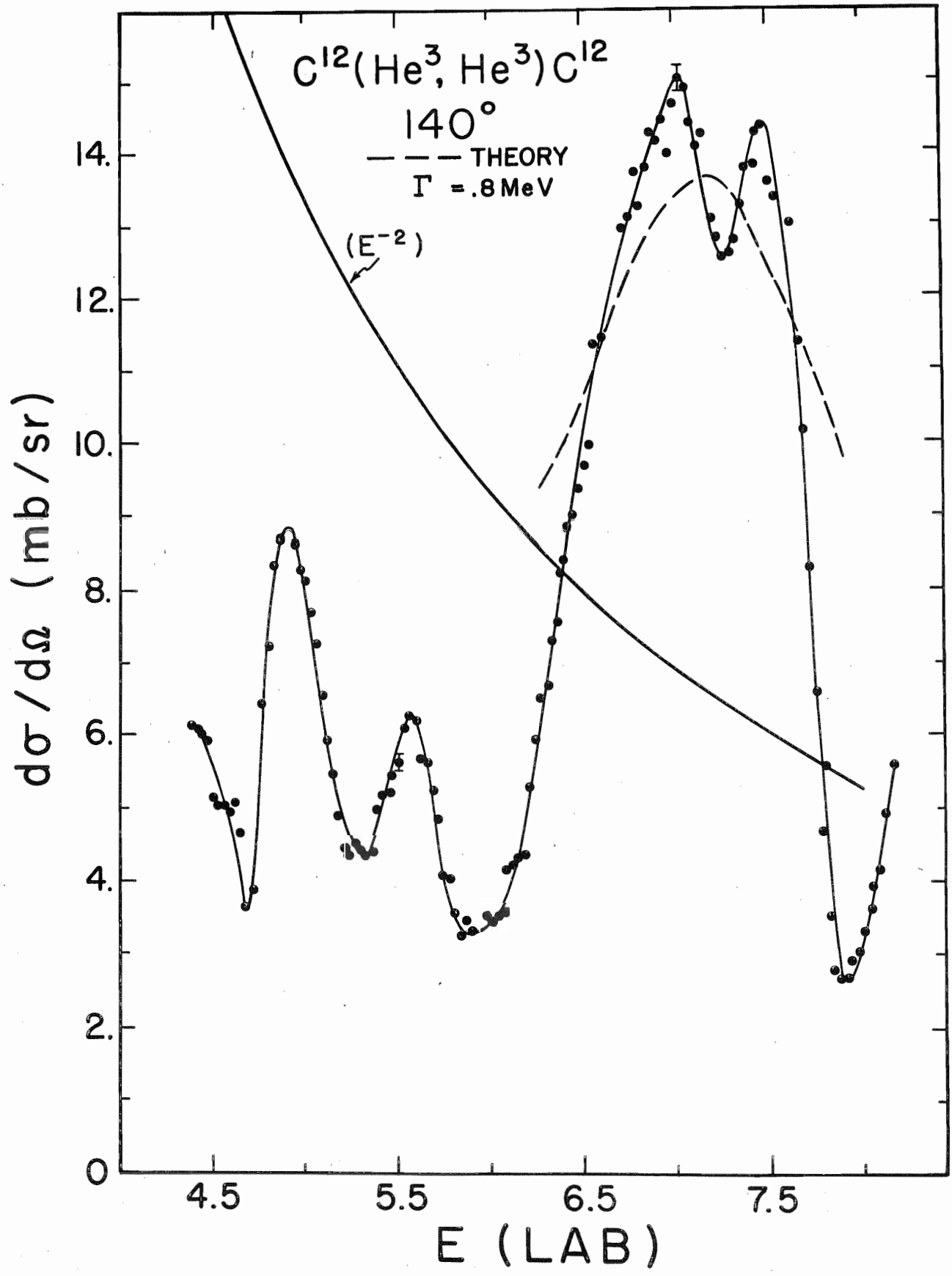
C12(He3, He3)C12
140°
— — — THEORY
Γ = .8 MeV
(E-2)
dσ/dΩ (mb/sr)
E (LAB)
0
2.
4.
6.
8.
10.
12.
14.
4.5
5.5
6.5
7.5

Figure 23. Experimental Data and Theoretical Fit for a p Wave Resonance Plus Optical Model Amplitude for 7.0 MeV He^3 Elastic Scattering from C^{12}.

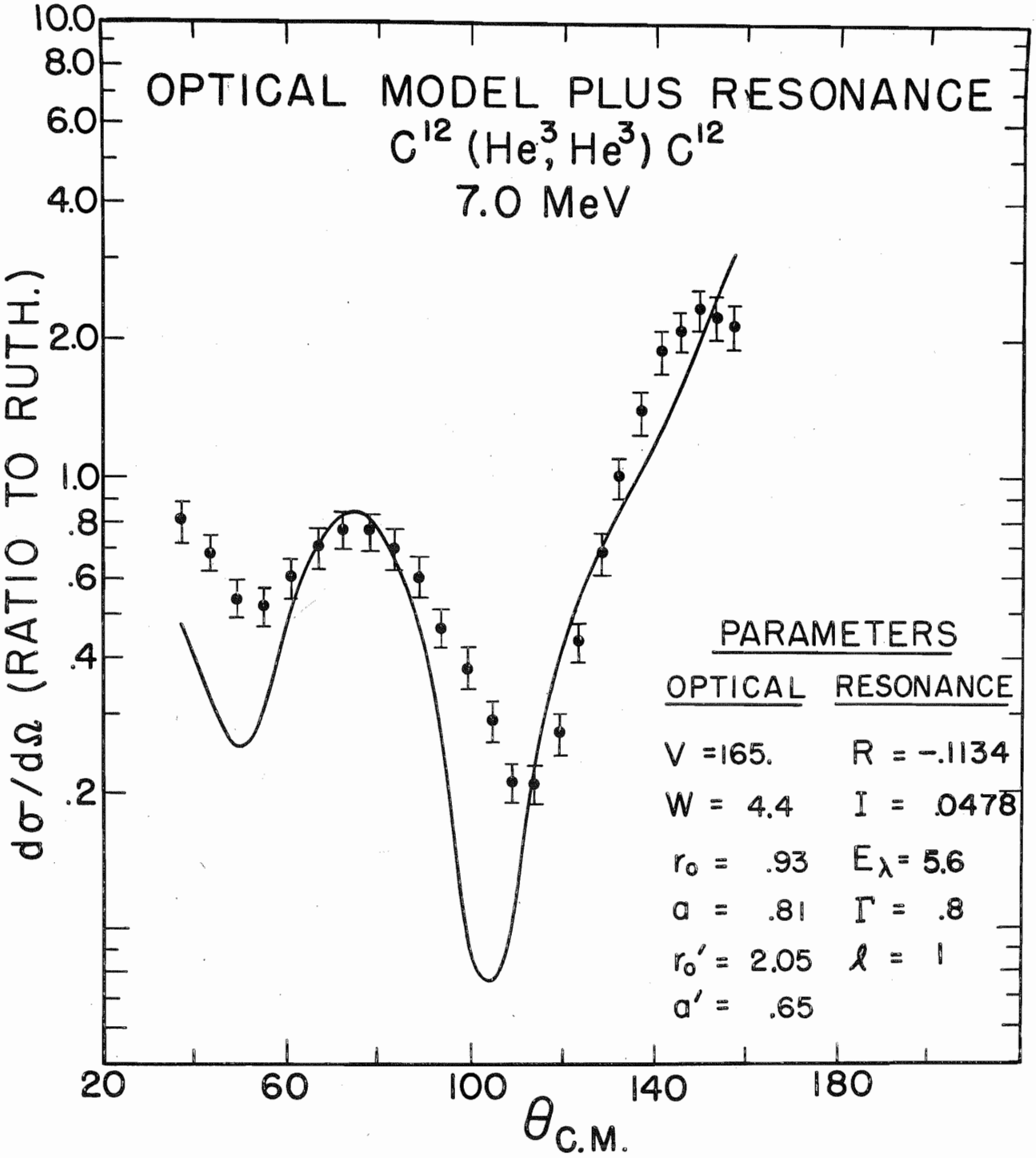
OPTICAL MODEL PLUS RESONANCE
C12 (He3, He3) C12
7.0 MeV
dσ/dΩ (RATIO TO RUTH.)
10.0
8.0
6.0
4.0
2.0
1.0
.8
.6
.4
.2
20
60
100
140
180
θC.M.
PARAMETERS
OPTICAL
RESONANCE
V =165.
R = -.1134
W = 4.4
I = .0478
r0 = .93
Eλ = 5.6
a = .81
Γ = .8
r0' = 2.05
ℓ = 1
a' = .65

with the excitation curve. The results are shown in figure 22. The equations used for this calculation are given below. One has a term in the amplitude (see equation (42)) which at E = Eres is

$$\frac{R_\lambda + i\, I_\lambda}{\frac{1}{2} i \Gamma_\lambda} = \frac{-\frac{1}{2}\Gamma_\lambda R_\lambda\, i + \frac{1}{2} I_\lambda \Gamma_\lambda}{\frac{1}{4}\Gamma_\lambda^2} = \frac{I_\lambda}{2\Gamma_\lambda} - i\, \frac{R_\lambda}{2\Gamma_\lambda} \qquad (57$$

We want to keep the magnitude and phase the same so

$$\left(\frac{I_\lambda}{2\Gamma_\lambda}\right)^2 + \left(\frac{R_\lambda}{2\Gamma_\lambda}\right)^2 = C \qquad (58)$$

and

$$\tan^{-1} \frac{R_\lambda}{I_\lambda} = K \qquad (59)$$

or

$$\left(\frac{I_\lambda}{2\Gamma_\lambda}\right)^2 \cdot \left[1 + (\tan K)^2\right] = C \qquad (60)$$

So with the constants C and K determined by the fit to the angular distribution at E = Eres, we can find I_λ and R_λ for a given Γ_λ.

As is clear from the data of figure 22, there is additional structure involved here which we have not accounted for. A study of the alpha and proton channels substantiated this observation. This indicates the need for a more careful study of this region. Perhaps a measurement of the angular distributions in small energy steps through this region would help to solve the problem.

D. Angular Distributions as a Function of Energy

With this collection of data it was now decided that a more detailed study of the alpha angular distributions would be useful in the case of C^{13}. For one thing we could examine the integrated cross section as a function of energy to look for signs of the 6.0 MeV state. A study of the coefficients of a Legendre polynomial expansion as a function of energy also seemed interesting. (52) Finally, additional statistical tests could be performed on such data. With these objectives, we took angular distributions in steps of 100 keV using 4 detectors as described earlier. The results including the integrated cross sections are shown in Figures 24, 25, 26, and 27. The consistent structure observed in a_2 as a function of energy indicated that the three dimensional presentation used in a_o and a_1 was unnecessary here. Some observations which can be made from these data are:

1. In the alpha one data we noticed a smooth trend of the nodes toward the forward angles as the energy increases. In fact there is a helical nature, for as the forward peaks dissolve, they reappear in the back angles.
2. The characteristic shapes change from forward peaking to symmetric about 90^o to backward peaking as the energy increases.
3. The effect of the statistical damping factor is apparent when comparing a_o with a_1 in that the relative fluctuations are damped in the case of a_1.

Figure 24. Three Dimensional Display of The Angular Distributions for the Reaction $C^{13}(He^3, a_o)C^{12}$ as a Function of Bombarding Energy. The Integrated Cross Section is also Shown.

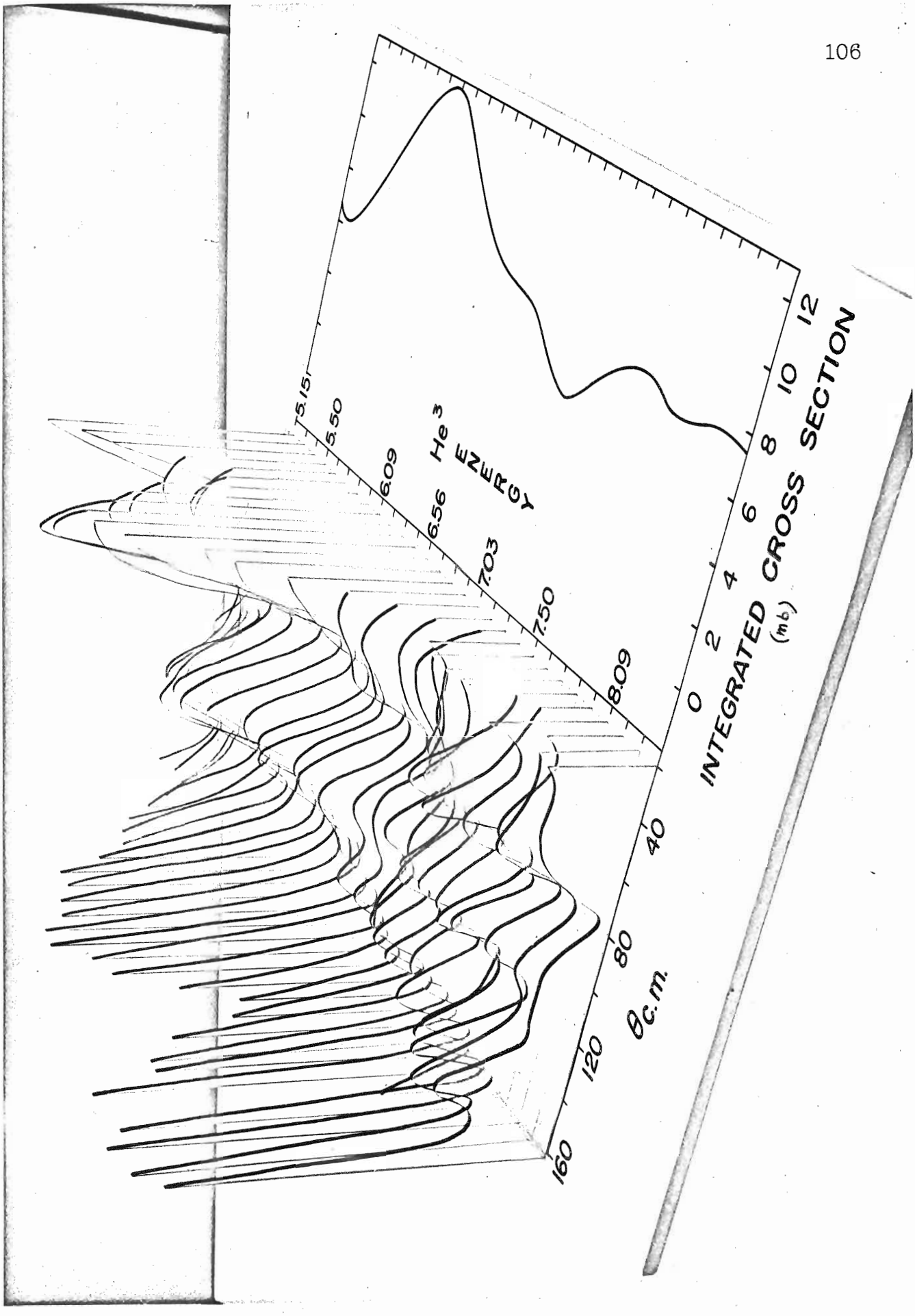
5.15
5.50
6.09
6.56
7.03
7.50
8.09
He³ ENERGY
0
2
4
6
8
10
12
INTEGRATED CROSS SECTION
(mb)
40
80
120
160
θc.m.

Figure 25. Three Dimensional Display of the Angular Distributions for the Reaction $C^{13}(He^{3}, a_{1})C^{12}$ as a Function of Bombarding Energy. The Integrated Cross Section is also Shown.

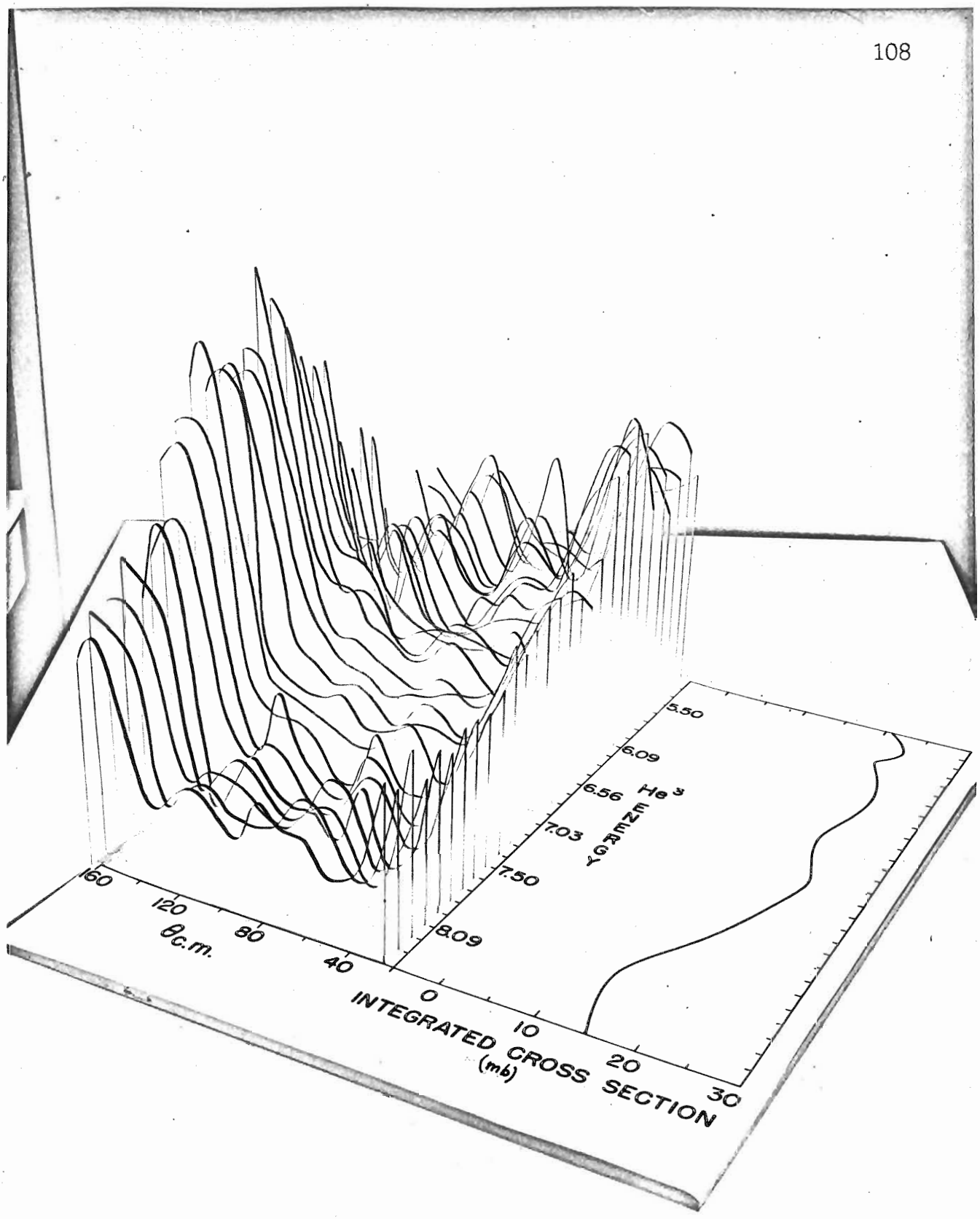
160
120
80
40
θc.m.
0
10
20
30
INTEGRATED CROSS SECTION
(mb)
5.50
6.09
6.56
7.03
7.50
8.09
He³
ENERGY

Figure 26. The Angular Distributions of the $C^{13}(He^3, a_2)C^{12}$ Reaction as a Function of Bombarding Energy. The Scales for the Solid Lines are on the Left, Those for the Dashed Lines are on the Right.

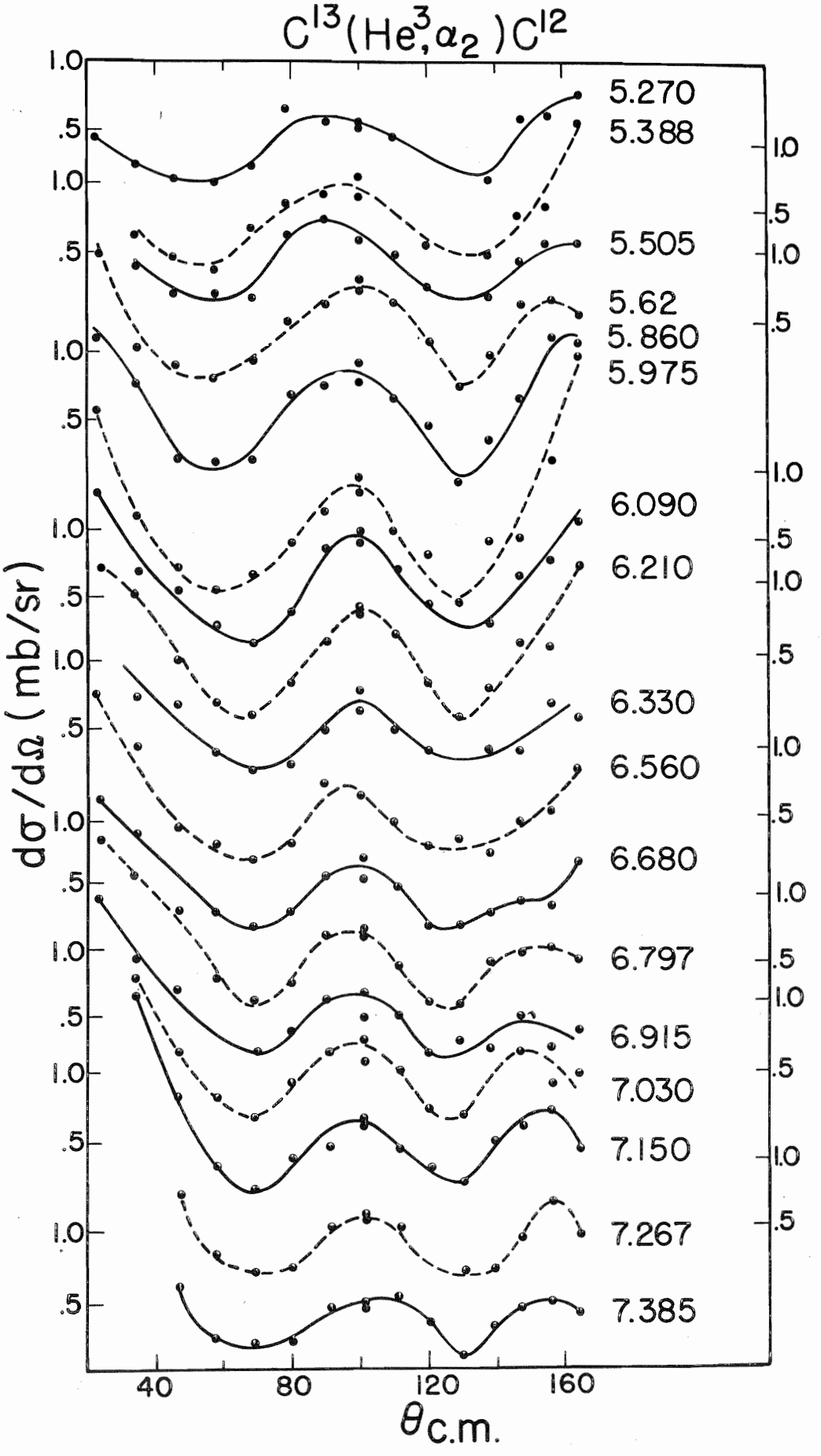
$C^{13}(He^3,\alpha_2)C^{12}$
5.270
5.388
5.505
5.62
5.860
5.975
6.090
6.210
6.330
6.560
6.680
6.797
6.915
7.030
7.150
7.267
7.385
1.0
.5
40
80
120
160
$\theta_{c.m.}$
$d\sigma/d\Omega$ (mb/sr)

Figure 27. The Integrated Cross Section for the Reaction $C^{13}(He^3, a_2)C^{12}$ as a Function of Bombarding Energy.

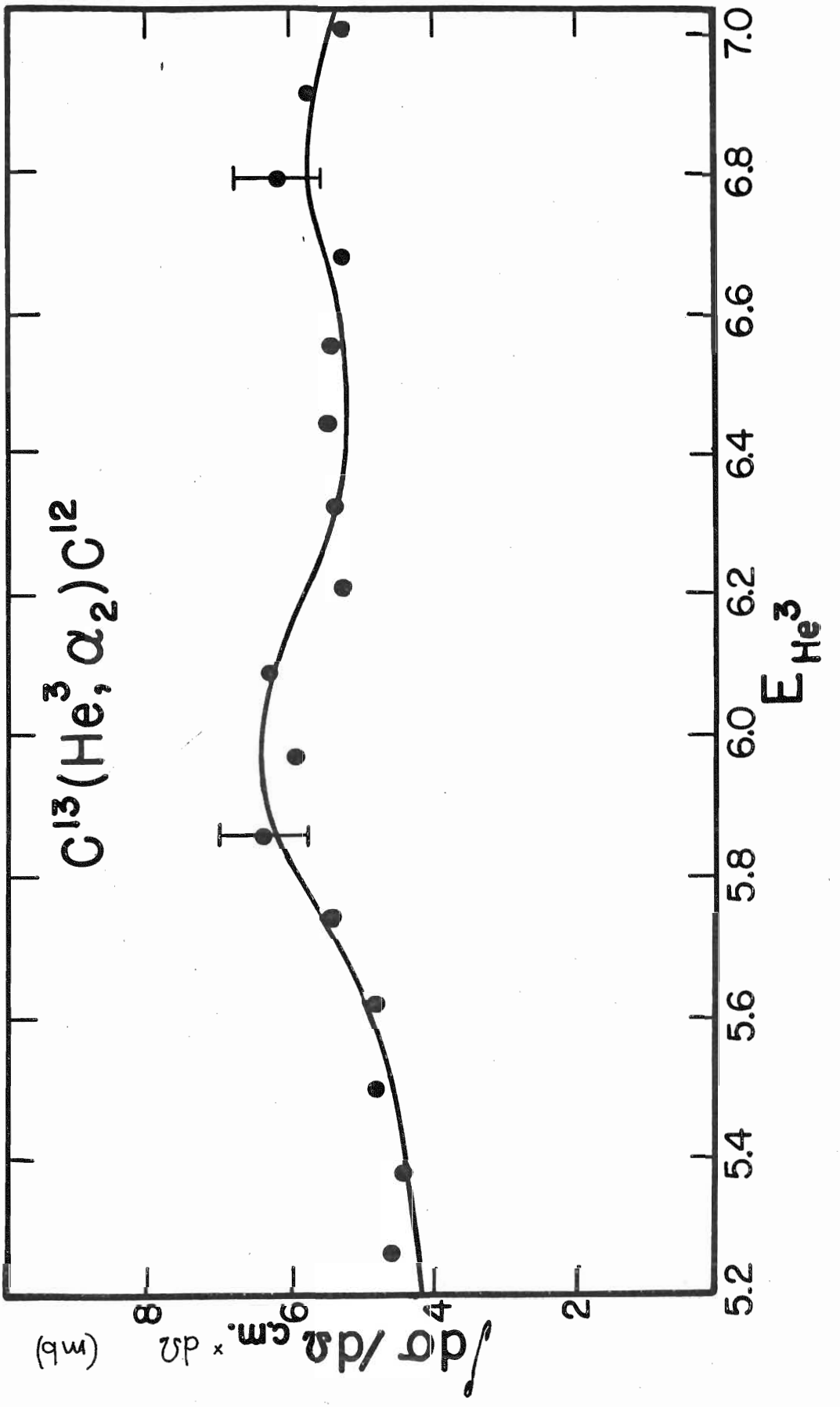
$C^{13}(He^3, \alpha_2)C^{12}$
$\int d\sigma/d\Omega_{c.m.} \times d\Omega$ (mb)
8
6
4
2
5.2
5.4
5.6
5.8
6.0
6.2
6.4
6.6
6.8
7.0
E_{He^3}

The average angular distribution is expected to be symmetric about 90° if a statistical assumption is valid and a sufficient sample of data is taken. In Figure 28 we show the average angular distributions obtained for a_0 and a_1 from the 30 energies measured. Due to a background problem the data for a_2 did not cover the entire energy range. However, it is clear (see Figure 26) that the available data will yield a symmetric average. So in all cases we see that the effect of averaging results in a trend towards symmetry about 90°.

We next expanded the angular distributions in terms of Legendre Polynomials in a least squares manner. The resulting coefficients are shown as a function of energy in Figures 29 and 30. The behavior of P_7 and the good fits obtained indicate that higher order terms are not required. The resonance is seen in P_6 at 6.0 MeV. The fact that the lower order terms show the resonance in a shifted position suggests an interference due to another amplitude. This result supports the $J = 3$ assignment, for it follows from the properties of the $\bar{Z}$ coefficients (23) that

$$L_{max} \leq 2\ell_{max} \qquad L_{max} \leq 2\ell'_{max} \tag{61}$$

So for the coefficients of P_8 to be zero we have $\ell'_{max} = 3$, $J = \ell' + s' = 3$.

It is also to be noticed in these curves that P_o shows the resonance at 6.0 MeV. Due to the orthonormality of the Legendre Polynomials the curve P_o represents the integrated cross section (actually divided by 4π).

Figure 28. Average Angular Distributions Obtained from the 30 Measured Energies.

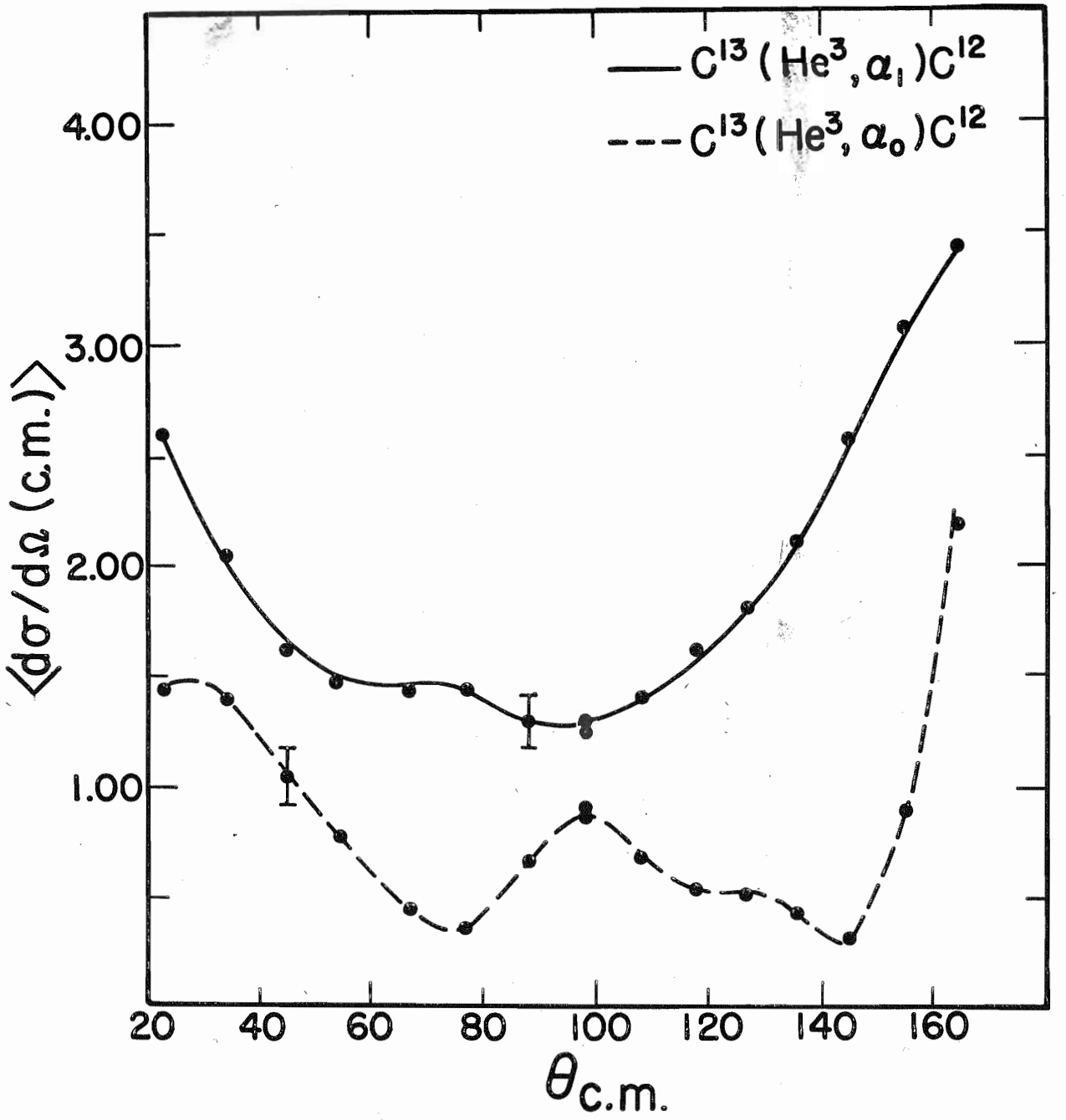
C13 (He3, α1) C12
C13 (He3, α0) C12
4.00
3.00
2.00
1.00
⟨dσ/dΩ (c.m.)⟩
20
40
60
80
100
120
140
160
θc.m.

Figure 29. Coefficients of the Legendre Polynomial Expansions of the 30 Angular Distributions for the $C^{13}(He^{3}, a_{o})C^{12}$ Reaction. The scales for the solid lines are on the left, those for the dashed lines are on the right.

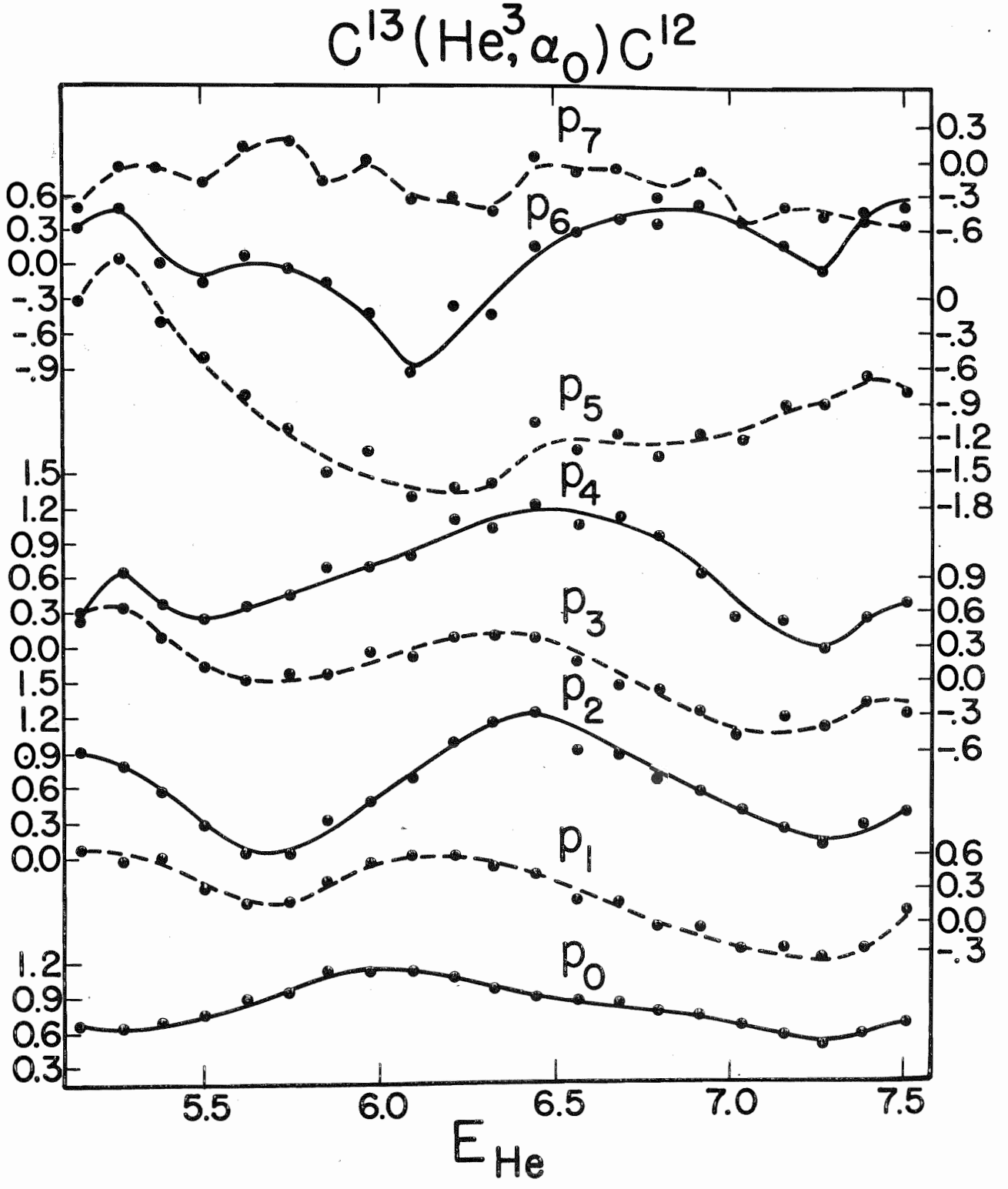
$C^{13}(He^3,\alpha_0)C^{12}$
p_7
p_6
p_5
p_4
p_3
p_2
p_1
p_0
0.6 0.3 0.0 -.3 -.6 -.9
0.3 0.0 -.3 -.6
0 -.3 -.6 -.9 -1.2 -1.5 -1.8
1.5 1.2 0.9 0.6 0.3 0.0
0.9 0.6 0.3 0.0 -.3 -.6
1.5 1.2 0.9 0.6 0.3 0.0
0.6 0.3 0.0 -.3
1.2 0.9 0.6 0.3
5.5 6.0 6.5 7.0 7.5
E_{He}

Figure 30. Coefficients of the Legendre Polynomial Expansions of the 30 Angular Distributions for the $C^{13}(He^3, a_1)C^{12}$ Reaction. The scales for the solid lines are on the left, those for the dashed lines are on the right.

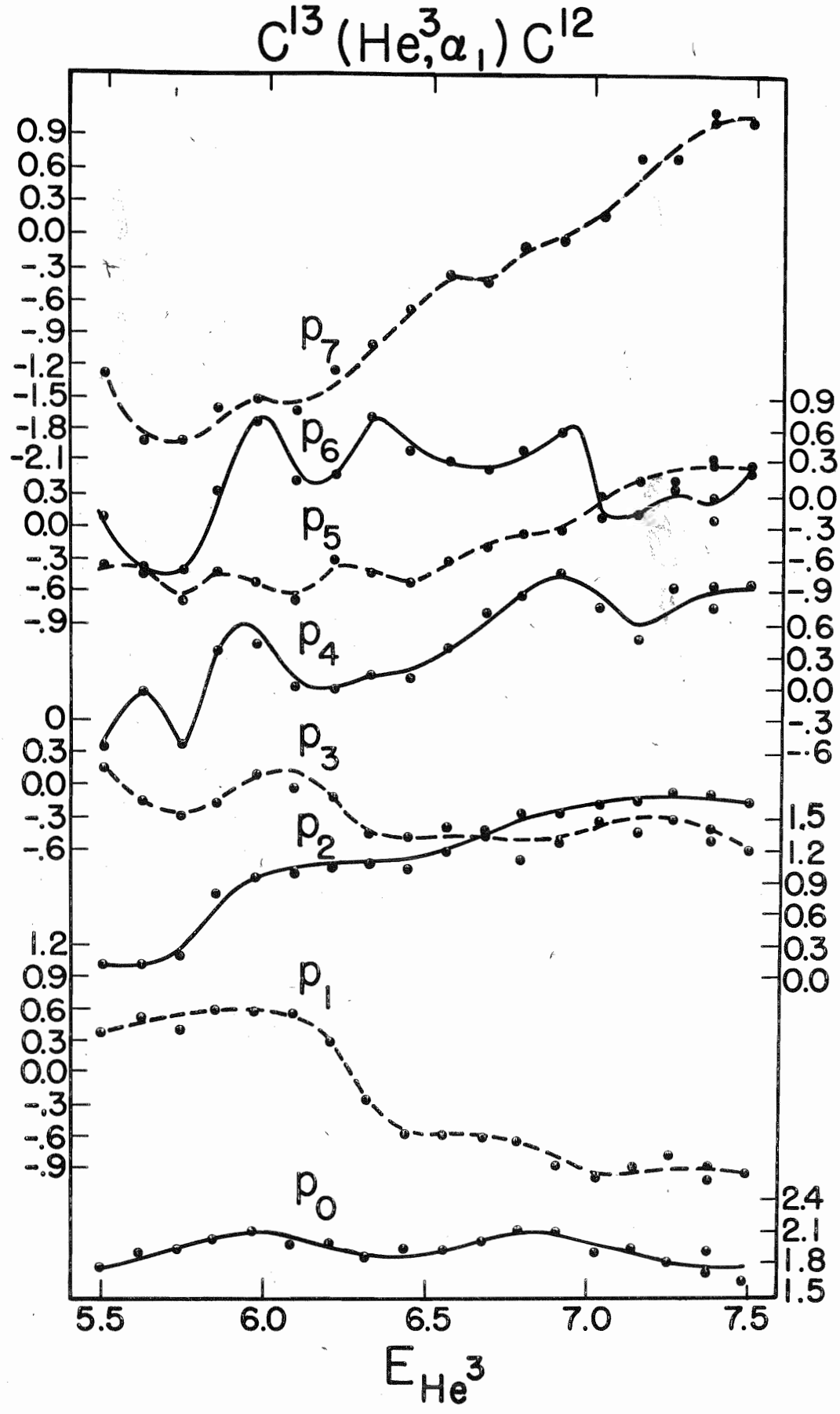
$C^{13}(He^3,\alpha_1)C^{12}$
p_7
p_6
p_5
p_4
p_3
p_2
p_1
p_0
0.9
0.6
0.3
0.0
-.3
-.6
-.9
-1.2
-1.5
-1.8
-2.1
0.3
0.0
-.3
-.6
-.9
0
0.3
0.0
-.3
-.6
1.2
0.9
0.6
0.3
0.0
-.3
-.6
-.9
0.9
0.6
0.3
0.0
-.3
-.6
0.6
0.3
0.0
-.3
-.6
1.5
1.2
0.9
0.6
0.3
0.0
2.4
2.1
1.8
1.5
5.5
6.0
6.5
7.0
7.5
E_{He^3}

In the case of a_1 (see Figure 30) there is some indication of a resonance in the vicinity of 6.0 MeV. However, terms as high as P_8 are permitted for this channel for J = 3. This means that one must expand the angular distribution including terms as high as P_9 before a conclusion concerning a spin assignment of J = 3 can be made. It was found that the accuracy of our data made such an expansion meaningless in the present case.

Finally, the coefficients $F(L_1, L_2)$ were evaluated as defined in equation (27). It was found that the terms for $L_1 + L_2$ odd were non zero, in fact the even and odd terms were of equal magnitude, indicating appreciable direct reaction contribution. This result is consistent with previous statistical theory analysis.

E. Summary

At this point we can summarize our results as follows:

1. The DWBA as formulated in code JULIE does not appear to be satisfactory for the $C^{13}(He^3, a)C^{12}$ reaction in the energy range from 5.0 to 8.0 MeV, although there is some indication that it is beginning to work near 8.0 MeV.
2. The theory of the statistical compound nucleus which includes the effects of direct reactions appears to describe much of the data, however, no detailed behavior can be explained by this theory.

3. There appears to be a resonant structure in the region of 6.0 MeV He^3 energies. Although it is not a pure single level, it behaves very much like a single level.

How do we reconcile the resonant structure with the statistical behavior? Here we can take two viewpoints. The first would be to use Feshbach's terminology. One would say that a simple resonance behavior at a high excitation energy where one might expect $\Gamma >> D$ is indicative of a doorway state mechanism operating. In this region Feshbach has described a doorway state as being a linear combination of open channel wave functions which are particularly stable, i.e., have a relatively small width. One expects the resonances to occur amongst the Ericson-Brink fluctuations. The problem is to separate the two. Perhaps this is indeed what we have accomplished.

Rather than looking at these "single level like" structures as foreign to the statistical region, Moldauer (6) has recently suggested that a proper statistical theory can give rise, by virtue of the distribution of resonance pole widths and strengths, to intermediate structure resonances in the cross section. These statistical model intermediate resonances will have many properties in common with doorway states. For example, they will be associated with a definite total angular momentum, and each will have a characteristic angular distribution.

F. The Eigenchannel Reaction Theory Results

Finally, we wish to compare our results with a calculation of the 3^- continuum states of O^{16} in the eigenchannel reaction theory performed by Wahsweiler, Danos, and Greiner. (53) Here no mechanism is involved, since the cross section is computed directly from the nuclear structure as has been discussed in section III. C. This calculational technique may be looked at as one means of finding the states which Feshbach calls doorway states in the continuum. In this calculation the complete 3^- part of the S matrix of O^{16} has been computed in the 1p1h approximation. Examining the eigenphases as a function of energy as shown in Figure 31, which is taken from reference 53 reveals that the eigenphase which originates from the $(d\,3/2\ p\,3/2^{-1})_p$ configuration (i.e., no. 4) passes through 90° in the vicinity of 27.0 MeV. Thus, as has been discussed, one would expect a single level like behavior near 27.0 MeV.

In order to compare the results of the eigenchannel calculation more carefully with our experiment, Wahsweiler (54) has performed more detailed calculations at Frankfurt, Germany. A list of the 3^- eigenphases resulting from this calculation as a function of energy in half MeV steps is given in table 4. Eigenphase 4 (as was seen in Figure 31 of the older calculation) is the one which passes through 90 degrees. Wahsweiler has suggested that since all the inelastic partial particle-particle cross sections display a local maximum at about 27.0 MeV this is the only one which possibly could be related to the resonance which we have observed.

Figure 31. Eigenphases as a Function of Energy in O^{16}.

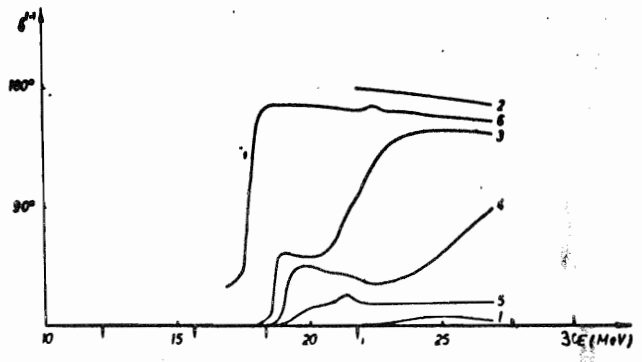

FIG. 2. Eigenphases for the 3^- states as a function of the excitation energy of the compound system. The numbers on the different curves label the channels presumably predominant in the neighbourhood of the corresponding threshold. The sequence is (1) $(d_{3/2}p_{3/2}^{-1})_n$, (2) $(d_{5/2}p_{3/2}^{-1})_n$, (3) $(d_{5/2}p_{1/2}^{-1})_n$, (4) $(d_{3/2}p_{3/2}^{-1})_p$, (5) $(d_{5/2}p_{3/2}^{-1})_p$, (6) $(d_{5/2}p_{1/2}^{-1})_p$. The arrows indicate the various thresholds.

Table 4. List of the 3^- Eigenphases as a Function of Energy.

V \ E_{exc}	$25.5_{(Mev)}$	26	26.5	27	27.5
1	6.84^o	6.31	5.80	4.83	3.78
2	171.21	169.64	167.85	166.75	165.19
3	142.38	142.61	142.25	141.77	141.13
4	52.99	59.41	66.48	73.33	79.11
5	19.64	18.83	18.48	17.94	17.46
6	156.10	155.31	154.54	153.77	152.75
	$28_{(Mev)}$	28.5	29	29.5	30
	2.60^o	0.96	179.89	178.47	177.21
	164.00	162.70	161.52	160.36	159.35
	140.18	139.54	138.52	137.74	136.86
	83.89	87.93	90.80	93.32	95.04
	16.49	16.07	14.32	13.64	13.14
	152.01	150.91	150.05	149.10	147.75

Eigenchannel 4 is the one which contains the largest octupole strength.

It was also decided to investigate the 4^{th} eigenvector with regard to isospin. If we assume that the compound nucleus has an isolated level with definite isobaric spin T, then the decay or formation of such a level is governed by the selection rules of vector addition

$$\vec{T}_t + \vec{t} = \vec{T} = \vec{T}_r + \vec{t}' \qquad (62)$$

where the subscripts t and r refer to the target and residual nucleus respectively. The above equation holds provided we assume charge independence in the decay and formation mechanisms. (55) So we see that the relatively strong α decay of our state suggests T = 0.

From the calculation of Wahsweiler (54) it appears that the strongest amplitudes in the 4^{th} eigenvector of the S matrix are those of channel c = 1 $((d3/2\, p3/2^{-1})_n)$ and channel C = 4 $((d3/2\ p3/2^{-1})_p)$ through the region from 27.0 to 30.0 MeV. The amplitudes of the assymptotic 4^{th} eigenchannel function are given in table 5a. The approximate equality of the amplitudes to $\pm\ 1/\sqrt{2}$ respectively indicates that the resonance is almost T = 0. One can also investigate the amplitudes of the wave function of the inside region as given in table 5b in the same manner. Thus it may be concluded that the 1p1h contribution to the total 3^- compound state of O^{16} has T = 0, and shows a weak resonance aroung 27.0 MeV.

Since this calculation does not consider higher order particle hole configurations, it is not complete with regard to a comparison with our experiment. However, the observation of the resonance in the (He^3, p) channel implies, in a time independent description, that there is a signifi-

Table 5a. Amplitudes of the Asymptotic 4^{th} Eigenchannel Function

E_{exc}	$\delta^{(4)}$	c = 1	c = 4
27 Mev	73.33°	0.658	-0.723
27.5	79.11	0.684	-0.702
28	83.89	0.704	-0.683
28.5	87.93	0.720	-0.668
29	90.80	0.738	-0.650
29.5	93.32	0.746	-0.649
30	95.04	0.751	-0.628

Table 5b. Amplitudes of the Wave Functions of the Inside Region

E_{exc} (Mev)	$\delta^{(4)}$	$(d_{3/2}\bar{p}_{3/2})_n$			$(d_{3/2}\bar{p}_{3/2})_p$		
		N_r=1	N_r=2	N_r=3	N_r=1	N_r=2	N_r=3
27	73.33	+.064	0.707	-.119	-.072	-.630	.21[illegible]
28	83.89	.174	.707	-.123	-.125	-.612	.185
29	90.80	.196	.720	-.116	-.144	-.593	.163
30	95.04	.189	.736	-.105	-.152	-.581	.146

(N_r denotes the radial quantum number)

cant 1p1h component. In addition the observation of alpha particles indicates that the 4p4h configurations are also involved. The width of the state as calculated by Danos et al. (53) appears to be somewhat broader than that observed here. Including the higher configurations would be expected to have the desired effect of narrowing the width by decreasing the amplitude of the decaying configuration in the configuration mixture.

How would a proper description of O^{16} proceed? First we point out that the description of the state is taken to be in the time independent formulation, so that everything which is there exists when a state is formed. Initially one may have a set of states such as those in the sketch below

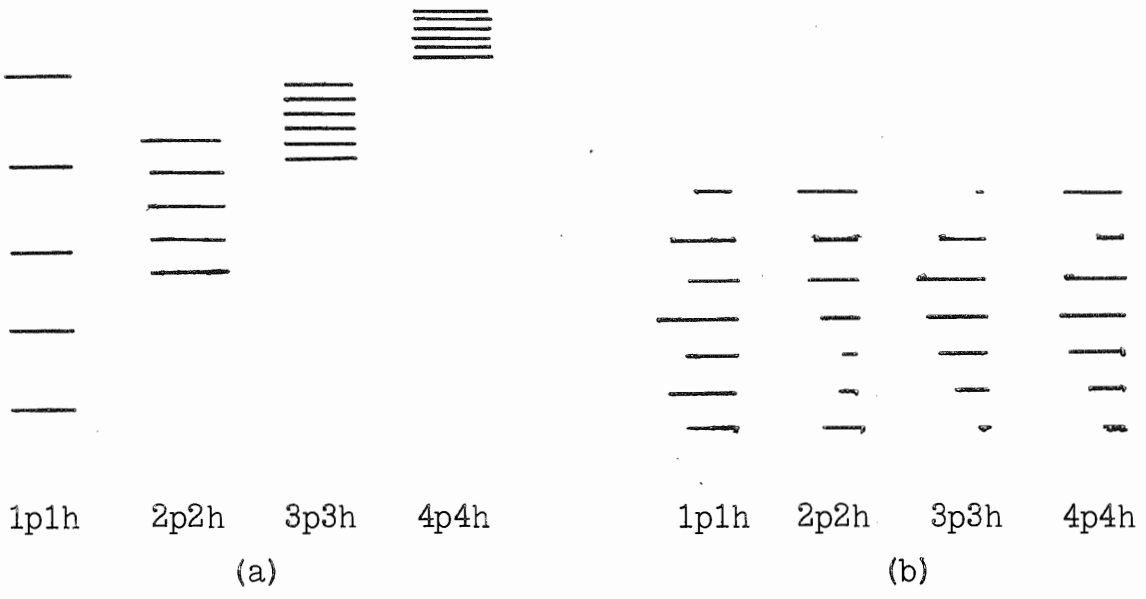

Diagonalizing the Hamiltonian in this space will result in a new set of states which can be pictured as having certain components given by the length of the line in the sketch (b). Each 1p1h state is now a linear combination of the 1p1h states we started with; the same is true for all configu-

rations. We see that the higher generations will in general shift the 1p1h states slightly and take some strength from them.

In the case of O^{16} one would at first suppose that there would be an astronomical number of states in going out to 4p4h states, and that therefore the problem would be essentially unsolvable. Gillet (56) has recently argued that in the case of the 2p2h states only a few are important in the 20 - 30 MeV region. This is because the 2p2h configurations of odd parity arise at energy $3\hbar\omega$ (40 MeV). Therefore, the residual interaction must account for shifts of about 20 MeV. It was found that only 4 out of 50 2p2h states are important. So perhaps the 3p3h and 4p4h states will also turn out to be simple enough to be included in a calculation. In the present case it is expected that including the higher generations will shift the resonant energy to a slightly higher position and reduce its width some. Calculations are under way by Wahsweiler at Frankfurt to enable a more complete solution of this problem. (54).

APPENDIX

Appendix I

The C^{13} targets used in this experiment were self supporting foils made by the technique of cracking C^{13} enriched methyl iodide on a .00012 inch nickel foil.

To begin with the one inch square nickel foil was carefully folded in half without creasing the edge and placed between two electrodes. The purpose of this was to keep the inside surface relatively free from deposite during the cracking process. The electrodes were now covered with a small bell jar which was subsequently evacuated. A mercury manometer was used to measure the pressure when the methyl iodide was introduced. A pressure of about 3 centimeters of mercury was used. After introducing the vapor, the current was raised until the foil was bright red and cracking began (as indicated by the deposite on the bell jar surface). After about 15 seconds, the current was slowly decreased.

After removing the cracked foil from the bell jar, it was unfolded and cut in half along the fold. The two pieces were dropped, carbon side up, into an acid solution of 2 parts water, 1 part Sulfuric Acid, and 2 parts Nitric Acid. After the nickel dissolved, the resulting carbon foils

were picked up on a target ring and rinsed in distilled water. The thickness of the foils ranged from 10 to 40 keV for 5. MeV alpha particles.

To assure success this procedure was practiced by using normal methyl iodide to make C^{12} targets. By doing this two satisfactory C^{13} targets could be obtained for each cracking attempt.

LIST OF REFERENCES

REFERENCES

1. N. Bohr, Nature, 137, 344 (1936).

2. P. P. Singh, B. A. Watson, J. J. Kroepfl, and T. P. Marvin, Phys. Rev. Letters, 17, 968 (1966).

3. H. Buttner, W. Greiner and G. Sussmann, Phys. Letters 20, 521 (1966).

4. K. Izumo, Nucl. Phys. 62, 673 (1965).

5. K. J. LeCouteur, Phys. Letters 11, 53 (1964).

6. P. A. Moldauer, Phys. Rev. Letters 18, 249 (1967).

7. J. J. Griffin, Phys. Rev. Letters 17, 478 (1966).

8. H. Feshbach, Nuclear Structure Study with Neutrons, Proceedings of the International Conference, Antwerp, July 19-23, 1965.

9. H. Feshbach, A. K. Kerman, and R. H. Lemmer, Ann. of Phys. 41, 230 (1967).

10. N. G. Puttasswamy and D. Kohler, Phys. Letters 20, 288 (1966).

11. G. E. Owen and L. Madansky, NYO Report 2054 (1958).

12. V. K. Deshpande, Nucl. Phys. 70, 561 (1965).

13. E. M. Kellogg, Ph.D. Thesis, University of Pennsylvania (1965).

14. G. M. Temmer, Phys. Rev. Letters, 12, 330 (1964).

15. I. Nonaka, T. Mikumo, M. Koike, K. Matsuda, A. Suzuki, Y. Nagahava, K. Kikuchi and T. Maki, Journal of the Phys. Soc. of Japan, 22, 949 (1967).

16. M. Danos and W. Greiner, Phys. Rev. 146, 708 (1966).

17. N. R. Roberson, D. R. Tilley and H. R. Weller, Nucl. Instr. and Methods 33, 84 (1965).

18. O. Meier, private communication.

19. D. Gerke, Ph.D Thesis (unpublished), Duke University (1962).

20. R. R. Carlson, private communication.

21. H. D. Holmgren, Phys. Rev. 106, 100 (1957).

22. H. Feshbach, Nuclear Spectroscopy, Part B, P625 (Academic Press, N. Y., 1960.

23. L. C. Biedenharn, J. M. Blatt, and M. E. Rose, Reviews of Mod. Phys., 24, 249 (1952).

24. W. Sharp, J. Kennedy, B. Sears and M. Hoyle, "Tables of Coefficients for Angular Distribution Analysis", AECL No. 97 (1960).

25. P. A. Moldauer, ANL-6323 (1961).

26. T. Ericson, Ann. of Phys. 23, 390 (1963).

27. D. M. Brink and R. O. Stephen, Phys. Letters 5, 77 (1963).

28. R. O. Stephen, Report of the Clarendon Laboratory, Oxford (1963).

29. B. W. Allardyce, W. R. Graham and I. Hall, Nucl. Phys. 52, 239 (1964).

30. T. Ericson and Mayer-Kuckuk, Annual Reviews of Nuclear Science 16, 183 (1966).

31. R. Bassell, R. Drisko and G. Satchler, ORNL 3240.

32. S. Fernbach, R. Serber, and T. Taylor, Phys. Rev. 75, 1352 (1949).

33. L. Cook, E. McMillan, J. Peterson and D. Sewell, Phys. Rev. 75, 7 (1949).

34. R. LeLevier and D. Saxon, Phys. Rev. 87, 40 (1952).

35. P. E. Hodgson, The Optical Model of Elastic Scattering (Clarendon Press, Oxford, 1963).

36. H. Feshbach, C. E. Porter, and V. F. Weisskopf, Phys. Rev. 96, 448 (1954).

37. T. Tamura and T. Terasawa, Phys. Letters 8, 41 (1964).

38. M. Danos and W. Greiner, Phys. Rev. 138, B93 (1965).

39. M. Danos, private communication.

40. E. B. Carter, G. E. Mitchess, and R. H. Davis, Phys. Rev. 133, B1421 (1964).

41. E. F. Bennett, NYO Rept. 8082 (1958); Princeton University Ph.D. Thesis, 1958.

42. R. M. Drisko, private communication

43. B. Buck and J. Rook, Nucl. Phys. 67, 504 (1965).

44. J. French and M. Mac Farlane, Rev. of Mod. Phys. 32, 567 (1960).

45. Jae Young Park, private communication.

46. Steve Edwards, private communication.

47. M. Abramowitz and I. Stegun, Handbook of Mathematical Functions, Dover, 1965.

48. J. Janecke, Nucl. Phys. 48, 129 (1963).

49. M. Gursky, private communication.

50. M. A. Chaudri, Ph.D. Thesis, University of Heidelberg, (1964).

51. J. P. Schiffer, Nuclear Spectroscopy with Direct Reactions, Vol. II, 279 (1964).

52. G. S. Mani and G. C. Dutt, Nucl. Phys. 78, 613 (1966).

53. H. Wahsweiler, M. Danos, and W. Greiner, Phys. Rev. Letters 17, 395 (1966).

54. H. G. Wahsweiler, private communication.

55. D. Robson, Annual Rev. of Nuclear Sci., 16, 119 (1966).

56. V. Gillet, M. A. Melkanoff and J. Raynal, Nucl. Phys. A97, 631 (1967).

BIOGRAPHY

Henry R. Weller

Date of Birth: March 15, 1941

Place of Birth: Hackensack, New Jersey

Colleges Attended:

Fairleigh Dickinson University	B.S.	1962
Duke University	Ph.D.	1968

Publications:

The Acceleration of Doubly-Ionized He^3, N. R. Roberson, D. R. Tilley, and H. R. Weller, Nuclear Instruments and Methods 33, 84 (1965).

Abstracts:

$C^{13}(He^3, \alpha)$ Reaction, with Roberson and Tilley, Bull. Am. Phys. Soc. 11, 317 (1966).

Excitation of O^{16} via He^3 Bombardment of C^{13}, with Roberson and Tilley, Bull. Am. Phys. Soc. 12, 518 (1967).

Positions Held:

Teaching Assistant at Duke	1962 - 1963
Research Assistant at Duke	1963 - 1967